LIST OF ABBREVIATIONS

A_c	the PV array area $[m^2]$
a, b	fuel cost coefficients
$B_C(0)$	the initial state of charge of the battery
$B_C^{\min}$	the minimum allowable battery bank capacity (kWh)
$B_C^{\max}$	maximum allowable battery bank capacity (kWh)
$B_C(t)$	the state of charge of the battery bank at any hour
$B_C(t-1)$	the state of charge of the battery bank at the previous hour
DOD	the depth of discharge
I_B	the hourly global irradiation (kWh/m^2)
I_D	the hourly diffuse irradiation (kWh/m^2)
η_B	the battery round trip efficiency
η_C	the battery charging efficiency
η_D	the battery discharging efficiency
η_{pv}	the PV generator efficiency
η_R	the PV generator efficiency at reference temperature
η_{WG}	the wind generator efficiency
NT	standard and nominal cell operating temperature conditions
$P_1(t)$	control variable representing energy flow from the diesel generator to the load at any hour (kW)
$P_2(t)$	control variable representing energy flow from the PV array to the load at any hour (kW)
$P_3(t)$	control variable representing energy flow from the PV array to the battery at any hour (kW)
$P_4(t)$	control variable representing energy flow from the battery to the load at any hour (kW)
$P_L(t)$	control variable representing the load at any hour (kW)
$P_1(k)$	control variable representing energy flow from the diesel generator to the load at the k^{th} hour $[kW]$
$P_2(k)$	control variable representing energy flow to and from the battery at the k^{th} hour$[kW]$

$P_3(k)$	control variable representing energy flow from the PV array at the k^{th} hour $[kW]$
$P_4(k)$	control variable representing energy flow from the wind generator at the k^{th} hour $[kW]$
P_{DG}	generator rated power output (kVA)
$P_L(k)$	control variable representing the load at the k^{th} hour $[kW]$
P_{pv}	the hourly energy output from a PV generator of a given array area (kWh/m^2)
$P_{pv}(k)$	the hourly energy output from a PV generator of a given array area at the k^{th} hour$[kWh/m^2]$
$P_{wind}(k)$	the hourly energy output from a wind generator at the k^{th} hour$[kW]$
R_B	the ratio of beam irradiance incident on a tilted plane to that incident on a horizontal plane
SOC	the state of charge
$SOC(k)$	the current state of charge of the battery bank
T_A	the ambient temperature (^{0}C)
T_C	the cell temperature (^{0}C)
T_R	reference cell temperature (^{0}C)

TABLE OF CONTENTS

LIST OF FIGURES

LIST OF TABLES

CHAPTER 1

INTRODUCTION

1.1 BACKGROUND

Many drivers are mentioned in literature to promote use the of renewable energy options [1, 2, 3, 4]. The global increase in population growth and development has led to over-dependency by many nations on energy generation from fossil fuels. At the same time, concerns about global warming and depletion of fossil fuel reserves have led many nations to turn to the exploitation of renewable energy (RE) sources. In most developing countries, the main driver for RE exploitation is access to electricity, especially in remote and rural areas that are not connected to the grid. Poor access to electricity in developing countries is mostly due to poor distribution of grid electricity and financial resources to aid grid extension [5]. The relatively low energy demand in rural and isolated areas in most cases does not compensate for the cost of long-range transmission lines from the national grid justifying the use of distributed energy resources. Solar photovoltaic (PV) and/or wind-diesel hybrid power generation system technologies promise great opportunities for energy supply in both advanced and developing countries. These RE technologies are gaining increased importance, as they offer advantages such as little maintenance, absence of fuel cost, and easy expansion to meet growing energy needs [6, 7, 8, 9]. The policy drivers, such as reduction of carbon dioxide emissions and related credits, energy sources diversification, and energy efficiency encourage use of RE sources. Wind and solar PV generation are established clean technologies that are free, environmentally friendly and easy to expand to meet growing energy needs [7, 10]. PV and wind technology modularity is one of their major strengths, as this allows the users to match the system capacity to the desired situation. RE-based power systems are being deployed globally to provide autonomous power for various off-grid applications [1, 2, 3, 4].

The disadvantages of these RE technologies are that they are capital-cost-intensive and their sunshine-dependent output may not match the load on a daily basis. Stand-alone diesel generator (DG) sets have traditionally been favored solutions for off-grid applications, as they are generally inexpensive to purchase. However, their operational and maintenance costs are high and they have negative environmental impacts, especially when they operate at partial loads.

It should be noted, however, that PV generators and DGs have complementary characteristics in terms of capital cost, operating cost, maintenance requirements and resource availability. The major challenges associated with the use of these RE technologies in stand-alone installations are their intermittent nature and dependence on weather and climatic changes, which render them incapable of providing continuous uninterrupted power. Solar and wind resources also have naturally complementary characteristics in certain locations in terms of power production and this provides a strong case for RE-based hybrid systems with DGs and battery storage in terms of the capability of the system to provide reliable and continuous power supply in remote locations not connected to the grid power supply. The combination makes the most of the site's seasonal wind and solar resources owing to the fact that wind is relatively more available in winter months and during the night, while solar energy is relatively more available in summer months and during sunlit days in winter. Incorporation of battery storage improves supply reliability but it is often necessary to over-size both the storage and RE systems excessively to meet demand, resulting in high capital costs and inefficient use of the system. PV-diesel-battery (PDB) or PV-wind-diesel-battery (PWDB) hybrid power systems offer great opportunities by overcoming single source problems, providing environmentally friendly, reliable systems that reduce DG running costs and are considered a cost-effective way to meet energy requirements of areas not easily accessible for grid connection [6, 11, 12]. Hybrid energy systems therefore present a resolution to the time correlation of intermittent RE sources [13, 14, 4]. The fact that the hourly solar radiation incident on the PV module and the wind speed at a given location are functions of the day and time of the year means that the fraction of the load supplied by PV or wind is not constant. In the hybrid systems considered in this work, the solar/wind fraction and battery bank capacity are expected to have a great impact on the DG fuel consumption, depending on the season and load profile. A high RE resource output will result in reduced fuel consumption, as the RE sources will be able to generate enough power to serve the load and/or charge the battery. The variable

nature of RE sources means that the battery banks in RE-based applications experience a wide range of operational conditions, including varying rates of charge and discharge, depth of discharge (DoD), temperature fluctuations and charging strategies [15, 16]. These operating conditions vary significantly in different locations and applications and this provides the grounds for considering the lifetime characteristics of battery energy storage systems, as they have not been fully considered in many RE-based hybrid energy management optimization studies. Battery wear is determined by operating conditions, which are a function of the system sizing and the dispatch strategy.

The hybrid RE system is not an entirely new concept. A lot of research work is being done in this area [17]. Various authors have proposed hybrid PDB systems for off-grid applications in which the cost of energy is the main criterion used to select the optimal power system [2, 12]. RE systems incorporating DGs and batteries have been studied by various authors, such as [14, 18], but battery wear has not been evaluated in the analyses. In most RE-based hybrid systems, battery banks constitute a major part of the investment costs and are often the most expensive component when considering the lifetime costs, as their lifetime is considerably shorter than that of any of the other hybrid components [19], hence consideration of battery cost in this work. The selection and sizing of components of a hybrid power system in [2] are done using the Hybrid Optimisation Model for Electric Renewables (HOMER) software developed by the National Renewable Energy Laboratory, USA. HOMER is a simplified optimization model that can perform many hourly simulations in order to come up with the best possible matching between supply and demand to design the optimum system. It uses life cycle cost to rank different systems and also calculates the annual diesel costs. The main algorithm used in [12] obtains the optimal configuration of PV panels, batteries and DG while minimizing the total net present cost of the system, which includes all the life cycle costs throughout the useful lifetime of the system. It is shown in this work that the minimum output power of the DG and the minimum state of charge (SoC) of the batteries have an influence on the total net present cost and the optimal dispatch strategy. The PDB systems are found to be economically better than PV or diesel stand-alone systems for peak load profiles.

An economic analysis and environmental impact modeling of a PV with a diesel–battery system are proposed by [20], in which the fuel cost is calculated over a one-year period and simple payback is worked out for the PV module. The electric power sources in the hybrid

system consist of a PV array, a battery bank, a DG, and a wind generator (WG). The model calculates the annual cost of electricity for different systems and also the annual cost of fuel. The results show that the PDB hybrid power system reduces the operating costs and the greenhouse gases, as well as the amount of particulate matter emitted to the atmosphere. However, the work done by [2, 12, 20] assumes a constant load and also a uniform daily operational cost, which does not reflect the variation of radiation output throughout the year or the varying consumption patterns. These variable aspects are taken into account in this thesis.

RE systems incorporating DGs and batteries have been studied by various authors, such as [14, 12, 18, 21], but battery wear has not been evaluated in the analyses. The lifetime characteristics of battery energy storage systems have therefore not been fully considered in many RE-based hybrid energy management optimization studies. In [15] the performance and expected lifetimes of different sized batteries using a previously developed lead acid battery model are investigated. The results, based on the lifetime algorithm assumptions used, show that the lifetime of a battery should increase linearly with battery size. In [22] a battery management system that considers the various characteristics of the individual battery strings and decides how the strings are treated considering the load profile is developed. A grid-tied microgeneration and storage model has been developed for quantifying the performance of energy storage options and the challenges of relying on microgeneration for autonomy are highlighted. In [23, 24] a grid-tied system with a peak-shaving service as a way of increasing the penetration of PV production in the grid and consider battery ageing, but the PV generation is not optimized is also proposed. An optimal hybrid scheme of micro-grid including combined heat and power, gas-engine, WG, and PV, with the objective of minimizing fuel consumption, is proposed in [25]. The bone of contention is that in most optimization work battery wear cost is neglected, yet battery lifetime in RE-based applications poses a lot of uncertainty for investors owing to the replacement cost during the hybrid system's lifetime.

Hybrid energy systems have been used to power satellite earth stations, systems in rural communities, radio telecommunications and other off-grid applications [13]. In Central Africa, in countries such as the Congo, many mines are operating on DGs and RE hybrid systems can be useful in such industrial applications. The main challenge is the design of an optimal energy management system that satisfies the load demand, considering the variable nature of

the RE energy sources and the real-time variations in demand. Considerable research effort has been put into optimizing hybrid system components and operations, using various methods [26, 27, 28, 29]. However, these do not solve the problem in real-time in order to analyze the actual performance of the system, hence the application of a receding horizon strategy in the performance analysis of the hybrid system in this work. Unlike most similar works, this work focuses on the optimal dispatch of the various powers while minimizing operational cost, maximizing the utilization of RE sources and considering battery life improvement by minimizing the charge-discharge cycles of the battery. Model predictive control (MPC) is employed in this work owing to its advantages over the open loop approach and its capability to handle constraints of the system explicitly using a user-defined cost function [30]. Closed-loop models automatically adjust to changes in output due to external disturbance, measure states and give feedback to the optimization model repeatedly; hence the optimal solution is updated accordingly [31, 32]. The open loop model is unable to compensate for disturbances occurring from external sources owing to the absence of a feedback mechanism. When compared with the open loop optimization approaches, MPC results in reduced dimensions, easier computation, convergence and robustness, which are well demonstrated by its application to power economic dispatching problems with a six-unit system [31, 33, 34]. The MPC approach has been applied to a building heating system in order to analyze the energy savings that can be achieved [35]. Implementation of the receding horizon in controlling a single conventional power plant output to balance the demand has been explored by [36]. However, the work done so far does not specifically apply the on-line methodology to PWDB hybrid power supply options. MPC approaches have been applied previously to dispatching problems, such as optimal dynamic resource allocation [34], cost-optimal operation of a water pump station [37], fuel cost minimization of power generation [33], and current management of a hybrid fuel cell power system [32]. Besides, there are other approaches for energy dispatching of hybrid power systems (genetic algorithm [12], for example). A few researchers have applied this approach to the analysis of electric energy systems that incorporate intermittent resources [38].

1.2 MOTIVATION

RE technologies in stand-alone hybrid off-grid systems are gaining increased importance in most developing or remote areas that are not linked to the grid for both financial and infra-

structural reasons. PV-based power systems are being deployed globally to provide autonomous power for various off-grid applications. Improvements in the performance of these systems for off-grid applications occur continually globally in many research communities. The main challenge in this work is the design of an optimal energy management system that satisfies the load demand, considering the variable nature of the RE energy sources and variations in demand. The combination of various system components in a hybrid results in increased complexity of the system, which makes optimal energy management difficult. Optimum energy management of the hybrid system becomes complicated owing to the following aspects: non-linear characteristics of the components, variable load demand, unpredictable RE supplies and also interdependency of the optimum configuration and optimum control strategy of the hybrid system. The dynamic interaction between the load demand and the RE source can result in critical problems of stability and power quality that are not very common in conventional power systems, hence the need for proper control and management of power flow in the hybrid system to ensure continuous power supply for the load demand. Another challenge is that remote or off-grid home-owners are usually left with many decisions and little knowledge about the most cost-effective system for providing power to their homes and the expected operational costs. This work contributes to addressing these concerns.

It is important to note that the recent technological advancement of RE hybrid energy systems is due to activities in a number of research areas, including:

- On-going development of versatile hybrid energy system simulation software
- Continuing advances in the manufacturing process and improved efficiency of PV modules
- Availability of more efficient and reliable AC and DC appliances.
- Improved efficiency, system quality and reliability owing to advancements in electrical power conversion resulting from the introduction of new power electronic semiconductor devices
- Development of improved storage technologies, such as deep-cycle, lead-acid batteries for renewable energy systems.

- On-going development of customized, automatic controllers, which improve the operation of hybrid energy systems and reduce maintenance requirements.

The various optimization approaches used in literature, such as probabilistic, iterative and other classical approaches do not consider weekday, weekend and seasonal changes in demand. The optimization model proposed in this work takes into account the non-linearity of the operational costs associated with the hybrid systems, necessitating the use of quadratic programming. Heuristic techniques such as the one employed in this study are more efficient than classical techniques in terms of their ability to handle complex non-linear problems with many decision variables without extending computing time. The approach used in this work also has low computational requirements achieving results in reasonable time. The fuel costs and power flows are analyzed taking into account weekday, weekend and seasonal changes in demand. The emphasis of this work is, however, not on the optimization approach employed but on the power flow management. Daily energy consumption variations for weekdays and weekends are considered in order to compare the corresponding fuel costs and evaluate the operational efficiency of the hybrid system. Previous studies have assumed a fixed load and uniform daily operational cost, which can be extrapolated to get the monthly or yearly cost. However, the assumption is not accurate because of variations in consumer behavior patterns, hence a more practical daily operational cost is considered in this work. The model can assist solar energy practitioners or companies to give consumers accurate estimates of fuel costs they could expect to incur daily, seasonally or yearly.

The main role of the current hybrid energy management system is to control and optimize the interaction of various system components and control power flows within the system to provide a stable and reliable source of energy. The energy management system also has to deal with many conflicting objectives, such as minimizing battery wear and fuel costs, maximizing system components' service lives, providing a reliable system, maximizing operational efficiency and satisfying all operational constraints. The hybrid power system proposed in this thesis aims to satisfy the daily requirements of power of a rural Zimbabwean public clinic. The battery is used to store surplus energy generated by the RE sources. The DG is used to cover the imbalance whenever load demands cannot be satisfied by the RE sources and the battery. During the working process of the hybrid power system, RE usage is prioritized because of environmental and economic concerns, followed by the battery; the DG is the last choice since it consumes expensive fossil fuels and emits greenhouse gases. A dispatching

problem arises on scheduling uses of different components of the hybrid system, such that load demands are supplied, and fuel consumption can be reduced as much as possible.

The current work focuses on the minimization of the operational cost during a 24-hour period for a chosen diesel dispatch strategy. The work looks at the optimization of the operational cost of the PDB power supply system from an energy efficiency perspective, as one of the key characteristics of energy efficiency is the search for optimality. Energy efficiency is defined as the ratio of energy output and input and is summarized as having the following components: performance efficiency, operational efficiency, equipment efficiency, and technology efficiency. Operational efficiency is a system-wide measure, which is evaluated by considering the proper sizing and matching of different system components, time control and human coordination. Operational efficiency can be improved through mathematical optimization and optimal control approaches; for instance, pump operations [39] and conveyor belt systems [40] are investigated in literature. However, operational efficiency has not been explored in RE based systems such as the ones described in this work. In the current study the operational efficiency is measured in monetary terms so as to minimize the fuel cost during a 24-hour period. The objective of this work is also to illustrate the daily variation of demand and supply, as well as real operational issues in improving efficiency.

Unlike most similar works, this work focuses on the optimal dispatch of the various powers while minimizing operational cost and maximizing the utilization of renewable energy sources and simultanously considering battery life improvement by minimizing the charge-discharge cycles of the battery. Another effective approach for energy dispatching is MPC.

MPC is employed in this work owing to its advantages over the open loop approach and its capability to handle constraints of the system explicitly using a user-defined cost function. One advantage of MPC for energy dispatching over optimal control is that MPC is a closed-loop approach achieving better performance during a relatively long period when disturbances would possibly occur. Closed-loop models automatically adjust to changes in outputs due to external disturbance, measure states and give feedback to the optimization model repeatedly and hence the optimal solution is updated accordingly. For the PDB hybrid power system, a practical concern is that the battery must not charge and discharge simultaneously. A typical route to solving the dispatching problem for this situation is to design MPC for a switched model. Switched MPC approaches have been studied extensively [41, 42, 43];

however, current research is based on complicated switched predictive models, which may potentially render the optimization unsolvable in MPC design. This approach is beneficial to search for less complicated MPC strategies, hence its application to the hybrid system proposed in this thesis. In this thesis, a new adaptive switched MPC is proposed for the PDB hybrid power system to ensure that battery charging and discharging do not take place at the same time. The optimal dispatching problem is modeled into a control problem and solved by the approach of MPC, so that the closed-loop system could benefit from advantages such as feedback and prediction. The switched modes (charge and discharge) of the battery are described by switched constraints (instead of a switched state-space model), such that a unified linear multiple-input-multiple-output (MIMO) state-space model could be used to design a simple predictive model. Adaptive parameters with updating law are employed to estimate uncertain constant parameters of the battery. Simulation results demonstrate that, with the proposed switched MPC strategy, the energy efficiency of the closed-loop system is satisfactory.

A few researchers have applied this approach to the analysis of electric energy systems that incorporate intermittent resources. Also, the work done so far does not specifically apply the on-line methodology to the PDB or PWDB hybrid power supply options.

The results of this work enable consumers and practitioners to obtain an idea of the system operations and also to appreciate the need for optimal control of the system. Application of multi-objective optimization means that optimal decisions can be achieved in the presence of trade-offs between conflicting objectives. Varying weights and solving each multi-objective problem for its optimum result in various optimal solutions, depending on the weighting factors. Typically, there is an entire curve or surface of points, whose shape depicts the nature of the trade-off between different objectives. In this research, weights could be determined taking into account factors such as energy prices, environmental concerns, etc. However, in the absence of adequate data concerning such factors, cases with different weights are proposed to determine the overall tendency by considering fuel and battery wear cost while maximizing PV output. It would therefore be convenient to select appropriate weights if corresponding data are available. It is important to note that weight scheduling is still an open question in optimization.

From the above it is evident that there is a research gap that should be addressed to ensure

that the energy requirements of off-grid consumers are met fully at all times. The variable nature of RE sources which render them non-dispatchable, is complemented by dispatchable DGs and energy storage batteries, which is an important motivating aspect with regards to the use of hybrid energy systems such as the one considered in this thesis. Furthermore, maximization of the use of RE sources means that there is less use of fossil-based energy sources, hence the work addresses the global need to reduce greenhouse gas emissions. The optimization approach employed means that optimal use is made of the various hybrid system technologies. The main concern of this work is to design a reliable system that satisfies demand and minimizes the overall system operational cost. The role of such hybrid energy systems in providing energy to developing nations and remote areas, as highlighted in the preceding paragraphs should not be over-emphasized. Although a lot of work has been done on energy models, there is no one model that captures all aspects justifying the on-going works in various research communities. The multi-objective optimization used in this work also enables designers, performance analyzers, control agents and decision-makers who are faced with multiple objectives to make appropriate trade-offs, compromises or choices.

1.3 OPTIMIZATION AND MODELLING

Optimization is considered an effective tool for identifying optimal strategies in complex energy management systems. It entails obtaining the set of design parameters that maximizes a desired attribute or minimizes an undesirable attribute subject to a number of constraints. The levels of difficulty of optimization problems differ depending on the nature of the variables (continuous, discrete, integer), the existence of constraints (constrained, unconstrained), the nature of the objectives and constraints functions (linear, non-linear), the number of objectives (single-objective, multi-objective) and the convexity of the problem [44]. There are many well-documented optimization methods in literature [45, 46] and various optimization techniques for hybrid solar-wind systems such as graphic construction methods, probabilistic approach, iterative technique, artificial intelligence methods and multi-objective design, but no single method that can solve all problems has been reported. The complexity of the optimization problem increases as the number of optimization variables increases and this results in an increase in the time and effort required to solve the problem. It is therefore vital for designers to find the most effective optimization technique to select the optimum system configurations accurately and quickly. Mathematical optimization methods are designed to solve

specific types of problems, for instance, when applied to the right problem, a mathematical method can give an accurate optimal solution in a relatively short period. Linear and convex problems involving many variables can be effectively solved by an appropriate method and these methods can provide proofs for the optimality of the solution in these cases [47].

Optimization techniques to solve power system planning and operational problems have been an area of active research in many research communities. Optimal power flow is a generic term that is used to describe a broad class of problems that seek to optimize a specific objective function while satisfying constraints dictated by operational and physical particulars of the electrical system [48]. Non-linear programming has been applied to problems involving non-linear objective and constraint functions. These constraints may be made up of equality and/or inequality formulations. Formulations of this nature have been used for both real-time on-line and off-line operational problems. Linear programming has been applied to problems with constraints and objective functions that are linear. The simplex method and revised simplex methods have been effective for solving linear programming problems that include economic dispatch problems. Mixed integer programming handles linear programming problems in which the constraints involve variables restricted to being integers. The optimization problem may constitute a linear objective function that is subject to a combination of linear and and non-linear constraints with integer or discrete variables. Newton-based solutions have been applied to power system planning and operational problems and in this case the Kuhn-Tucker conditions, which are the necessary conditions of optimality, are achieved. They are generally used to solve non-linear problems that require iterative methods of solution and are favored for their quadratic convergence properties. Quasi-Newton and sensitivity-based methods have been used for solving real on-line power system planning and operational problems. Quadratic programming has been applied to many optimal power flow problems and this a special form of non-linear programming in which the objective function is quadratic with linear constraints. Interior point methods have been applied to linear, non-linear and quadratic programming, and have proven to be faster and superior methods [47, 49]. It is important to note that our research focus is not on inventing a new optimization algorithm, so whenever possible, we always make an effort to model the system into a quadratic optimization problem.

In this work, the RE sources are modeled as variable power sources controllable in the range of zero to the maximum available RE power for the 24-hour interval. The battery is modeled as

a storage entity with minimum and maximum available capacity levels. The DG is modeled as a controllable variable power source with minimum and maximum output power. In this way the constraints are all formulated as linear equalities or linear inequalities. Fuel consumption costs are modeled as a quadratic function of generator output power combined. In this thesis, the mathematical optimization method employed is the quadratic programming method.

An open loop optimal control optimization model is developed for a PDB off-grid power supply system with the objective of minimizing fuel costs during winter and summer seasons on weekdays and on weekends. The model is further developed to incorporate battery wear cost in order to cater for battery life. A wind model is then added to the original PDB open loop model and MPC techniques are applied to the optimal model. Discrete linear MPC is a control approach for a given system expressed as follows:

$$x(k+1) = Ax(k) + Bu(k), \tag{1.1}$$

$$y(k) = Cx(k), \tag{1.2}$$

where $x \in R^n$, $u \in R^m$ and $y \in R^l$ are states, inputs and outputs, respectively.

MPC is employed to solve the optimal control problem at each sampling instant. In the proposed MPC approach, the optimal control problem over the prediction horizon is repeatedly solved ($k = 1, \ldots, N - N_p + 1$). The optimal control problem, including the objective function and the set of constraints, is defined. The optimization variable is the sequence of power flows for each sampling period. At the kth sample, an optimal solution $[\overline{u}(k), \overline{u}(k+1), \ldots, \overline{u}(k+N_p-1)]^T$ can be obtained after solving the optimal problem. Only the first part of solution $\overline{u}(k)$ will be used in the current period. According to the proposed rules, the disturbance of input that applied to the system in the period $(k-1, k]$ can be computed. When the planning period gets shorter than the prediction period N_p, i.e. $k > N - N_p + 1$, the prediction period will be decreased by one at each sample.

1.4 RESEARCH AIM AND OBJECTIVES

This thesis investigates the optimal planning and operation of hybrid energy systems for off-grid applications. The aim is the development of an optimal power flow management system for the hybrid system for off-grid applications. The system control algorithm has to be robust

with the ability to handle various changes, by establishing new management criteria depending on information data and environmental changes. Such an algorithm will be designed to optimize and coordinate the power flow between the hybrid power system components in order to satisfy the load requirements completely. To illustrate the benefits of the energy management and system reliability offered by RE-based hybrid systems, optimization models are developed for specific cases considered in this thesis for minimizing system operational costs. The main objectives of this thesis are the following:

- Develop an optimization model for power flow between components of a PDB system in order to minimize fuel cost.
- Develop an optimization model for power flow between components of the system in order to minimize the fuel and battery wear costs.
- Develop a MPC model for power flow between components of a PWDB system in order to minimize system operational costs.

1.5 OUTLINE AND CONTRIBUTION OF THE THESIS

The contribution of this research is found in the following published works: Journal papers [50, 51, 52, 53, 54, 55] and conference papers [56] and [57] as listed under the publications section. The maim contributions of this work are as follows:

- Development of an optimal control and management platform for power flow in RE-based hybrid systems to ensure continuous power supply for the load demand.
- Addressing of challenges faced by remote or off-grid home-owners who are usually left with many decisions and little knowledge about the most cost-effective system for providing power to their homes and the expected operational costs through the development of an optimization model for power flow between components of the system in order to minimize the fuel and battery wear costs.
- Development of MPC models for power flow between components of a hybrid system in order to minimize system operational costs that has not been applied to such hybrid systems and is a more practical approach to the energy dispatching problem as it is

able to respond to system disturbances.

- Development of a model that can assist designers, performance analyzers, control agents and decision-makers who are faced with multiple objectives to make appropriate trade-offs, compromises or choices.

- Development of optimal dispatch models that minimize operational cost, maximize the utilization of renewable energy sources and simultaneously consider battery life improvement by minimizing the charge-discharge cycles of the battery.

- Development of models that can assist solar energy practitioners or companies to give consumers accurate estimates of fuel costs they could expect to incur daily, seasonally or yearly.

- Consideration of variable as opposed to fixed demand and also variation of RE sources, introduced as uncertainties to analyze system performance.

The author thus investigated control approaches to solving the developed models in order to cope with the intermittent nature of RE sources and uncertainties in demand; developed RE-based hybrid system models (PDB/PWDB) that minimize fuel cost and satisfy load demand and determined the optimal dispatch strategies for different seasonal load profiles; integrated battery wear cost into the model formulation with the ability to show practical battery operation and dynamic constraints, and investigated the usefulness of the developed models on a case study of a remote Zimbabwean site.

The thesis focuses on developing optimization frameworks for optimal planning and operation of off-grid RE-based hybrid energy systems using the mathematical optimization approach. The remaining chapters of the thesis are organized as follows:

Chapter 2 reviews the current state of modeling, optimization, and control studies of the PDB and PWDB hybrid systems in terms of what has been done by various authors and their applications. It reviews the system components such as the DGs, battery storage and solar and wind energy generation, as well as the methodologies for incorporating the data for power output calculations. Possible methods of modeling of these technologies are reviewed. The chapter explains the role of DGs in hybrid energy systems and the problems associated with

conventional constant speed DGs of low part-load efficiency and minimum loading. It also explains how variable speed types of DGs can overcome these problems and the advantages of using these generators in terms of fuel savings.

Chapter 3 considers the optimal control model of the PDB hybrid energy system considering seasonal variations in demand while minimizing fuel costs. The proposed hybrid system is composed of the PV system, battery bank and DG; the optimization model that includes the objective function, constraints and model parameters is developed. The model proposed considers the daily energy consumption variations for winter and summer weekdays and weekends in order to compare the corresponding fuel costs and evaluates the operational efficiency of the hybrid system for a 24-hour period. Annual average hourly radiation is also considered under the different load profiles. It presents an open loop model that gives a new dimension to the time correlation of intermittent renewable energy sources while minimizing fuel costs. A load-following diesel dispatch strategy is employed in the proposed model and the fuel costs and energy flows are analyzed. The results obtained are compared in terms of fuel savings achieved by the PDB hybrid model case and by the case where the DG satisfies the load on its own, for winter and summer days.

In Chapter 4, a new adaptive switched MPC strategy is designed for energy dispatching of a PBD hybrid power system proposed in the previous chapter, to ensure that the battery cannot charge and discharge at the same time. The distinguishing feature of the proposed switched MPC is that, new switched constraints are constructed to describe the different modes (charging and discharging) of the battery, such that the burden of using a switched MIMO state-space model could be circumvented. Based on optimization with the switched constraints, receding horizon control is utilized to obtain the dispatching strategy for the hybrid power system. The performance of the closed-loop system with the proposed switched MPC is verified by simulation results.

In Chapter 5 the model proposed in the previous chapters is developed further to incorporate battery wear cost and penalizing factors for the conflicting objectives. An optimal energy management model of a solar PDB hybrid power supply system for off-grid applications is presented. The aim is to meet the load demand completely while satisfying the system constraints. The proposed model minimizes fuel and battery wear costs and finds the optimal power flow, taking into account PV power availability, battery bank SOC and load power

demand. The optimal solutions are compared for cases when the conflicting objectives (fuel and battery wear costs) are weighted equally and when a larger weight is assigned to battery wear. The results are important for decision makers, as they depict the optimal decisions considered in the presence of trade-offs between conflicting objectives.

In Chapter 6, the model is further developed to incorporate wind energy. An energy dispatch model that satisfies the load demand, taking into account the intermittent nature of the solar and wind energy sources and variations in demand, is proposed and MPC techniques are applied in the management and control of such a power supply system. The emphasis is on the co-ordinated management of energy flow from the battery, wind, PV and DGs when the system is subject to disturbances. The results of the open loop model and the closed-loop model are compared in terms of the model capability to attenuate against uncertainties and external disturbances in demand and renewable output. Diesel consumption is also compared for winter and summer seasons. The results indicate that the developed model can achieve a more practical estimate of the fuel costs, reflecting variations in power consumption behavior patterns for any given system.

In each of chapters 3, 4, 5 and 6, the methodologies employed and modeling of power generated by each of the generation source and the battery bank models are discussed. The objective functions and constraints are formulated for each optimization problem. The simulation results for each case are discussed. Chapter 6 summarizes the results of the thesis and conclusions are drawn from the various results discussed in chapters 3, 4, 5 and 6 and the rest of this thesis.

1.6 CONCLUSION

An overview of the thesis has been presented. In the next chapter a review of related literature will be done to reveal the knowledge and ideas that have been established on the topic by various authorities. Hybrid energy sub-systems, which include solar PV, wind, DGs and battery storage will be taken into consideration. Various RE-based hybrid energy systems and the methodologies employed will be discussed.

CHAPTER 2

OVERVIEW OF HYBRID ENERGY SYSTEMS

2.1 INTRODUCTION

This section makes a review of literature pertaining to energy optimization and management of RE-based hybrid power systems for off-grid applications. The various energy system components, which include solar PV, wind, DGs and battery storage, are reviewed. The merits and demerits of the various technologies are revealed, explaining the motivation for the usage of technologies chosen for this work. The methodologies used by various authors to model the hybrid energy system components, depending on the data available, are explored. Part of the literature is obtained from authors' published papers [50, 51, 53, 55].

2.2 HYBRID ENERGY SYSTEM CONFIGURATION

The RE-diesel-battery hybrid power supply system proposed in this study is made up of the following main sub-systems: RE systems (PV and wind), the battery storage system and the DG. Controllers and inverters have been left out for simplicity purposes and are assumed to be 100% efficient in this work. Priority for power supply is given to RE sources. The load is met by the RE generators and the battery comes in and discharges when the RE output is not enough to meet the load if it is within its operating limits. If RE output is above the load requirements, the battery is charged by the RE generator(s). The DG comes in when the RE generators and/or the battery cannot meet the load but does not charge the battery. Fig. 2.1 shows the proposed hybrid energy management system. A

supervisory system controller is incorporated just to show the principle of energy management in terms of the input or database, the data base support and the output. The main role of the hybrid energy management system is to control and optimize the interaction of various system components and control power flows within the system to provide a stable and reliable source of energy.

Sources:www.orientalcopper.com;www.gentek.co.za;www.georator.com;
www.aiosystems.com

2.2.1 Solar energy

Solar PV is an established technology that is being used throughout the world to supply autonomous power for many off-grid applications. There is therefore a need for accurate estimates of available solar irradiation, as it is site-specific and crucial in the optimal design of conversion systems for various applications. Many meteorological or radiometric stations measure global and diffuse irradiation received on horizontal surfaces, but data on inclined surfaces are not available and are estimated using different models from those measured on horizontal surfaces. Radiation on a horizontal surface is the only radiation record available at many meteorological stations, especially in developing countries. Total radiation incident on a tilted plane consists of three components: beam radiation, diffuse radiation and reflected radiation from the ground. The direct and reflected components are easily computed with good accuracy by using simple algorithms, but the nature of the diffuse component is more complicated and the required algorithms need to be assessed and evaluated. Various models have been developed for this purpose and some of these models are available in literature [58, 59, 60, 61]. The methods used to estimate the ratio of diffuse solar radiation on a tilted surface to that on a horizontal are categorized as isotropic and anisotropic models. The isotropic models assume that the intensity of diffuse sky radiation is uniformly distributed over the sky dome, implying that the diffuse radiation incident on a tilted collector depends on the fraction of the sky dome seen by the collector. The anisotropic models assume the anisotropy of the diffuse sky radiation in the circumsolar region and the isotropically distributed diffuse part from the rest of the sky dome[62, 63]. The circumsolar model [64] applies to clear and cloudless skies and predicts the sky diffuse radiation component. Another isotropic model of Liu and Jordan [65], [66] incorporates the intensity of sky diffuse radiation and assumes this

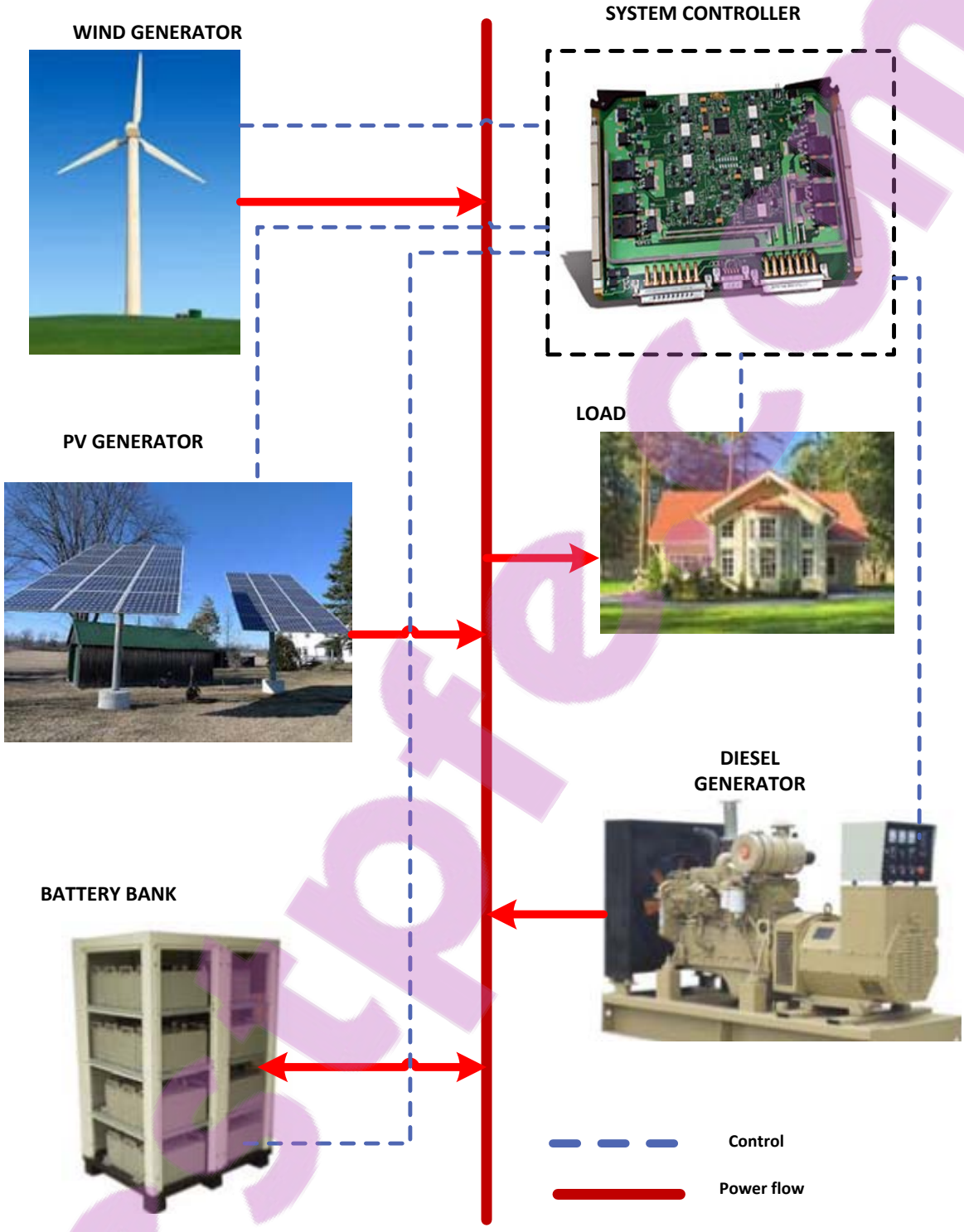

Figure 2.1: RE hybrid power supply system configuration

to be uniform over the sky dome. The anisotropic model of Klucher [67] modified the Temps and Coulson [68] model by incorporating the effect of cloudy skies. The Hay [69] model is composed of an isotropic and circumsolar component and predicts the radiation on a tilted

surface from the available data on a horizontal surface. The hourly solar irradiation incident on the PV array is a function of time of day, expressed by the hour angle, the day of the year, the tilt and azimuth of the PV array, the location of the PV array site as expressed by the latitude, as well as the hourly global solar irradiation and its diffuse fraction [70, 71, 72]. The actual expression relies on the sky model, which is a mathematical representation of the distribution of diffuse radiation over the sky dome presented in [70].

In this study, the simplified isotropic diffuse formula suggested in [71] is used. The hourly solar irradiation incident on the PV array is given by:

$$I_{pv} = (I_B - I_D)R_B + I_D. \tag{2.1}$$

In (2.1), I_B and I_D are respectively the hourly global and diffuse irradiation in kWh/m^2. R_B is a geometric factor representing the ratio of beam irradiance incident on a tilted plane to that incident on a horizontal plane. Monthly average hourly meteorological data, global irradiation, diffuse irradiation and ambient temperature are used as inputs in evaluating (2.1), (2.2) and (2.3) of the performance simulation model. The evaluation is performed at the mid-point of each hour of the day, on the "average day" of each month as defined in [70].

The instantaneous radiation incident on the PV array, I_{pv}, can be obtained [71, 73] as:

$$I_{pv} = I_{bn}\frac{cos\theta_{pv}}{cos\theta_z} + \frac{1}{C}I_d, \tag{2.2}$$

where I_{bn} represents the direct irradiance at normal incidence, θ_{pv} the angle of incidence of direct irradiance on the PV array, C the concentration ratio (=1 for a flat-plate collector) and I_d the diffuse irradiance. If it is assumed that all radiation in an hour is concentrated at the middle of the hour, the same expression also gives the hourly irradiation incident on the PV array, with θ_{pv} measured at the middle of the hour. Hourly radiation data or data resolved into the beam and diffuse components are usually not available from many meteorological stations, especially in developing countries [73]. Records available from most meteorological stations are those for monthly average daily hemispherical or global irradiation on a horizontal plane, H_h. In such circumstances, the procedure described below could be employed. The monthly average daily diffuse irradiation, H_d, can be predicted from H_h by applying any of the many correlations that relate the ratio H_d/H_h with monthly average clearness index, K_h given by various authors including [74, 75, 76, 73]. The following correlation for climates like

that of Zimbabwe is used in this work [77, 73]

$$H_d/H_h = 1.0294 - 1.14K_h \quad \text{for } 0.47 \prec K_h \prec 0.75 \tag{2.3}$$

$$= 0.175 \quad \text{for } K_h \geq 0.75. \tag{2.4}$$

H_d can be calculated by considering that:

$$K_h = H_h/H_o, \tag{2.5}$$

where H_o is the monthly average extraterrestrial radiation. H_h and H_d are then resolved into monthly average hourly values, I_H and I_D respectively, by using conversion factors, r_h and r_d [71], as follows [73]:

$$I_H = r_h H_h \tag{2.6}$$

and

$$I_D = r_d H_D. \tag{2.7}$$

The formulae for the above factors, which are functions of sunset hour angle, are cited by various authors [70, 71].

The direct irradiance at normal incidence can then be expressed in terms of the radiation on a horizontal plane (hemispherical) and diffuse radiation as:

$$I_{bn} = (I_h - I_d)\frac{cos\theta}{cos\theta_z}, \tag{2.8}$$

where θ_z is the zenith angle. When the monthly average hourly irradiation values are replaced by the hourly (instantaneous) irradiation values, the following expression is obtained:

$$I_{pv} = (I_h - I_d)\frac{cos\theta_{pv}}{cos\theta_z} + I_D. \tag{2.9}$$

A geometric factor representing the ratio of beam irradiance incident on a tilted plane to that incident on a horizontal plane is represented by R_B. In the case of a fixed flat-plate collector located at latitude, ϕ, with azimuth equal to zero and angle of tilt β, the ratio is given by [73]:

$$R_B = \frac{cos\theta_{pv}}{cos\theta_z} = \frac{cos(\phi - \beta)(cos\omega - cos\omega_s')}{cos\theta(cos\omega - cos\omega_s)}, \tag{2.10}$$

where ω is the hour angle and ω_s' is the sunset hour angle. The angle ω_s' is given by:

$$cos\omega_s' = -tan(\phi - \beta)tan\delta, \tag{2.11}$$

for the Northern Hemisphere and

$$cos\omega_s' = -tan(\phi + \beta)tan\delta, \tag{2.12}$$

for the Southern Hemisphere, where δ is the sun's declination angle. For a solar array with tilt, β, equal latitude, ϕ, as assumed in this thesis, R_B is evaluated with $\omega_s' = 0$ [73]. The fact that the operating temperature plays a crucial role in the PV conversion process is well documented in literature. The efficiency, η, of a PV cell is actually a function of cell temperature and array irradiation [78, 73]. It has been shown that PV cell performance decreases with increase in temperature, as carrier concentrations increase, resulting in increased internal carrier recombination rates. There are many correlations in literature, as given by [78], that express the PV cell temperature as a function of weather variables such as the ambient temperature, wind speed, solar radiation, material and system-dependent properties such as glazing-cover transmittance and plate absorbance. The temperature dependence of the electrical efficiency of a PV cell can be traced to the fundamental power, P, equation which can be used to investigate the effect of temperature on the current, I, and the voltage, V, output of a PV cell as follows:

$$P_m = I_m V_m = (FF) I_{sc} V_{oc}, \tag{2.13}$$

where subscript m refers to the maximum power point in the cell's I-V curve, FF is the fill factor, and subscripts sc and oc denote open-circuit and short-circuit values respectively. Investigations by various authors have shown that V_{oc} and FF decrease substantially with temperature while the I_{sc} increases slightly, leading to a linear relation in the general form:

$$\eta_{pv} = \eta_{TR}[1 - \beta_R(T_C - T_R) + \gamma log_{10} I_{pv}], \tag{2.14}$$

where η_{pv} is the PV module efficiency measured at reference cell temperature, T_R, i.e., under standard test conditions (25°C). β_R is the temperature coefficient for cell efficiency (typically 0.004–0.005/°C) and this is relatively constant for the operating temperature ranges

encountered in flat-plate arrays [79, 73], I_{pv} is the average hourly solar irradiation incident on the module at nominal operating cell temperature, NT ($0.8kWh/m^2$); T_C is the PV module temperature and γ is a radiation-intensity coefficient for cell efficiency, which is often assumed to be zero by many authors [79, 80], reducing the traditional cell efficiency to:

$$\eta_{pv} = \eta_{TR}[1 - \beta_R(T_C - T_R). \tag{2.15}$$

The temperature of the module is not readily available and in many of the correlations in literature, it has been replaced by the nominal operating cell temperature. By adding and subtracting the ambient temperature, T_A, to and from the two temperature terms in the expression above and changing the parentheses of parameters measured at the nominal operating cell temperature to NT, and making some assumptions according to [73], the following expression is obtained:

$$\eta_{pv} = \eta_R[1 - 0.9\beta(\frac{I_{pv}}{I_{pv,NT}})(T_{c,NT} - T_{A,NT}) - \beta(T_A - T_R)], \tag{2.16}$$

where $T_{C,NT}$ (typically 45°C) and $T_{A,NT}$ (20°C) are, respectively, the cell and ambient temperatures at NT test conditions. The hourly energy output from the PV generator, P_{pv}, of a given area, A, is therefore obtained by:

$$P_{pv} = \eta_{pv} A_c I_{pv}. \tag{2.17}$$

The power output of a PV module also depends on the type of mounting used. Solar module mountings can be fixed, adjustable or tracking. The above methodology can be applied to both the fixed and adjustable types. The fixed type is the most common, as it is the simplest and least expensive type; the array is completely stationary at a particular tilt angle facing the equator. Various rule of thumb tilt angle adjustments have been proposed in literature in an effort to increase the array output throughout the year [62, 81]. Some authors have used mathematical optimization approaches to optimize the tilt angle [82]. The angle of inclination of an adjustable type of mounting can be changed twice or more times during the year to cater for the lower angle of the sun in winter as the earth turns around the sun, causing seasonal changes. This type has proven to produce increased output compared to the fixed type. The third type is the tracking one, which follows the path of the sun during the day to maximize the solar radiation that the solar array receives. This type can be a single-axis

tracker that tracks the east-to-west or a two-axis tracker, tracking the daily east-to-west and north-south movements of the sun and the seasonal declination movement of the sun. The latter type is the most efficient but this is achieved at a cost.

Another way of maximizing module power output is by employing a Maximum Power Point Tracking (MPPT) system. This is an electronic system that operates the PV module and enables it to produce all the power it is capable of producing. The MPPT system varies the electrical operating point of the modules so that the modules are able to deliver maximum available power. This system can be used together with a mechanical tracking system. The additional power harvested from the modules is made available as increased battery charge current. When a conventional charge controller charges a discharged battery, it just connects the modules directly to the battery, forcing the modules to operate at battery voltage, which is typically not the ideal operating voltage at which the modules are able to produce their maximum available power. All types of solar installations can benefit from using MPPT technology as they would be able to operate at operating voltages.

The power output of the PV array is also given by the expression [83] :

$$P_{pv} = N_{pvp}.N_{pvs}.V_{pv}.I_{pv}.F_c.F_o, \tag{2.18}$$

where N_{pvs} is the number of series-connected modules, N_{pvp} the parallel-connected modules; and F_c and F_o are the connection and other losses respectively. This is very useful for practical applications.

The power of the PV array is calculated by [84] as:

$$P_{pv} = N_{pvp}.N_{pvs}.P_{mod}.\eta_{MPPT}.Fo, \tag{2.19}$$

where P_{mod} is the module maximum power and η_{MPPT} the efficiency of the MPPT, usually taken as 95%.

2.2.2 Wind energy

Wind energy is one of the RE sources that has huge potential and has been in use for centuries. Wind is the movement of air from high-pressure areas to low-pressure areas caused

by uneven heating of the earth's surface by the sun. Wind will always exist as long as solar energy exists. Ancient mariners made use of wind to sail to distant lands. Wind power has been used by farmers to pump water and for grinding grain. Currently wind energy is mainly converted to electrical energy to meet critical energy needs. It is one of the fastest growing sources of electricity and one of the fastest growing markets. The wind turbines harvest kinetic energy and convert it into usable power, which can provide electricity for residential, commercial and industrial purposes. Wind turbines are a mature technology that has been used by many customers, utilities and independent power producers to produce electricity from wind energy. Because of the space requirements of WGs, they are more suitable for remote area applications [85] and for supply reliability; they are usually incorporated in a hybrid system. Wind farms are a common feature in countries where there is vast land and good wind resources.

There are basically two designs for modern wind turbines, namely the horizontal axis and vertical axis. Vertical axis turbines, whose axis of rotation is vertical or perpendicular to the ground, have the advantage of being omnidirectional (powered by wind coming from all directions), with gears and the generator at the tower base. They are, however, disappearing from the mainstream commercial market owing to the weight and cost of the transmission shaft, low starting torque, low efficiency and less power production owing to less wind speed closer to the ground, compared to horizontal axis designs. Attempts are currently being made to commercialize vertical axis design for building-rooftop applications [86]. The gearbox and generator in vertical axis designs can be lowered to the ground, making construction costs lower and maintenance easier. Moreover, there is no need for the turbines to point towards the wind, making them ideal for installations in areas with inconsistent wind patterns. Horizontal axis wind turbine, whose axis of rotation is horizontal, or parallel with the ground, dominate the wind industry. While horizontal axis wind turbines are common in big wind applications, vertical axis turbines are found in small and residential wind applications. The advantage of horizontal wind turbines is that they can produce more power from a given amount of wind, though they are generally heavier and do not perform well in turbulent winds. In this work, small horizontal axis turbines with three blades are considered.

The power output of wind a turbine at a given site depends on wind velocity at hub height and turbine speed characteristics. As the standard height or reference for wind speed measurements for wind resource assessment is 10 m above the effective ground level, there is a

need to determine the wind speed at hub height. This is important because it is the wind speed seen by the rotor of the wind turbine (hub height wind speed) that determines the actual power radiated by a particular turbine. The most common expression used for this purpose is the power-law equation, expressed as [13, 87]:

$$v_{hub} = v_{ref}.\left(\frac{h_{hub}}{h_{ref}}\right)^{\varphi}, \tag{2.20}$$

where v_{hub} is the wind speed at the desired height h_{hub}, v_{ref} is the wind speed at the reference height h_{ref} and φ is the power law exponent, which represents the ground surface friction coefficient. The exponent is a function of height, time of day, season, nature of the terrain, wind speed, and temperature. It is low for smooth terrains, high for rough terrains and the values for typical classes are given in [87]. The coefficient ranges from $\frac{1}{7}$ to $\frac{1}{4}$. $\frac{1}{7}$ is used in this work, which is typical for open land. The v_{hub} obtained is then used in the wind power equation.

The power output of a wind turbine depends on the wind speed pattern at the specific location, air density, rotor swept area and energy conversion efficiency from wind to electrical energy. Various models are used to simulate the wind turbine power output [88, 87]. The mechanical power, P, in a moving mass of air is given by:

$$P = 0.5\rho AV^3, \tag{2.21}$$

where ρ is the air density in kg/m^3, A is the area swept by rotor blades in m^2, and V is the air velocity (v_{hub}) in m/s. It is important to note that ρAV represents the mass flow rate m per second, and ρ can be calculated using the ideal gas law :

$$\rho = \frac{P_{ab}}{R_g}A_T, \tag{2.22}$$

where P_{ab} is the absolute pressure in N/m^2, R_g is the gas constant, and A_T is the absolute temperature. The actual power that can be extracted is much lower owing to the fact that the air mass would be stopped completely in the intercepting rotor area for complete energy extraction. The theoretical maximum power that can be extracted from a wind turbine is 59.3%, (Betz limit) of the power in the wind [89, 90]. The power output, P_w, of a wind turbine is given by the expression [88]:

$$P_w = 0.5\rho C_p AV^3, \tag{2.23}$$

where C_p is the coefficient of performance of the turbine expressed as:

$$C_p = 0.5\left(1 + \frac{V_2}{V_1}\right)\left(1 - \left(\frac{V_2}{V_1}\right)^2\right). \tag{2.24}$$

Its value for each wind speed, V_i, can be obtained by:

$$C_p(V_i) = \frac{P_w(V_i)}{P(V_i)}. \tag{2.25}$$

The actual power, P_w, extracted by rotor blades depends on the upstream and downstream wind velocities, V_1 and V_2, respectively. The average of these velocities is used in the mass flow rate equation since in the macro-scope perspective, air velocity is discontinuous at the plane of the rotor blades.

The turbine power performance curve, is characterized by three speeds, namely, the cut-in speed, nominal or rated speed, and cut-out speed for a pitch-regulated turbines. When the speed is below the cut-in speed, the output power is zero and the rotor cannot be loaded. At the nominal speed, the power output is at the rated value. The output power remains constant as wind speed increases by using power control mechanisms until the cut-out speed is reached, at which point, the turbine will be turned off to prevent any damage to the mechanical structure. After the cut-in speed, the power output increases as the speed increases until the turbine reaches its maximum capacity. Variable-speed wind turbines have the capability of tracking the locus of maximum power, corresponding to the locus of maximum coefficient of performance, as wind speed varies by adjusting the speed of the turbine [89, 90]. Typical wind output characteristics are found in various texts [88].

The hub height velocity is used in the output power model to calculate the power generated by the wind turbine generator. The models used to describe the performance of WGs are different since different WGs have different power output performance curves. Various authors have developed different models for calculating the power output by making various assumptions and assuming that the turbine power curve has a linear, quadratic or cubic form [89, 90]. The general expression used is as follows:

$$P_w = \begin{cases} P_r \frac{V^k - V_{in}^k}{V_r^k - V_{in}^k}, & (V_{in} \leq V \leq V_r) \\ P_r, & (V_r \leq V \leq V_{out}) \\ 0, & (0 \leq V_{in} \text{ and } V \leq V_{out}) \end{cases} \tag{2.26}$$

where V is the wind speed at the hub height, k is the Weibull shape parameter, P_r is the rated electrical power; V_{in} is the cut-in wind speed; V_r is the rated wind speed and V_{out} is the

cut-off wind speed. Others have simplified models for wind speeds higher than the rated speed and a quadratic function has been used by [91]. Authors such as [90] have approximated the power curve with a piecewise linear function with nodes. The following expression is useful if the power characteristics of the particular wind turbine are provided [92] and [93]:

$$P_w = \begin{cases} 0, & (V \leq V_{in} \text{ or } V \geq V_{out}) \\ a_1V^3 + b_1V^2 + c_1V + d_1 & (V_{in} < V < V_1) \\ a_2V^3 + b_2V^2 + c_2V + d_2 & (V_1 < V < V_2) \\ \quad \ldots\ldots & \\ a_nV^3 + b_nV^2 + c_nV + d_n & (V_{n-1} < V < V_r) \\ P_r, & (V_r < V < V_{out}) \end{cases} \tag{2.27}$$

where n is the number of cubic spline interpolation functions corresponding to $n+1$ value couples (speed, power) of data provided by the manufacturers, and a, b, c and d are the polynomial coefficients of the cubic spline interpolation functions, which depend on the wind turbine generator type. The mathematical model adopted in this work to convert hourly wind speed to electrical power is as proposed by [88]:

$$P_w = 0.5\eta_w.\rho_{air}.C_p.A.V^3, \tag{2.28}$$

where η_w is the WG efficiency as obtained from the manufacturer's data.

2.2.3 Diesel generator

DGs have been used widely to supply power to isolated and remote areas where there is no grid connection, owing to their affordability and dispatchability, as they have low initial capital costs and can generate power on demand. These systems can be operated with or without battery storage. The major disadvantages of these systems are that they have high operational and maintenance costs and negative environmental impacts. RE sources and battery storage systems have been incorporated in DG-based hybrid systems in an effort to reduce the the ever rising fuel costs. In recent years, RE-based hybrid systems have dominated the market, with DGs as back-up systems to ensure continuous supply reliability. In RE-based systems, DGs can be directly connected to the load, in which case the rated capacity of the generator must be at least equal to the maximum load. If the main purpose of the DG is to charge the battery, then the current produced by the generator should not be greater than CAh/5 A, (CAh is the ampere hour capacity of the battery). Sizing the DG for maximum or peak power entails less efficiency when the load ratio is low.

Two main types of generators used in hybrid applications are the constant speed DG and the variable speed DG. Constant speed type DGs have been favored for a long time due to their low initial cost, however, if designed for peak power power, they operate at partial load for most of their operating life. Specific fuel consumption characteristics of a typical diesel engine show that a DG must be operated above a certain minimum load level in order to maintain efficiency and to reduce the possibility of premature failures. These operating limits are normally specified by the manufacturer range between 30% and 50 % of the rated power to prevent premature ageing of the engine and inefficient burning of fuel [94]. Generator units generally perform best when operated near their rated output. The generator efficiency decreases as the load decreases and if it is run for long periods at very low loads, significant maintenance problems can occur, including wet stacking. At supervisory control level, the rigid operational range of the constant speed DGs reduces system flexibility. Variable speed DGs, on the other hand, are on the expensive side owing to the incorporated embedded controls, but can be operated between the sub-synchronous and super-synchronous speeds that give efficient operation. They are capable of using optimum speed for a particular output power, which results in higher efficiency of the generator operation. They can thus operate at relatively low speeds for low power demand and vice versa and at lower fuel consumption compared to the constant speed type [94]. The variable speed type DG has been used in [94] for grid connected applications. A PV-diesel system incorporating a variable speed DG has been proposed in [95], as a feasible alternative of power supply system for remote area applications without relying on the energy storage component. In this work a variable speed Rush generator type is employed in which an electronic control system is used to vary the output by sensing the load and sending an electrical signal to the fuel injection system to adjust the fuel supply and engine revolutions in response to the load. The advantage of this type of generator is its ability to supply the required power output at any given time [50, 51]

In many RE-based applications, such as the one in this thesis, DGs are incorporated in the hybrid power supply systems as back-up and are usually required to cover the load at times when the RE and the battery cannot meet the load [96]. The manufacturer of the DG usually recommends the DG operating limits. The maximum efficiency of a DG corresponds to the rated power of the DG, therefore the DG has to be operated between the rated power and

specified minimum value [12, 97, 46] as represented by the following constraint:

$$P_1^{\min} \leq P_1(t) \leq P_1^{\max}. \tag{2.29}$$

A variable speed DG is employed in this thesis because of its lower fuel consumption compared to the constant speed type and its ability to use optimum speed for a particular output power, resulting in higher efficiency of the generator operation, as explained in preceding sections. In this way, the engine is able to operate at relatively low speed for low power demand and vice versa [98, 99].

2.2.4 Battery storage

The intermittent and unpredictable nature of RE sources, the need to minimize fuel costs and the need to have continuous power supply to the load necessitate the incorporation of storage systems in RE-based hybrid power systems. Various types of energy storage technologies are available on the market such as flywheels, magnetic energy storage, super-conducting magnetic energy storage, super-capacitors, pumped hydro storage, hydrogen fuel cells and batteries. The choice of storage technology however, depends on many factors including cost, reliability, life span, environmental impact, efficiency and technical maturity of the technology as well as the type of project and the people involved [100]. The main purposes of storage systems in RE hybrid energy systems are to store energy during times of excess production, supply energy to the load during times of low generation and maintain stability within the system. Battery technology is used in this work and there are many type of batteries on the market that could be used in energy systems such as, zinc bromine, sodium sulphur, nickel cadmium, lithium ion and lead acid batteries. In order to determine which type of battery technology to use, a number of factors must be considered as well, such as maturity of the technology, DoD of the battery, cost, charge/discharge cycles, self-discharge and efficiency.

The lead acid and nickel cadmium batteries are the most technologically advanced of the types mentioned above, but lead acid batteries are easier to use and are cheaper. Lithium ion batteries have high efficiency and a long life span at high DoDs, but their high cost limits their usage especially in large scale applications. Sodium sulphur battery usage is also limited by the high cost involved in addition to the need to maintain a temperature of 300°C for optimal utilization. Nickel cadmium batteries, on the other hand, have an

excellent life span with 100% DoD, but they exhibit very high self-discharge rates and are therefore less ideal for long-term energy storage. Zinc bromine batteries are still immature in terms of technology and age and this hinders their application in off-grid systems [100, 101]. Considering the above reasons, lead acid batteries are chosen for use in this work owing to the fact that they have been used in many off-grid applications, are the cheapest and most mature type of battery technology, though their maintenance requirements and shorter life span are areas that still need to be improved [102]. When compared with other battery technologies, lead acid batteries are considered the best option for isolated hybrid RE systems where minimization of costs is an important aspect.

Batteries in RE-based off-grid systems are subject to varying operating conditions and they form a large part of the capital investment, hence the importance of managing the system to ensure that the maximum life span of the battery is improved by controlling the charging and discharging cycles. Modeling and simulation of these batteries aim to analyze their performance in the hybrid system, and to enable the optimization so as to minimize the overall system operating costs. Modeling of these storage systems can be challenging owing to the number of parameters to be considered, such as the internal resistances, voltages, capacitance, charge/discharge rates, SoC, operating temperatures and other parameters that are not constant. Various authors have adopted various complex to simple methodologies for modeling batteries by instituting various assumptions. Since batteries in off-grid applications are exposed to various operating conditions, some conditions must be considered in order to improve their life span, such as ensuring that they operate within the minimum and maximum limits of SoC as dictated by the manufacturers, and not allowing them to stay at a low SoC for long periods of time, as well as minimizing the charge/discharge cycles.

In a hybrid set-up with PV, DG and battery, the power output from the PV and the load demand at given a hour t, determine the charge or discharge power into and out of the battery bank. t is an integer representing the t^{th} hour interval used in this work. The SoC of the battery bank at any hour t, $B_C(t)$, depends on the SoC at the previous hour $B_C(t-1)$. The following conditions need to be taken into consideration for energy flows from $t-1$ to t: At any given hour the battery SoC will be given by the expression:

$$B_C(t) = B_C(t-1) + \eta_C P_3(t) - \frac{1}{\eta_D} P_4(t), \tag{2.30}$$

in which, η_C is the battery charging efficiency, η_D is the battery discharging efficiency, and

$P_3(t)$ and$P_4(t)$ are the powers accepted or discharged by the battery at time t.

The available battery bank capacity must not be less than the minimum allowable capacity $B_C^{\min}$ and must not be higher than the maximum allowable capacity $B_C^{\max}$ [103, 99]. The SoC of a battery is simulated as follows [46] :

$$SoC(t+1) = SoC(t).(1-\sigma(t)) + \frac{I_b(t).\Delta t.\eta_c}{C_b}, \tag{2.31}$$

for the charging process and,

$$SoC(t+1) = SoC(t).(1-\sigma(t)) - \frac{I_b(t).\Delta t.\eta_c}{C_b}, \tag{2.32}$$

for the discharging process, where $I_b(t)$ is the charging or discharging current, C_b is the nominal battery capacity (A h), $\sigma(t)$ is the hourly self-discharge rate, which is determined by the accumulated charge and the battery state of health, and is approximately 0.02% [46, 104]. This value is neglected in most work as it is very small.

The SoC of the battery is also expressed as [105, 96]:

$$SoC(t) = SoC(t-1).(1-\sigma(t)) + \frac{P_b(t)}{V_{bus}}.\eta_c.\Delta t, \tag{2.33}$$

where $P_b(t)$ is the battery bank power at any given moment and V_{bus} is the nominal operating DC bus voltage.

Modeling of the lifetime characteristics of battery energy storage systems is a vital aspect of hybrid power system simulation that has not been fully considered in many RE-based hybrid energy management optimization studies [106]. The uncertainty associated with the expected lifetime of the batteries used in RE-based hybrid energy systems makes the estimates of cost of energy of the systems uncertain, as the life cycle cost of the batteries is one of the significant hybrid system expenses. This makes modeling of battery lifetime characteristics an important aspect of hybrid power system simulation.

There are two common lead acid battery lifetime models, namely post-processing models and performance degradation models. Among these there are also numerous methods for calculating the lifetime consumption, of which the most commonly used are the Ah-throughput and the cycle-counting methods. In this work the Ah-throughput counting method which assumes that an amount of energy can be cycled through a battery before it requires replacement is used. The estimated throughput (the total throughput over a battery bank lifetime),

obtained mostly from the DoD vs. cycles to failure curve provided by the manufacturer, is obtained by getting the average throughput of the product of the nominal battery capacity, at the specific DoD being considered and the cycles to failure to the specific depth of discharge. The cycles to failure, and specific DoDs are specified by the manufacturer[107].

2.3 HYBRID ENERGY SYSTEM SIZING

Proper sizing of components of a hybrid energy system is an important factor for its technical and economic feasibility. This entails determination of the PV generator capacity (number of PV panels), WG capacity (number and size of wind turbines), DG capacity and battery storage capacity required for the stand-alone system. This is not an easy task, as this involves formulating one or more optimization problems, selecting an objective function and identifying associated constraints. The problem is further complicated by non-linear characteristics of system components, the intermittent nature of RE sources (e.g. solar or wind), and the number of optimization variables and design constraints [108]. Owing to the system complexity, many sizing methodologies have been developed and applied in the design of hybrid energy systems. Optimization techniques for hybrid energy system sizing work, such as particle swarm optimization, genetic algorithm and simulated annealing, have been reported in various research works [13, 108].

Sizing tools such as HOMER, LINDO, Hybrid Power System Simulation Model (HYBRID2), Dividing Rectangles (DIRECT), General Algebraic Modeling System (GAMS), and many other commercial software tools have been used in hybrid system designs [109, 110]. Other sizing methods found in literature, include [108] the yearly monthly average sizing method; in which the sizing is based on the average annual monthly solar and wind data; the worst case scenario or most unfavorable month method in which data for the worst case month are used for sizing and the loss of power supply probability method, which portrays the probability that an insufficient power supply results when the system is unable to satisfy the load demand. The worst case scenario method gets more complex when both wind and solar generators are hybrid components, as in most cases the month most unfavorable in wind is favorable in irradiation and the system should be sized using both unfavorable irradiation and unfavorable wind months. A design tool for the system sizing was developed by defining the hybrid system design space by generating a set of system sizing curves that plot PV array

size required to attain a prescribed loss of load fraction, against battery size, for different discrete values of DG size. The sizing curves were generalized for all sizes of daily loads with the same diurnal profile by representing the hybrid system component sizes by dimensionless variables [111].

2.4 CASE STUDY

This work is based on a case study of a remote community in Zimbabwe with a PV-Diesel-Battery system. PV and battery systems were integrated into the diesel only system in order to minimize fuel and maintenance and also to make use of environment friendly solar technology. The techno-economic analysis was done in [111]. In this work a variable type of generator is employed and the possibility of incorporating wind energy explored. The meteorological data was obtained from a nearby weather station. The I_{pv} values are obtained from measured meteorological data of hourly global and diffuse radiation. Annual average hourly radiation for the year 2005 for the site is as shown in the following figure: There are

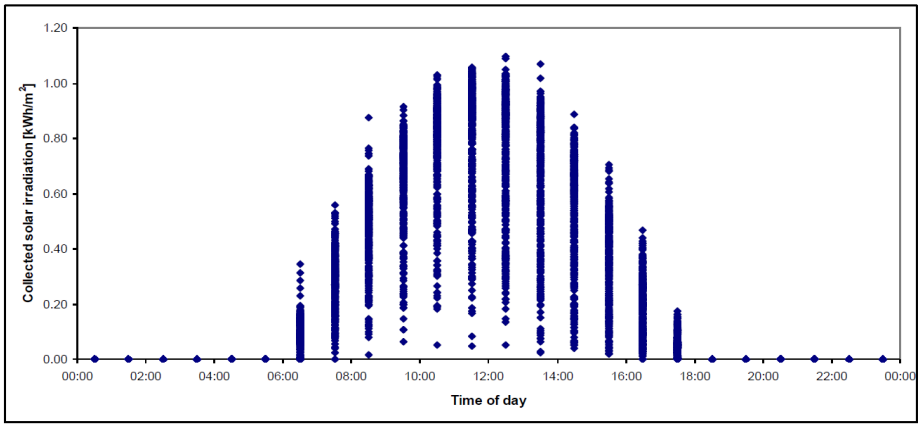

Figure 2.2: Average annual hourly distribution of I_{pv} for Harare

8760 dots in the Figure 2.2, each representing the calculated value of I_{pv} for an hour of the year. In this work long term averages for winter, summer seasons and annual values of I_{pv} are calculated using Klein's average days. Demand profiles for winter and summer weekdays and weekends for typical days are used.

Figure 2.3 shows the yearly average wind data for the site. The load demand information and other parameters are given in the respective chapters.

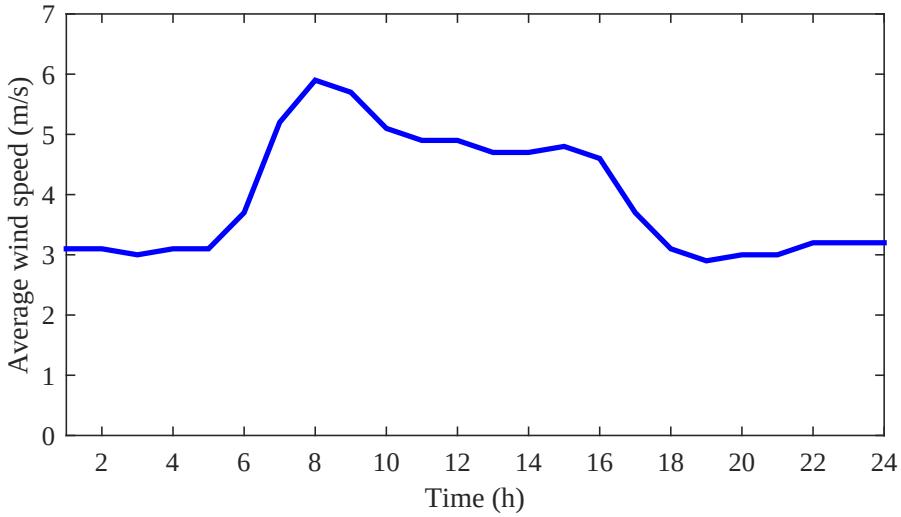

Figure 2.3: Average hourly wind velocity for Harare

2.5 CONCLUSION

A review of literature related to this thesis has been provided. The various methods used in the evaluation of the components of the hybrid energy system have been described. The following chapters will dwell on published work on the various models developed in this work, namely [50, 51] and [53]. The next chapter deals with optimal modeling of a PDB model with the objective of minimizing fuel costs.

CHAPTER 3

OPTIMAL CONTROL MODEL FOR OFF-GRID APPLICATIONS: CASE OF FUEL COST MINIMIZATION

This chapter is based on author's published work on fuel cost minimization of PDB hybrid energy system for off-grid applications [50]. The proposed hybrid system, which is composed of the PV system, battery bank and DG, as well as the optimization model, which includes the objective function, constraints and model parameters, is presented. The model proposed considers the daily energy consumption variations for winter and summer weekdays and weekends in order to compare the corresponding fuel costs and evaluates the operational efficiency of the hybrid system for a 24-hour period. It presents an open loop model that considers the intermittent nature of RE sources while minimizing fuel costs. A load-following diesel dispatch strategy is proposed and the fuel costs and energy flows are analyzed. The results obtained are compared in terms of fuel savings achieved by the PDB hybrid model case and by the case where the DG satisfies the load on its own, for winter and summer days.

3.1 INTRODUCTION

The hybrid system considered in this work is made up of PV modules with battery storage and a DG set as stated above. The hybrid operational costs are the costs incurred after installation in order to run the system. These costs are usually determined on an annual basis or any other time interval and then discounted for the project life. The long-term operational costs of a project include maintenance, fuel, component overhaul and replacement

costs. These costs are estimated for the future and are therefore more difficult to determine than the initial costs. In the short term, the operational costs of the battery and PV are negligible during the time interval considered, so only the fuel cost of the DG is taken into account. The PDB hybrid system operational costs are generally non-linear, as they depend on the component size and type, and the dispatch strategy [99].DGs use a quadratic fuel cost function such as the one in this work based on a particular fuel cost curve that allows consideration of a wide range of economic dispatch practices such as total operating cost of a system, incremental cost and minute by minute loading of DGs. The fuel cost function becomes more non-linear when the actual generator response is considered. Quadratic and cubic cost functions more accurately model the actual response thermal units including DGs, gas micro turbines, biomass power plants etc. Energy sources such as solar, wind and hydro are not usually included since the fuel that drives the power generation is priceless.

3.2 THE HYBRID SYSTEM

In this section the three main sub-models of the hybrid system are described.The load is met by the PV array and the battery comes in and discharges when the PV output is not enough to meet the load if it is within its operating limits. If PV output is above the load requirements, the battery is charged by the PV array. The DG comes in when the PV and/or the battery cannot meet the load but does not charge the battery. Fig. 3.1 shows the proposed simulation process in terms of the input or database, the database support and the output.

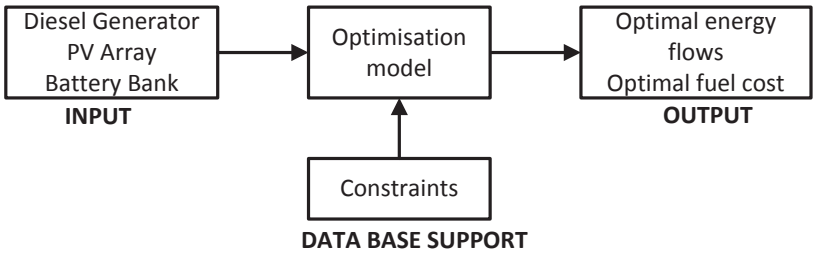

Figure 3.1: Simulation of a PV-diesel-battery hybrid power supply system

3.2.1 Photovoltaic system model

The hourly energy output from the PV generator of a given area is written as:

$$P_{pv} = \eta_{pv} A_c I_{pv}. \tag{3.1}$$

In equation (3.1), η_{pv} is the efficiency of the PV generator, which can be expressed as a function of the hourly solar irradiation incident on the PV array, I_{pv} (kWh/m^2), and the ambient temperature, T_A, as well as the test parameters of the PV generator at standard and nominal cell operating temperature (NT) conditions. A_c is the PV array area and P_{pv} is the hourly energy output from a PV generator of a given array area. The efficiency of the PV generator is given by:

$$\eta_{pv} = \eta_R[1 - 0.9\beta(\frac{I_{pv}}{I_{pv,NT}})(T_{c,NT} - T_{A,NT}) - \beta(T_A - T_R)]. \tag{3.2}$$

The hourly solar irradiation incident on the PV array is a function of time of day, expressed by the hour angle, the day of the year, the tilt and azimuth of the PV array, the location of the PV array site as expressed by the latitude, as well as the hourly global solar irradiation and its diffuse fraction [70, 71, 72]. The actual expression relies on the sky model, which is a mathematical representation of the distribution of diffuse radiation over the sky dome presented in [70]. In the study, the simplified isotropic diffuse formula suggested in [71] is used. The hourly solar irradiation incident on the PV array is given by:

$$I_{pv} = (I_B - I_D)R_B + I_D. \tag{3.3}$$

In (3.3), I_B and I_D are respectively the hourly global and diffuse irradiation in kWh/m^2. R_B is a geometric factor representing the ratio of beam irradiance incident on a tilted plane to that incident on a horizontal plane. Monthly average hourly meteorological data, global irradiation, diffuse irradiation and ambient temperature are used as inputs in evaluating (3.1), (3.2) and (3.3) of the performance simulation model. The evaluation is performed at the mid-point of each hour of the day, on the "average day" of each month as defined in [70]. For any energy supply system, the hourly average energy demand depends on the energy demand profile for the particular application. Typical load profiles for summer and winter seasons for rural community clinics in Zimbabwe are shown in Table 1. The load profile is for the clinic and nurses' houses. The methodology for calculating the load demand developed in [112, 113] is used to obtain the weekday and weekend demand profiles based on an energy demand survey carried out in rural communities by the same authors.

Table 3.1: Weekday and weekend demand profiles

Time	Winter Load [kW]		Summer Load [kW]	
	Weekend	Weekday	Weekend	Weekday
00:30	1.5	1.5	1.5	1.5
01:30	1.5	1.5	1.5	1.5
02:30	1.5	1.5	1.85	1.85
03:30	1.5	1.5	1.95	1.95
04:30	1.5	1.5	1.85	1.85
05:30	1.95	1.65	1.5	1.5
06:30	1.95	1.65	1.65	1.15
07:30	1.65	1.35	1.65	1.25
08:30	1.35	1.35	1.7	1.3
09:30	3.25	3.0	1.75	1.32
10:30	3.25	3.0	1.75	1.35
11:30	2.15	1.95	1.75	1.32
12:30	2.15	1.95	1.25	1.25
13:30	2.15	1.95	1.32	1.32
14:30	2.15	1.95	1.35	1.35
15:30	2.15	1.95	1.35	1.35
16:30	2.15	1.65	1.45	1.45
17:30	1.8	1.65	2.1	2.15
18:30	2.31	3.25	2.4	2.31
19:30	3.81	3.25	3.8	3.25
20:30	2.31	2.31	3.8	3.25
21:30	2.31	2.15	2.0	2.0
22:30	2.31	2.15	1.95	1.95
23:30	1.35	1.35	1.65	1.65

3.2.2 Battery bank model

The power output from the PV and the load demand at a given hour t, determine the charge or discharge power into and out of the battery bank. t is an integer representing the t^{th} hour interval. The SOC of the battery bank at any hour t, $B_C(t)$, depends on the SOC at the previous hour $B_C(t-1)$. The following conditions need to be taken into consideration for energy flows from $t-1$ to t:

At any given hour the battery SOC will be given by the expression:

$$B_C(t) = B_C(t-1) + \eta_C P_3(t) - \frac{1}{\eta_D} P_4(t), \tag{3.4}$$

in which, η_C is the battery charging efficiency, and η_D is the battery discharging efficiency. The following general expression derived from (3.4) applies to the battery dynamics:

$$B_C(t) = B_C(0) + \eta_C \sum_{\tau=1}^{t} P_3(\tau) - \frac{1}{\eta_D} \sum_{\tau=1}^{t} P_4(\tau), \tag{3.5}$$

where $B_C(0)$ is considered as the initial SOC of the battery.
$\eta_C \sum_{\tau=1}^{t} P_3(\tau)$ is the power accepted by the battery at time t, and $\frac{1}{\eta_D} \sum_{\tau=1}^{t} P_4(\tau)$ is the power discharged by the battery at time t.

3.2.3 Diesel generator model

DGs are incorporated in hybrid power supply systems as back-up and are usually required to cover the load at times when the PV and the battery cannot meet the load [96]. The manufacturer of the DG usually recommends the minimum diesel operation. The maximum efficiency of a DG corresponds to the rated power of the DG, therefore the DG has to be operated between the rated power and specified minimum value [12, 97, 46] as represented by the following constraint:

$$P_1^{\min} \leq P_1(t) \leq P_1^{\max}.$$

The conditions for switching on or off depend on the DG energy dispatch strategy. In the present study, a load-following strategy is employed in which the DG is switched on when the PV and/or the battery is unable to meet the load. This strategy promises to be more economical in terms of usage of DG energy, as the generator is dispatched only when required.

Under the load-following strategy, the DG produces only enough power to meet the load demand and is not used as a battery charger. The DG is more likely to operate at high load factors, resulting in low specific fuel consumption and longer DG life [14, 114]. In this work a 5 kVA Power Rush generator type is employed in which an electronic control system is used to vary the output by sensing the load and sending an electrical signal to the fuel injection system to adjust the fuel supply and engine revolutions in response to the load. The advantage of this type of generator is its ability to supply the required power output at any given time.

3.3 OPTIMIZATION MODEL

The PV module is modeled as a variable power source controllable in the range of zero to the maximum available PV power for the 24-hour interval. No PV operating costs are incorporated. The battery is modeled as a storage entity with minimum and maximum available capacity levels. The DG is modeled as a controllable variable power source with minimum and maximum output power as indicated at the end of the previous section. Fuel consumption costs are modeled as a non-linear function of generator output power [99, 115]. The load demand is to be met by the PV generator. If the PV output is not enough to satisfy the load demand, the battery discharges to satisfy the load requirement. If the PV output is above the load requirement, the excess energy from the PV is stored in the battery until full capacity of the batteries is reached. In some instances the solar PV power and/or battery bank power available is supplied to the load and the DG supplies the deficit in order to satisfy the load completely. The DG switches off when the PV and/or the battery bank can fully satisfy the load. The economic dispatch problem is to determine the optimum scheduling of generation at any given time that minimizes the fuel cost while completely satisfying the demand and operating limits. The objective function is given by the following expression:

$$\min C_f \sum_{t=1}^{N} (aP_1^2(t) + bP_1(t)) + c, \tag{3.6}$$

subject to the following constraints:

$$P_2(t) + P_3(t) \leq P_{pv}(t), \tag{3.7}$$

$$P_1(t) + P_2(t) + P_4(t) = P_L(t), \tag{3.8}$$

$$P_1(t) \geq 0, P_2(t) \geq 0, P_3(t) \geq 0, P_4(t) \geq 0, \tag{3.9}$$

$$P_i^{min} \leq P_i(t) \leq P_i^{max}, \tag{3.10}$$

$$B_C^{min} \leq B_C(0) + \eta_C \sum_{\tau=1}^{t} P_3(\tau) - \frac{1}{\eta_D} \sum_{\tau=1}^{t} P_4(\tau) \leq B_C^{max}, \tag{3.11}$$

for all $t = 1, \cdots, N$, where a, b and c $\$/h$ are DG coefficients, N is 24 and C_f is the fuel price. $B_C(t)$ is equal to the sum of and the power accepted or discharged by the battery. $P_1(t)$, $P_2(t)$ and $P_4(t)$ are the control variables representing energy flows from the DG, PV and battery to the load at any time (t) respectively and $P_3(t)$ represents the energy flow to the battery during the 24-hour period. The first constraint (3.7) implies that the sum of the charging power and power supplied directly to the load from the PV array is less than or equal to the total power from the PV array. Constraint (3.8) ensures that the power supplied by the DG, PV array and battery at any hour equals to the demand at the same hour. Constraint (3.9) ensures that the charging power, power supplied directly to the load from the PV array and power supplied by the battery to the load are each greater than or equal to zero. Each energy source i is constrained by minimum and maximum values, as specified by constraint (3.10).

3.3.1 Model parameters

The generator cost coefficients a and b are specified by the manufacturer while the DG, PV and battery bank capacities are chosen based on a sizing model in [111]. c is very small and is generally less than 0.01% of b. The system sizing is such that demand will be met, at any given time. A small system means demand will not always be met while an oversized system means the demand will be met but the system will be unnecessarily costly and energy will be wasted, hence the need for an optimally sized system. In this work, the focus is mainly on the optimal energy management of any given system. The sizing is also within “rule of thumb" provisions, for example the PV array area for 1 kWp varies from 7 m^2 to 20 m^2 depending on cell material used. The energy generated by the PV array and the DG is consumed by the load

and the PV generator also charges the battery, depending on the instantaneous magnitude of the load and SOC of the storage battery. The switching on or off times of the DG depend on the DG energy dispatch strategy employed, which is herein referred to as the load-following strategy. The DG switches on when the PV hourly output is lower than the hourly load and the combined battery output and PV output cannot meet the load. The parameters used in this model are shown in Table 2. The quadratic optimization programming is solved using the "quadprog" function in MATLAB. This function solves problems in the form:

$$\min \frac{1}{2} x^T H x + f^T x,$$

subject to:

$$Ax \leq b,$$

$$A_{eq} x = b_{eq},$$

$$lb \leq x \leq ub.$$

The load demand is to be met by the PV generator. If the PV output is not enough to satisfy the load demand, the battery discharges to satisfy the load requirement. If the PV output is above the load requirement, the excess energy from the PV is stored in the battery until the full capacity of the batteries is reached. In some instances the solar PV power and/or battery bank power available is supplied to the load and the DG supplies the deficit in order to satisfy the load completely. The DG switches off when the PV and/or the battery bank can fully satisfy the load. The economic dispatch problem is to determine the optimum scheduling of generation at any given time that minimizes the fuel cost while completely satisfying the demand and operating limits.

3.4 RESULTS AND DISCUSSION

Figs. 3.2-5 show the energy flow during the 24-hour period. During the night and early morning the load is met by the battery if the SOC is within limits and can satisfy the load or by the DG or by a combination of the two sources. PV output supplies the load and charges the battery. The first constraint (3.7) means that for PV array output to be able to satisfy the load or satisfy the load and charge the battery, it must be equal to or greater than the load. The DG switches on when the PV and battery cannot satisfy the load. The charge and

Table 3.2: Parameters

Nominal battery capacity	54.5 kWh
Battery charge efficiency	85%
Battery discharge efficiency	100%
Battery allowable depth of discharge	50%
PV array capacity	$4kW$
DG capacity	$5kVA$
a	US \$0.246 /(kW)^{2}h
b	US \$0.1 /kWh
Fuel Cost	US\$1.2

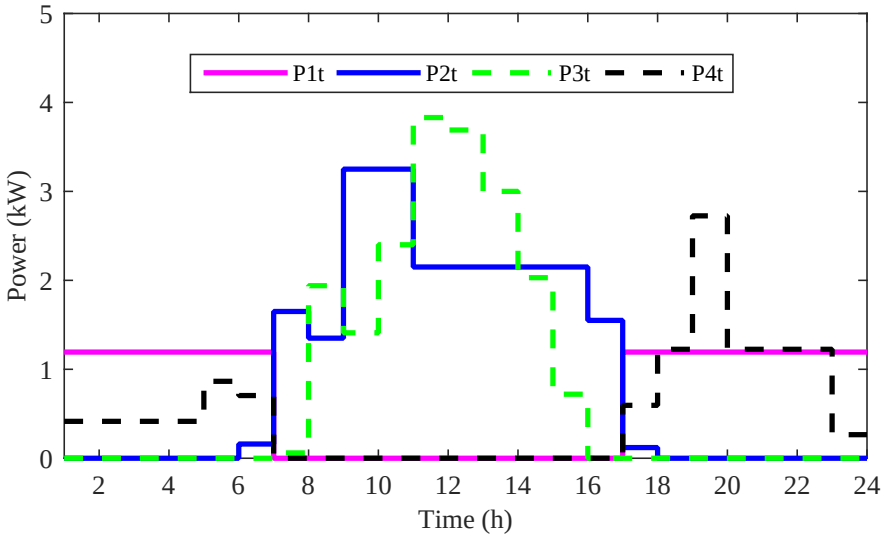

Figure 3.2: June weekend power flow

discharge processes of the battery are shown in Figs. 3.2-5 as $P_3(t)$ and $P_4(t)$ respectively. Generally the battery bank is charged during the day and supplies the load mostly during the night when there is no power from the PV. During the early hours of the day after sunrise and towards sunset the load is met by the DG, PV and battery bank. The DG turns off when the PV produces enough power to meet the load or when the combined power from the PV and battery can satisfy the load. In Figs. 3.2-5, it is shown that power from the PV to the load $P_2(t)$ is not enough to meet the load just after sunrise and just before sunset. The PV output continues to increase up to the point when it produces more than the load and is

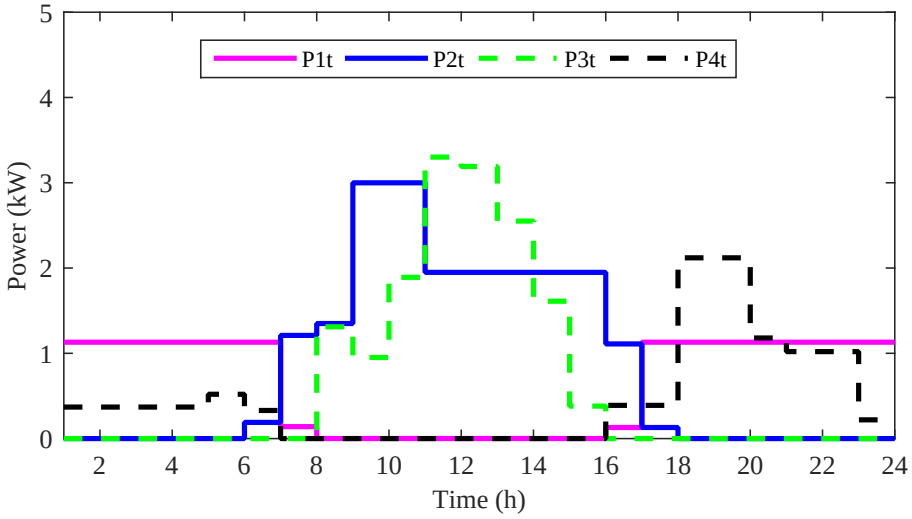

Figure 3.3: June weekday power flow

able to charge the battery bank. At that point the DG switches off until the point when the PV cannot produce enough power to meet the load and charge the battery, as shown in Figs. 3.2-5 in $P_1(t)$. The DG running time and amount of power supplied by the DG depends on the SOC of the battery and the amount of power from the PV array. It therefore follows that the DG runs for more hours and generates more power if the output from the PV and/or battery is low.

Figs.3.2 and 3.3 show the weekend and weekday power flows during winter while Figs. 3.4 and 3.5 show the weekend and weekday power flows during summer. The graphs show how seasonal variations in PV output and change in demand affect the diesel dispatch strategy. In summer the PV supplies more power than it does in winter. Figs. 3.2-5 generally show that the DG switches off earlier and switches on later in summer than in winter. The longer summer day-times, shorter winter day-times and the corresponding high and low radiation levels mean that the battery is charged more in summer than in winter. The DG also supplies more power in winter than in summer, especially during the early hours of the day and this is attributed to higher PV output and higher SOC of the battery bank in summer than in winter. Figs. 3.6-9 show the optimal power flows when the average hourly annual radiation output is used a the PV input.

It is observed that demand is generally lower in summer than in winter. Weekday and weekend fuel consumption value differences are attributed to differences in consumption patterns as

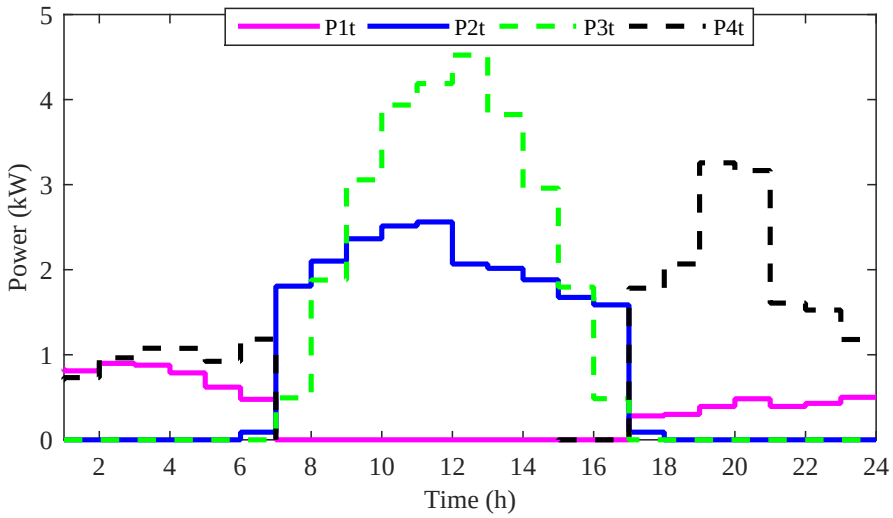

Figure 3.4: December weekend power flow

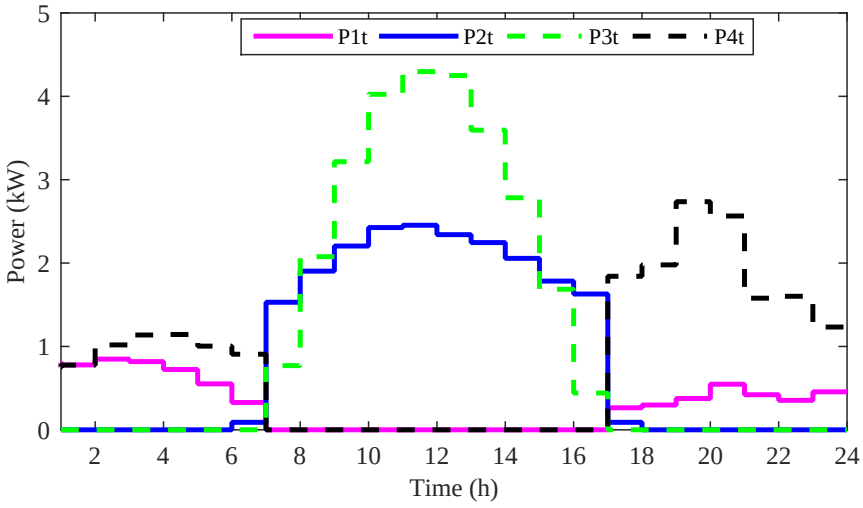

Figure 3.5: December weekday power flow

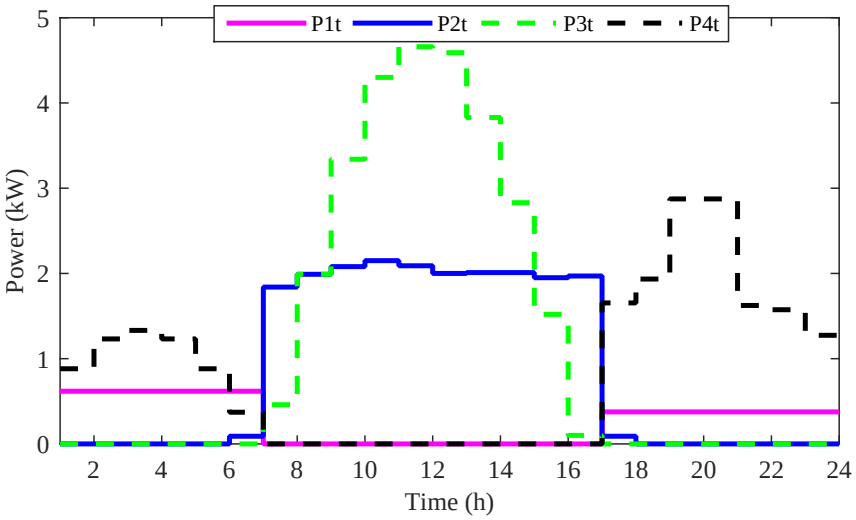

Figure 3.6: December weekday power flow

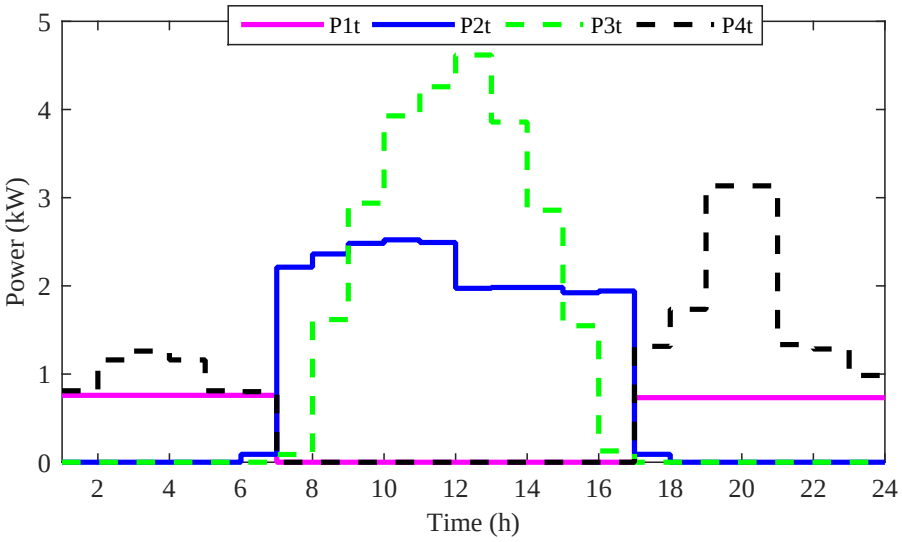

Figure 3.7: December weekend power flow

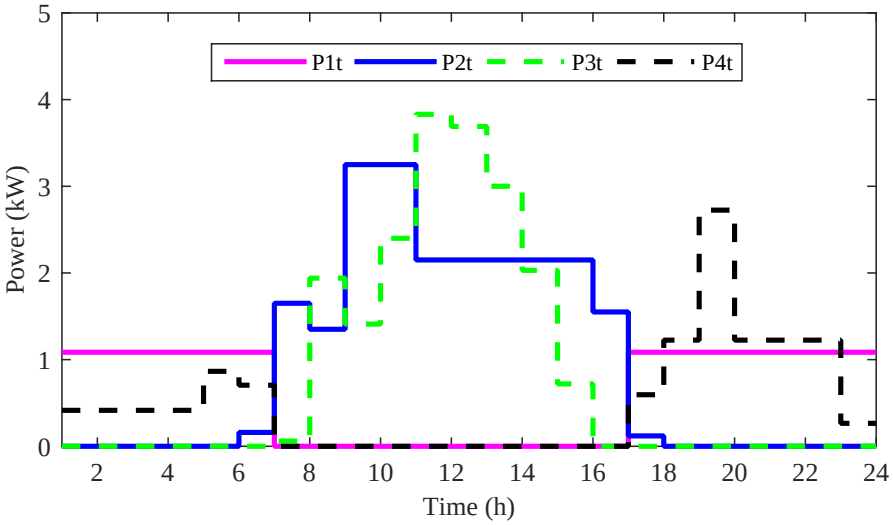

Figure 3.8: Winter weekend power flow

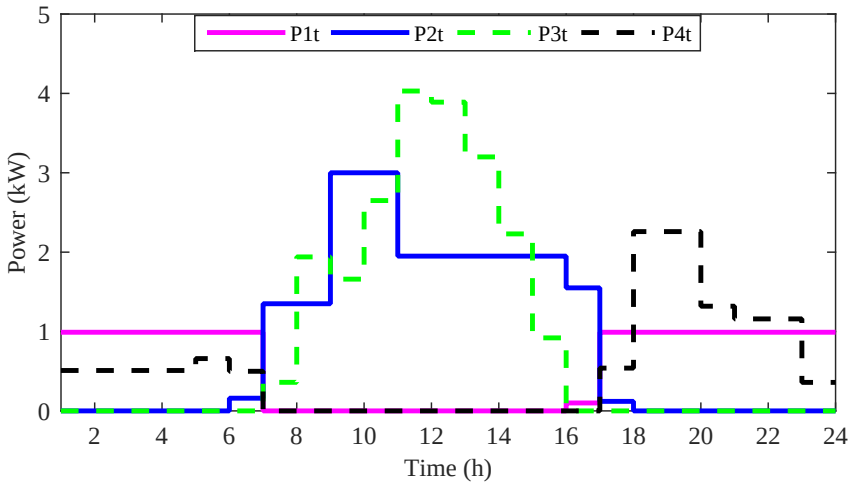

Figure 3.9: Winter weekday power flow

shown in Table 1. Generally the weekend demand is higher than weekday demand because in most rural communities during the week people will be busy with activities outside the home but during weekends they will be at home making more use of various appliances. The number of people who visit the clinic is also higher during weekends. The results show that more fuel is used in winter than in summer and also more is used during the weekends than on weekdays. The fuel cost for winter weekends is found to be 15% more than that for weekdays. The fuel cost for summer weekends is 19% more than that for weekdays. The fuel cost for winter weekends is found to be 36% more than that for summer, while that for winter weekdays is 39% more than that for summer weekdays.These results show that it is very important to consider seasonal demand changes when calculating operational costs. The results thus show how demand is optimally satisfied by the DG, PV array and battery bank and the corresponding energy flows during the 24-hour interval.

In the model configuration employed in this work, the battery is charged by the PV array only and the DG supplies the load when it is switched on. This configuration ensures maximum use of PV output and no energy is wasted when the DG runs, since the output matches the demand. The objective function is to minimize fuel costs while satisfying demand and other constraints using quadratic programming, as stated in preceding sections. No similar optimization model for PDB system is found in literature that minimizes fuel costs, taking into account variations in demand. Closer to this work is work done by [116] who use genetic algorithm to solve an economic model in which the annual cost of the system is minimized. The battery is utilized when both the DG and the PV cannot meet the load while in the model developed in this study it is utilized when PV output cannot meet the load but before the DG comes in depending on its SOC. [27] look at various dispatch strategies for various combinations of wind turbine generators, DGs, PV arrays and batteries using an analysis of cost trade-offs, a simple quasi-steady-state time-series model and HYBRID2. However, there is no basis for comparing the corresponding fuel costs, as the system configurations are different. The system configurations and the operational strategies employed are different from the optimization model developed in this work, making it difficult to compare the daily fuel costs.

Table 3 shows how the diesel fuel costs for typical weekdays and weekends in both summer and winter seasons compare to the diesel only scenario. Hybrid models 1 and 2 refer to seasonal and yearly applications of radiation data. The fuel savings are obtained by finding

Table 3.3: Fuel cost savings

	Winter Weekend	Winter Weekday	Summer Weekend	Summer Weekday
Diesel only scenario	US$51.4	US$46.5	US$43.7	US$37.8
Hybrid Model 1	US$13.2	US$11.3	US$8.4	US$6.80
Hybrid Model 2	US$14.7	US$12.1	US$9.3	US$7.50
Savings 1	US$38.2	US$35.2	US$35.3	US$31
Savings 2	US$40.7	US$34.4	US$34.4	US$30.3

the difference between the fuel cost values for the diesel-only scenario in which the load is met completely by the DG, and the PDB model for the days and consumption patterns considered. The results show that the PDB model achieves 73% and 77% fuel savings in winter, and 80.5% and 82% fuel savings in summer on weekends and weekdays respectively when compared to the diesel-only scenario. The differences in fuel cost obtained indicate the potential of the optimization model to reduce fuel costs for the DG dispatch strategy employed compared to the diesel-only scenario. When the annual daily average hourly radiation is used, the model achieves 79% and 80% fuel savings in winter, and 79% and 80% fuel savings in summer on weekends and weekdays respectively when compared to the diesel-only scenario. The reduction in summer savings is due the fact that the average summer PV output is more than the annual average, and the increase in winter savings is due to the fact that the average winter radiation is less than the annual average. As already mentioned, most of the work done so far assume a load that does not change and a uniform daily operational cost; this does not reflect the variation in consumption patterns. The current study results indicate that by making use of the described methodology and considering daily and seasonal variations in demand, more accurate costs can be obtained.

3.5 ECONOMIC ANALYSIS

The payback period analysis which determines the number of years required to recover an initial investment through project returns is considered in this section. In this work the diesel only system is the baseline and additional investment consists of the PV system and battery bank. Seasonal average cost savings are used in the analysis to obtain the annualized benefits

and these are assumed to be constant. Maintenance costs are also assumed to be constant over the entire period. The discounted present value method is employed in the cash flow analysis as follows:

$$DPV = \frac{FV}{(1+r)^n}, \tag{3.12}$$

where DPV is the discounted present value of future cash flow, FV is the nominal value of the cash flow amount in a future period, r is the interest or discount rate and n is the time in years.

Table 3.4: Payback period

Years	0	1	2	3	4	5	6	7	8
Solar photovoltaics	(72 000.00)								
Battery	(98 340.00)								
Controllers	(7 235.58)								
Inverters and accesories	(25 000.00)								
Installation cost	(20 000.00)								
Maintenance cost		(1 800.00)	(1 800.00)	(1 800.00)	(1 800.00)	(1 800.00)	(1 800.00)	(1 800.00)	(1 800.00)
Optimal benefit (saved costs on energy)		120060.00	120060.00	120060.00	120060.00	120060.00	120060.00	120060.00	120060.00
	(222 575.58)	118 260.00	118 260.00	118 260.00	118 260.00	118 260.00	118 260.00	118 260.00	118 260.00
Discount factor @ 5%	1.00	0.95	0.91	0.86	0.82	0.78	0.75	0.71	0.68
Discounted cashflows	(222 575.58)	112 628.57	107 265.31	102 157.43	97 292.79	92 659.80	88 247.43	84 045.17	80 043.02

Discounted Payback Period	Years	Discounted cashflows	Cumulative cashflows
	0	(222 575.58)	(222 575.58)
	1	112 628.57	(109 947.01)
	2	107 265.31	(2 681.70)
	3	102 157.43	99 475.73
	4	97 292.79	196 768.53
	5	92 659.80	289 428.33
	6	88 247.43	377 675.76
	7	84 045.17	461 720.94
	8	80 043.02	541 763.96
Payback is :	**2 years plus 2 months**	2.393987353	

Table 3.4 shows the cash flows illustrating the break even point occurring at 2 years and 2 months. The short payback period is attributed to the reduction in the operating time of the DG, owing to the optimal dispatching strategy employed that results in considerable fuel savings and prolonged DG lifespan and maintenance schedules. These results show the cost-effectiveness of such hybrid systems.

3.6 CONCLUSION

An optimal energy dispatch model of a PDB system has been presented and the optimal energy flows have been analyzed. The optimization model developed is shown to achieve more savings than the diesel-only scenario. The results show how daily and seasonal variations in demand affect the operational cost of the PDB power supply system. For both summer and winter seasons, the weekend fuel costs are higher than weekday costs. Winter fuel costs are

found to be higher than summer fuel cost because of higher demand in winter; the lower winter radiation levels imply more use of supplementary sources. This shows that the daily and seasonal demand changes are important aspects to be considered, as they affect the operational cost and the energy flows considerably. A more practical estimate of the fuel costs reflecting variations in power consumption behavior patterns is thus presented in this thesis, which can be extrapolated to give an accurate estimate of the daily diesel fuel cost. In the following chapter, the switched MPC design is introduced to improve the hybrid power system performance and cater for the weaknesses of the optimal control strategy used in this chapter when subjected to disturbances.

CHAPTER 4

ENERGY DISPATCHING OF A PHOTOVOLTAIC-DIESEL-BATTERY HYBRID POWER SYSTEM: SWITCHED MODEL PREDICTIVE CONTROL APPROACH

4.1 INTRODUCTION

To solve dispatching problems for hybrid power systems, an optimization control strategy [50] is proposed in the previous chapter; however, in case of disturbances in load demands and PV power, the performance of the optimization strategy in [50] may deteriorate significantly. Another effective approach for energy dispatching, MPC, is proposed in this chapter owing to its ability to achieve better performance during a relatively long period when disturbances would possibly occur. In this chapter, a new adaptive switched MPC is proposed for the PDB hybrid power system [55].

The configuration of this work is arranged as follows: the mathematical model of the PDB hybrid system is proposed in Section 4.2; the detailed switched MPC design for energy dispatch of the PDB hybrid power system is presented in Section 4.3; simulation results are displayed in Section 4.4; and the conclusion is drawn in the final section.

4.2 PROBLEM STATEMENT

4.2.1 Overall structure of the hybrid system

As is displayed in Fig. 4.1, the PDB hybrid power system is proposed by combining a DG, a PV array, and a battery bank [50]. The proposed hybrid system supplies the daily requirements of a remote off-grid area.

In this work, the mathematical model of the PDB hybrid power system is based on a previous version [50]. The difference lies in the control approach to the charging and discharging processes. The new model is more practical than the previously proposed one.

The hourly load profile used in this work is displayed in Table 4.1. The data are obtained from a Zimbabwean rural community clinic [50] located in an off-grid remote area.

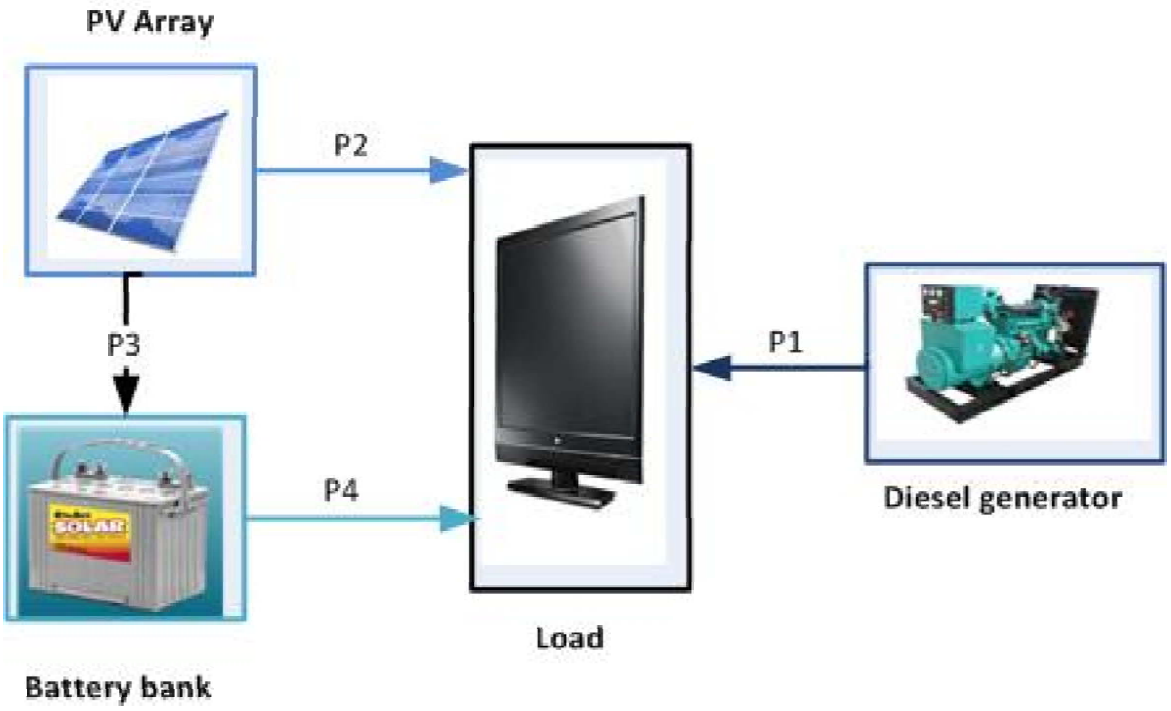

Figure 4.1: Configuration of the PDB hybrid system

Table 4.1: Load demand ($P_L(k)$, kW) of a Zimbabwean rural clinic

time	summer	winter	time	summer	winter
00:30	1.5	1.5	12:30	1.25	1.95
01:30	1.5	1.5	13:30	1.32	1.95
02:30	1.85	1.5	14:30	1.35	1.95
03:30	1.95	1.5	15:30	1.35	1.95
04:30	1.85	1.5	16:30	1.45	1.65
05:30	1.5	1.65	17:30	2.15	1.65
06:30	1.15	1.65	18:30	2.31	3.25
07:30	1.25	1.35	19:30	3.25	3.25
08:30	1.3	1.35	20:30	3.25	2.31
09:30	1.32	3.0	21:30	2.0	2.15
10:30	1.35	3.0	22:30	1.95	2.15
11:30	1.32	1.95	23:30	1.65	1.35

4.2.2 Photovoltaic array

In this thesis, data of energy output from the PV array are given for summer and winter, as shown in Table 4.2. The PV data are obtained from the aforementioned Zimbabwean rural community clinic, by using the methodology and solar radiation data proposed in [112]. As is shown in Fig. 4.1, energy from PV is used for supplying the load demand and charging the battery.

Remark 1 *Data from the aforementioned Zimbabwean rural community clinic are qualified for this research, because 1) this clinic is a typical energy-consuming unit located in an off-grid remote area where there is an energy shortage, and 2) the weather condition and solar radiation in this area are relatively stable, indicating that daily PV energy data are representative.*

Table 4.2: Energy provided by the PV array ($P_{pv}(k)$, kW)

time	summer	winter	time	summer	winter
00:30	0.00	0.00	12:30	6.59	5.14
01:30	0.00	0.00	13:30	5.84	4.50
02:30	0.00	0.00	14:30	4.84	3.56
03:30	0.00	0.00	15:30	3.47	2.33
04:30	0.00	0.00	16:30	2.07	1.11
05:30	0.00	0.00	17:30	0.09	0.13
06:30	0.09	0.19	18:30	0.00	0.00
07:30	2.30	1.21	19:30	0.00	0.00
08:30	3.98	2.66	20:30	0.00	0.00
09:30	5.42	3.95	21:30	0.00	0.00
10:30	6.45	4.89	22:30	0.00	0.00
11:30	6.75	5.25	23:30	0.00	0.00

PV powers for supplying the load demand and charging the battery are denoted by P_2 and P_3, respectively. They should be subject to the follows constraints:

$$0 \leq P_2(k) \leq P_2^{max},\ 0 \leq P_3(k) \leq P_3^{max},$$

$$0 \leq P_2(k) + P_3(k) \leq P_{pv}(k),$$

where P_2^{max} denotes the maximum amount of power that can be directly transmitted to the load from the PV array, and P_3^{max} is the maximum amount of power allowed to charge the battery during one hour.

4.2.3 Battery bank

Charging and discharging of the battery bank can be described by a simplified discrete dynamic equation:

$$S_{oc}(k+1) = S_{oc}(k) + \eta_c P_3(k) - \frac{1}{\eta_d} P_4(k), \tag{4.1}$$

where $S_{oc}(k)$ denotes the SoC at sampling time k; P_3 and P_4 are charged power and discharged power, respectively; η_c and η_d are charging efficiency and discharging efficiency, respectively.

In this work, it is considered that η_c and η_d are uncertain constant parameters, and are estimated online in the MPC design.

Remark 2 *The simplified discrete model of SoC* (4.1) *originates from the continuous model proposed in [32], where variation of the SoC is proportional to the (charging and discharging) current.*

It follows from (4.1) that the SoC at a given time τ could be expressed by

$$S_{oc}(\tau) = S_{oc}(0) + \eta_c \sum_{k=0}^{\tau} P_3(k) - \frac{1}{\eta_d} \sum_{k=0}^{\tau} P_4(k).$$

The SoC of the battery bank is subject to the constraint:

$$B_C^{min} \leq S_{oc}(k) \leq B_C^{max},$$

where B_C^{min} and B_C^{max} are its upper and lower limits. The discharged power of the battery P_4 should satisfy the constraint:

$$0 \leq P_4(k) \leq P_4^{max},$$

where P_4^{max} is the maximum hourly discharging.

In this work, it is considered that simultaneous charging and discharging are not permitted, that is

$$P_3(k)P_4(k) = 0. \tag{4.2}$$

Switches between charging and discharging are arranged in a heuristic manner according to data in Table 4.1 and Table 4.2. When the load demand exceeds PV power (between sunset and sunrise), the battery is set in discharging state; and when the PV power exceeds the load demand (during daytime), the battery is set in charging state.

Remark 3 *It should be acknowledged that the heuristic manner of switching time could possibly bring some drawbacks. For example, there might be disturbances in PV power and load demand. The disturbances could possibly result in lower PV power and higher load demand, such that charging would happen when PV power is in excess (and discharging would happen when PV power is insufficient). However, in another aspect, the performance of MPC with respect to disturbances can be well tested.*

4.2.4 Diesel generator

The DG is used to cover the imbalance, when the load demands cannot be satisfied by the PV array and the battery altogether. It is the final choice, because 1) the fuel is expensive, and 2) it generates greenhouse gases such as carbon dioxide (CO_2). The advantage of using a DG is that it can be operated at any time according to demands.

The energy from DG is subject to the constraint:

$$0 \leq P_1(k) \leq P_1^{max},$$

where P_1^{max} is the maximum amount of power that can be generated by the DG during one hour.

As mentioned before, the DG, PV array and battery bank should supply the daily requirements of power cooperatively:

$$P_1(k) + P_2(k) + P_4(k) = P_L(k).$$

4.2.5 Objective

The *objective* of this work is to design the scheduling of P_2, P_3 and P_4 for the PDB hybrid power system in case of uncertain constant charging and discharging coefficients (η_c and η_d), such that the usage of DG P_1 can be minimized. It is also intended that the battery should not be excessively used, such that its deterioration can be prevented.

4.3 SWITCHED MODEL PREDICTIVE CONTROL DESIGN

In this section, design procedures of switched MPC are presented, including parameter estimation, system model transformation, objective function design, constraints treatment, and MPC algorithm.

4.3.1 Online estimation of battery parameters

Define $u(k) \triangleq [P_2(k), P_3(k), P_4(k)]^T$. The dynamic process of the battery bank can be expressed by

$$S_{oc}(k) = S_{oc}(k-1) + b_m u(k-1), \tag{4.3}$$

where $b_m \triangleq [0, \eta_c, -\eta_d]$. or equivalently,

$$S_{oc}(k) = S_{oc}(k-1) + b_b u_b(k-1), \tag{4.4}$$

where $b_b \triangleq [\eta_c, -\eta_d]$, and $u_b \triangleq [P_3(k), P_4(k)]^T$.

The estimated battery dynamic system can be given by

$$\hat{S}_{oc}(k) = S_{oc}(k-1) + \hat{b}_b(k-1)u_b(k-1), \tag{4.5}$$

where $\hat{S}_{oc}(k)$ is the estimated SoC, and $\hat{b}_b \triangleq [\hat{\eta}_c, -\hat{\eta}_d]$ denotes estimated parameters.

The cost function for online identification is designed by

$$\begin{aligned} J_p =& \frac{1}{2}\tilde{S}_{oc}(k)^2 \\ =& \frac{1}{2}\left(S_{oc}(k) - S_{oc}(k-1) - \hat{b}_b(k-1)u_b(k-1)\right)^2. \end{aligned}$$

where $\tilde{S}_{oc}(k) \triangleq S_{oc}(k) - \hat{S}_{oc}(k)$. Its gradient with respect to $\hat{b}_b$ can be calculated by

$$\nabla J_p = -\left(\Delta S_{oc}(k) - \hat{b}_b(k-1)u_b(k-1)\right)u_b(k-1),$$

where $\Delta S_{oc}(k) \triangleq S_{oc}(k) - S_{oc}(k-1)$. Consequently, the updating law for $\hat{b}_b$ can be designed by

$$\hat{b}_b(k) = \hat{b}_b(k-1) - \lambda \nabla J_p$$

and the updating law for $\hat{b}_m$ is designed by

$$\hat{b}_m(k) = [0, \hat{\eta}_c(k), -\hat{\eta}_d(k)] = [0, \hat{b}_b(k)]. \tag{4.6}$$

It can be proved that [117], with the proposed updating law (4.6), estimated parameters converge to their actual values, if the control u_b is persistently exciting (PE [117]), and satisfies

$$u_b(k)^T u_b(k) < \frac{2-\alpha}{\lambda}, \tag{4.7}$$

where $0 < \alpha < 2$. In this work, (4.7) is treated as an additional constraint. PE of $u_b(k)$ is explained below.

PERSISTENT EXCITATION OF $U_B(K)$

PE of $u_b(k)$ can be explained as follows:

$$u_b(k)u_b(k)^T = \begin{bmatrix} P_3(k)^2 & P_3(k)P_4(k) \\ P_4(k)P_3(k) & P_4(k)^2 \end{bmatrix}$$

where $P_3(k)P_4(k) = 0$ since simultaneous charging and discharging are not permitted. Moreover, for this hybrid system, a time span $(h, h+H_0)$ always exists, containing both charging and discharging; it follows that $0 < \alpha_1 I_{2\times 2} \leqslant \Sigma_{k=h}^{h+H_0} u_b(k)u_b(k)^T \leqslant \alpha_2 I_{2\times 2}$, where $\alpha_1 = \min\left[\Sigma_{k=h}^{h+H_0} P_3(k), \Sigma_{k=h}^{h+H_0} P_4(k)\right]$, and $\alpha_2 = \max\left[\Sigma_{k=h}^{h+H_0} P_3(k), \Sigma_{k=h}^{h+H_0} P_4(k)\right]$. Consequently, $u_b(k)$ is persistently exciting in the time span $(h, h+H_0)$.

TRANSFORMATION OF CONSTRAINT (C)

Based on the battery dynamic equation Fig.4.3, predicted values of x_m can be calculated by

$$S_{oc}(k+i|k) = S_{oc}(k) + b_m \sum_{j=k}^{j\leq k+i-1} u(j), \tag{4.8}$$

where $S_{oc}(k+i|k)$ denotes the predicted value of S_{oc} from sampling time k. It follows from (4.8) that

$$X_m(k) = S_{oc}(k)[1, 1, \cdots, 1]^T + B_m U(k),$$

where

$$X_m(k) \triangleq [S_{oc}(k), S_{oc}(k+1|k), \cdots, S_{oc}(k+N_c-1|k)]^T,$$

$$B_m(b_m) = \underbrace{\begin{bmatrix} b_m & 0 & \cdots & 0 \\ b_m & b_m & \ddots & \vdots \\ \vdots & & \ddots & 0 \\ b_m & b_m & \cdots & b_m \end{bmatrix}}_{N_c}.$$

However, since b_m is uncertain, its estimated value $\hat{b}_m = [0, \hat{\eta}_c, \hat{\eta}_d]$ should be used in calculating B_m.

Each $S_{oc}(k+i|k)$ in the predictive SoC $X_m(k)$ should satisfy constraint (c); con-

sequently,

$$B_{min}\underbrace{[1,1,\cdots,1]}_{N_c}^T \leq X_m(k) \leq B_{max}\underbrace{[1,1,\cdots,1]}_{N_c}^T,$$

leading to (4.13).

4.3.2 MIMO linear state-space modeling

In this section, the model of the PDB hybrid system is transformed into a linear state-space form to facilitate MPC design.

Define outputs

$$\begin{aligned} y_m(k) &\triangleq c_1\left(P_L(k) - P_1(k)\right) = c_1\left(P_2(k) + P_4(k)\right), \\ y_a(k) &\triangleq c_3\left(P_2(k) + P_3(k)\right), \\ y_b(k) &\triangleq c_2\left(P_3(k) + P_4(k)\right), \end{aligned}$$

where c_1, c_2 and c_3 are positive weight coefficients. It can be seen that minimizing $\sum c_1^2 P_1(k)^2$ is equal to minimizing $\sum\left(c_1 P_L(k) - y_m(k)\right)^2$; the usage of PV can be encouraged by minimizing $\sum\left(c_3 P_{pv}(k) - y_a(k)\right)^2$; and the usage of the battery can be minimized by penalizing $\sum y_b(k)^2$.

Define the augmented system states

$$x(k) \triangleq [S_{oc}(k), y_m(k-1), y_a(k-1), y_b(k-1)]^T,$$

and the augmented output

$$y(k) \triangleq [y_m(k-1), y_a(k-1), y_b(k-1)]^T,$$

such that a linear state-space model can be obtained:

$$\begin{cases} x(k+1) &= Ax(k) + Bu(k), \\ y(k) &= Cx(k), \end{cases} \tag{4.9}$$

where

$$A = \begin{bmatrix} 1 & 0_{1\times 3} \\ 0_{3\times 1} & 0_{3\times 3} \end{bmatrix},\ B = \begin{bmatrix} 0 & \eta_c & -\eta_d \\ c_1 & 0 & c_1 \\ c_3 & c_3 & 0 \\ 0 & c_2 & c_2 \end{bmatrix},$$

$$C = \begin{bmatrix} 0_{3\times 1} & I_{3\times 3} \end{bmatrix}.$$

The linear state-space system (4.9) is considered as the plant to be controlled via the MPC approach.

CALCULATION OF MPC GAINS

According to classical MPC design [118], MPC gains can be calculated as follows:

$$F(k) = \left[\ (CA)^T \ , (CA^2)^T \ , \cdots \ , (CA^{N_p(k)})^T \ \right]^T ,$$

$$\Phi(k) = \begin{bmatrix} \Phi_{11} & 0 & \cdots & 0 \\ \Phi_{21} & \Phi_{22} & & 0 \\ \vdots & & \ddots & \vdots \\ \Phi_{N_p,1} & \Phi_{N_p,2} & \cdots & \Phi_{N_p,N_c} \end{bmatrix},$$

where $\Phi_{ij} = CA^{i-j}\hat{B}$, and $\hat{B}$ is in the form of B with η_c and η_d replaced by $\hat{\eta}_c$ and $\hat{\eta}_d$.

The output vector can be expressed with respect to the input vector: $Y(k) = Fx(k) + \Phi U(k)$. It follows that the objective functions can be given by

$$\begin{aligned} J(k) &= (Y(k) - R(k))^T (Y(k) - R(k)) \\ &= (Fx(k) - R(k))^T (Fx(k) - R(k)) \\ &\quad + 2(Fx(k) - R(k))^T \Phi U(k) + U(k)^T \Phi^T \Phi U(k). \end{aligned}$$

where $(Fx(k) - R(k))^T (Fx(k) - R(k))$ is independent of $U(k)$; consequently, according to [118], optimizing $J(k)$ can be transformed as follows:

$$\begin{aligned} &\min J(k) = \min (Y(k) - R(k))^T (Y(k) - R(k)) \\ \Leftrightarrow \ &\min \left[2(Fx(k) - R(k))^T \Phi U(k) + U(k)^T \Phi^T \Phi U(k) \right] \\ \Leftrightarrow \ &\min \left(U(k)^T E U(k) + 2HU(k) \right), \end{aligned}$$

where $E(k) = \Phi(k)^T \Phi(k)$, and $H(k) = (Fx(k) - R(k))^T \Phi$.

4.3.3 Objective function for MPC

The objective function comprises of the following three items:

1. $\min J_1(k) = \min \sum_k^{k+N_p} (c_1 P_L(k) - y_m(k))^2$, which indicates that usage of the DG should be minimized;

2. $\min J_2(k) = \min \sum_k^{k+N_p} y_b(k)^2$, which penalizes the use of the battery bank;

3. $\min J_3(k) = \min \sum_k^{k+N_p} \left(c_3 P_{pv}(k) - y_a(k)\right)^2$, which implies that usage of the PV generator is encouraged.

Here, N_p represents the predictive horizon for MPC design.

Define $Y(k) \triangleq [y^T(k), y^T(k+1|k), \ldots, y^T(k+N_p-1|k)]^T$, where $y(k+i|k)$ denotes the predicted value of y at step i $(i = 1, \ldots, N_p)$ from sampling time k. Define the reference value $R(k) \triangleq [c_1 P_L(k), c_3 P_{pv}(k), 0, c_1 P_L(k+1), c_3 P_{pv}(k+1), 0, \ldots, c_1 P_L(k+N_p-1), c_3 P_{pv}(k+N_p-1), 0]^T$. The overall objective function is then given by

$$\begin{aligned} \min J(k) =& \min(J_1(k) + J_2(k) + J_3(k)) \\ =& \min \left(Y(k) - R(k)\right)^T \left(Y(k) - R(k)\right). \end{aligned} \tag{4.10}$$

4.3.4 Constraints for the MIMO linear system

In this work, switched constraints are used to describe different modes (charging or discharging) of the battery, such that the plant to be controlled could be expressed by a unified linear MIMO state-space model without switching parts.

Constraints can be categorized as follows:

(a) Energy flows from the generators and battery are non-negative values and are subjected to their maximum values: $0 \leq P_1(k) = P_L(k) - y_m(k) \leq P_1^{max}$, $0 \leq P_i(k) \leq P_i^{max}$ $(i = 2, 3, 4)$, where P_i^{max} $(i = 1, 2, 3, 4)$ denote the maximum values of energy flows.

(b) Energy flow from the PV generator $(P_{pv}(k))$ is no less than the sum of PV energy directly used on the load $(P_2(k))$ and the battery charge rate $(P_3(k))$, that is

$$P_{pv}(k) \geq P_2(k) + P_3(k).$$

(c) The SoC of the battery is restricted between its minimum and maximum values:

$$B_C^{min} \leq S_{oc}(k) \leq B_C^{max}.$$

(d) $P_3(k)$, and $P_4(k)$ should satisfy the additional constraint (4.7), which can be rewritten

as follows:

$$P_3(k) + P_4(k) < \sqrt{\frac{2-\alpha}{\lambda}}.$$

(e) Charging and discharging cannot happen at the same time, as is implied by [2].

Constraints (a)-(d) are convex, while constraint (e) is non-convex. To achieve convex optimization in MPC design, we divide constraint (e) into two switched cases: 1) charging ($P_4 = 0$), and 2) discharging ($P_3 = 0$).

4.3.4.1 Charging

The constraint (e) can be rewritten by

$$\begin{cases} P_4(k) & \leq 0, \\ P_4(k) & \geq 0. \end{cases}$$

Constraints (a), (b), (d) and (e) can be compactly rewritten by

$$M_{11}u(k) \leq \gamma_{11}, \tag{4.11}$$

where

$$M_{11} = \begin{bmatrix} -1 & 0 & 0 \\ 0 & -1 & 0 \\ \mathbf{0} & \mathbf{0} & \mathbf{-1} \\ \mathbf{0} & \mathbf{0} & \mathbf{1} \\ 1 & 0 & 1 \\ 1 & 1 & 0 \\ 1 & 0 & 0 \\ 0 & 1 & 0 \\ 0 & 0 & 1 \\ -1 & 0 & -1 \\ 0 & 1 & 1 \end{bmatrix}, \ \gamma_{11} = \begin{bmatrix} 0 \\ 0 \\ 0 \\ 0 \\ P_L(k) \\ P_{pv}(k) \\ P_2^{max} \\ P_3^{max} \\ P_4^{max} \\ P_1^{max} - P_L(k) \\ \sqrt{\frac{2-\alpha}{\lambda}} \end{bmatrix}.$$

Define the predictive control vector:

$$U(k) \triangleq [u^T(k), u^T(k+1|k), \cdots, u^T(k+N_c-1|k)]^T,$$

where $u(k+i|k)$ is the predicted value of u from the sampling time k, and N_c denotes the control horizon. Since each $u(k+i|k)$ in the predictive control vector $U(k)$ should satisfy

(4.11), it follows that $U(k)$ should satisfy

$$\bar{M}_{11}U(k) \leq \bar{\gamma}_{11}, \tag{4.12}$$

where

$$\bar{M}_{11} = \underbrace{\begin{bmatrix} M_{11} & & \\ & \ddots & \\ & & M_{11} \end{bmatrix}}_{N_c}, \ \bar{\gamma}_{11} = \begin{bmatrix} \gamma_{11} \\ \vdots \\ \gamma_{11} \end{bmatrix}.$$

Constraint (c) is expressed with respect to SoC; to facilitate the MPC design, it should be transformed into a form with respect to predictive control vector $U(k)$. After some derivations (presented previously), constraint (c) can be transformed into a compact form:

$$\bar{M}_2U(k) \leq \bar{\gamma}_2, \tag{4.13}$$

where

$$\bar{M}_2 = \begin{bmatrix} -B_m \\ B_m \end{bmatrix}, \bar{\gamma}_2 = \begin{bmatrix} (S_{oc}(k) - B_C^{min})\,[1, 1, \cdots, 1]^T \\ (B_C^{max} - S_{oc}(k))\,[1, 1, \cdots, 1]^T \end{bmatrix},$$

$$B_m(\hat{b}_m) = \underbrace{\begin{bmatrix} \hat{b}_m & 0 & \cdots & 0 \\ \hat{b}_m & \hat{b}_m & \ddots & \vdots \\ \vdots & & \ddots & 0 \\ \hat{b}_m & \hat{b}_m & \cdots & \hat{b}_m \end{bmatrix}}_{N_c}.$$

In (4.13), $S_{oc}(k)$ can be obtained in real-time, and the constraint is expressed with respect to the predictive control vector $U(k)$.

Combining constraints (4.12) and (4.13) yields constraints for MPC design in charging state:

$$\bar{M}_cU(k) \leq \bar{\gamma}_c \tag{4.14}$$

where $\bar{M}_c = [\bar{M}_{11}^T, \bar{M}_2^T]^T$, $\bar{\gamma}_c = [\bar{\gamma}_{11}^T, \bar{\gamma}_2^T]^T$.

4.3.4.2 Discharging

The constraint (e) is equivalent to

$$\begin{cases} P_3(k) & \leq 0, \\ P_3(k) & \geq 0. \end{cases}$$

Constraints (a), (b), (d) and (e) can be compactly written by $M_{12}u(k) \leq \gamma_{12}$, where

$$M_{12} = \begin{bmatrix} -1 & 0 & 0 \\ \mathbf{0} & \mathbf{-1} & \mathbf{0} \\ 0 & 0 & -1 \\ \mathbf{0} & \mathbf{1} & \mathbf{0} \\ 1 & 0 & 1 \\ 1 & 1 & 0 \\ 1 & 0 & 0 \\ 0 & 1 & 0 \\ 0 & 0 & 1 \\ -1 & 0 & -1 \\ 0 & 1 & 1 \end{bmatrix}, \ \gamma_{12} = \begin{bmatrix} 0 \\ 0 \\ 0 \\ 0 \\ P_L(k) \\ P_{pv}(k) \\ P_2^{max} \\ P_3^{max} \\ P_4^{max} \\ P_1^{max} - P_L(k) \\ \sqrt{\frac{2-\alpha}{\lambda}} \end{bmatrix}.$$

It follows that the predictive control vector $U(k)$ should satisfy $\bar{M}_{12}U(k) \leq \bar{\gamma}_{12}$, where

$$\bar{M}_{12} = \begin{bmatrix} M_{12} & & \\ & \ddots & \\ & & M_{12} \end{bmatrix}, \ \bar{\gamma}_{12} = \begin{bmatrix} \gamma_{12} \\ \vdots \\ \gamma_{12} \end{bmatrix}.$$

Consequently, constraints for MPC design in discharging state can be expressed by:

$$\bar{M}_d U(k) \leq \bar{\gamma}_d \tag{4.15}$$

where $\bar{M}_d = [\bar{M}_{12}^T, \bar{M}_2^T]^T$, $\bar{\gamma}_d = [\bar{\gamma}_{12}^T, \bar{\gamma}_2^T]^T$; $\bar{M}_2$ and $\bar{\gamma}_2$ are give by (4.13) to satisfy the constraint (c).

4.3.5 Control horizon

Switching time is predefined in this work according to load demand profile and PV power supply. The battery is in the state of charging, when the PV power supply exceeds the load demand in a certain hour; the battery is in the state of discharging, when the PV provides insufficient power for the load demand in a certain hour. On summer weekdays, for example, the battery switches from discharging to charging at 7:30, and from charging to discharging at 17:30.

In this work, control horizon and predictive horizon vary according to switching times. At a given time k, find the nearest switching time $T_k > k$. The control horizon and predictive

horizon for time k are given by

$$N_c(k) = N_p(k) = T_k - k. \tag{4.16}$$

4.3.6 Switched MPC algorithm

Standard linear MPC algorithm can be referred to [118]. With the linear state-space equations (4.9), the objective function (4.10) and the constraints (4.14) or (4.15), a switched MIMO MPC algorithm can be designed for the PDB hybrid system:

i. For time k, find the control horizon $N_c(k)$ and the predictive horizon $N_p(k)$ through (4.16).

ii. Optimization: find optimal $U(k)$, such that the following optimization problem is solved:

$$\begin{aligned} \min \quad & \left(U(k)^T E U(k) + 2HU(k)\right), \\ \text{s.t.:} \quad & (4.14) \text{ for the case of charging,} \\ \text{or} \quad & (4.15) \text{ for the case of discharging,} \end{aligned}$$

where E and H are MPC gains calculated based on the objective function (4.10). Detailed calculation of E and H is presented in previous sections (PE).

v. Receding horizon control:

$$u(k) = [I_{3\times 3}, 0, \cdots, 0]\, U(k).$$

vi. Update the estimated parameters $\hat{\eta}_c$ and $\hat{\eta}_d$ by using the proposed updating law (4.6).

vii. Set $k = k + 1$, and update system states, inputs and outputs with control $u(k)$ and state-space equations (4.9). Repeat steps i-vi until k reaches its predefined value.

Remark 4 *It should be noted that, although MPC is applied, the dispatching of the hybrid power system is fundamentally an optimization problem (instead of a control design problem); consequently, stability of the closed-loop system is not assured by the proposed adaptive switched MPC. However, states of the closed-loop system are guaranteed bounded, since the optimization in MPC is processed with constraints on P_1, P_2, P_3, P_4, and S_{oc}.*

Table 4.3: Values of system parameters

Notations	Values	Notations	Values
P_1^{max}	5 kW	B_c^{max}	54.5 kWh
P_2^{max}	5 kW	B_c^{min}	27.25 kWh
P_3^{max}	5 kW	η_c	0.8
P_4^{max}	5 kW	η_d	1.0

Table 4.4: Values of control parameters

Notations	Values	Notations	Values
c_1	1.0	λ (summer)	0.1
c_2	0.2	λ (winter)	0.2
c_3	0.8	α	0.01

4.4 SIMULATION AND DISCUSSION

In this section, simulation results of the PDB hybrid system with the proposed switched MPC are presented. The daily demand and PV power supply in a Zimbabwean clinic are listed in Tables 4.1 and 4.2, respectively. To test the performance of the closed-loop system with disturbances, it is assumed that actual demands are 20% larger than expected, and PV provides 20% less power than expected. Values of system parameters and control parameters are listed in Table 4.3 and Table 4.4, respectively. Initial values of $P_i(k)(i = 1, 2, 3, 4)$ are set to zeros. Initial values of SoC are set to $x_m(1) = 0.7B_C^{max}$.

4.4.1 Simulation results of the proposed switched MPC

For the proposed switched MPC with online estimation for uncertain parameters, initial values of estimated parameters are given by $\hat{\eta}_c(0) = 1.0$ and $\hat{\eta}_d(0) = 1.0$. "Interior Point" [119] is used as the numerical approach for solving optimization problem at each MPC cycle. The time spans of simulation cases are assigned to four days (96 hours).

On summer days, switching times are 7:30 (from discharging to charging) and 17:30 (from

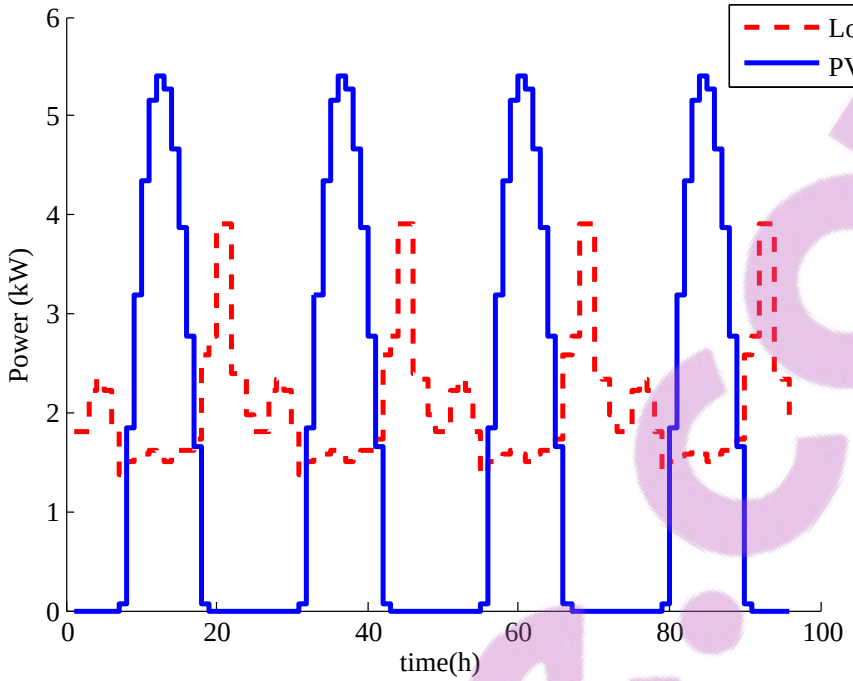

Figure 4.2: Load demand and PV power in summer

charging to discharging) every day. Results are displayed in Fig. 4.2 and 4.3. As can be seen from Fig. 4.2 and 4.3, whenever the PV power is sufficient for demands, it is used directly to satisfy demands, and the battery is in charging state. When PV power is insufficient, the battery switches into discharging state to satisfy the load demands. On summer days, it seems that PV power is quite sufficient, so that the DG is only used for covering the imbalance resulting from disturbances. The estimated parameters are found to converge to actual values of the uncertain parameters ultimately. This shows that PE is necessary for the estimated parameter to approach the uncertain parameter. Otherwise the estimated parameter will converge to other values that will affect negatively the performance of the closed loop system

On winter days, switching times are 8:30 (from discharging to charging) and 16:30 (from charging to discharging) every day. Results are shown in Fig. 4.4 and 4.5, where principles are similar to those in summer. The main difference in summer is that, PV power is relatively insufficient, and the DG covers the imbalance resulting from both insufficient PV power and external disturbances. The estimated parameters are also found converge to actual values of the uncertain parameters ultimately.

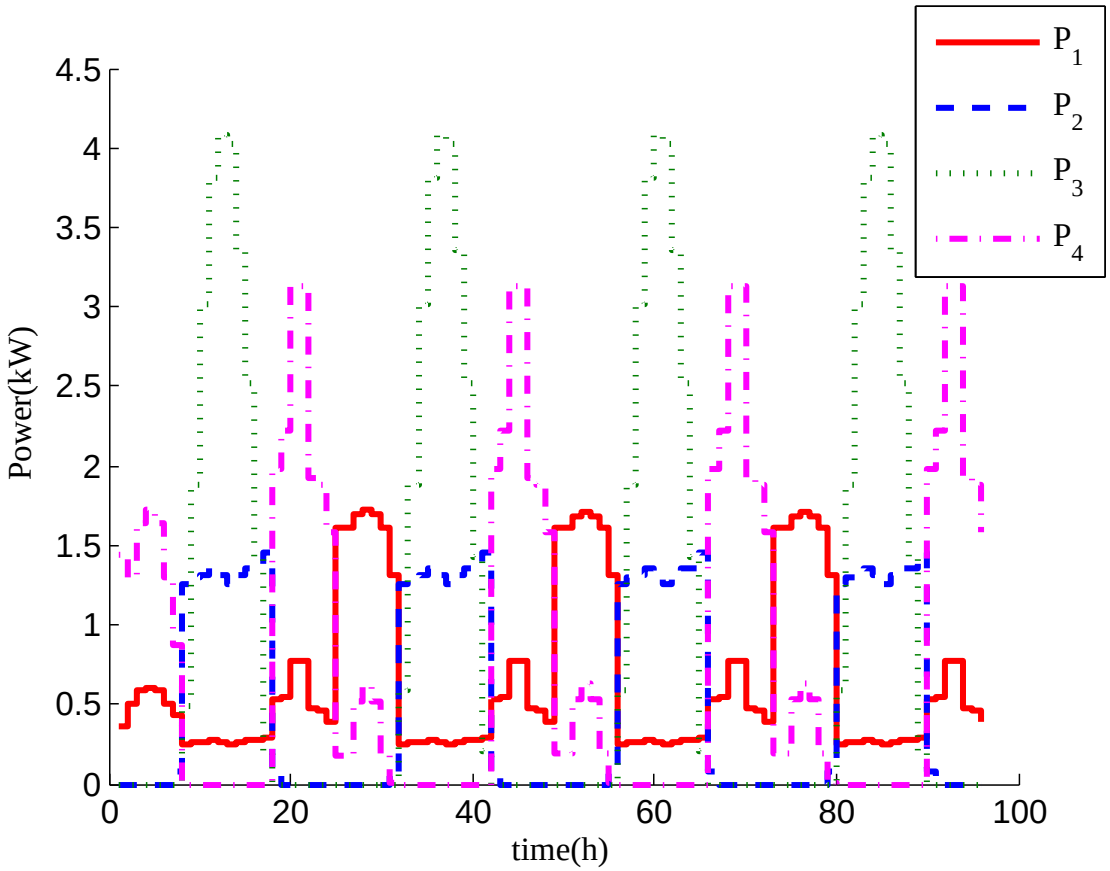

Figure 4.3: Energy flows of the closed-loop system (summer)

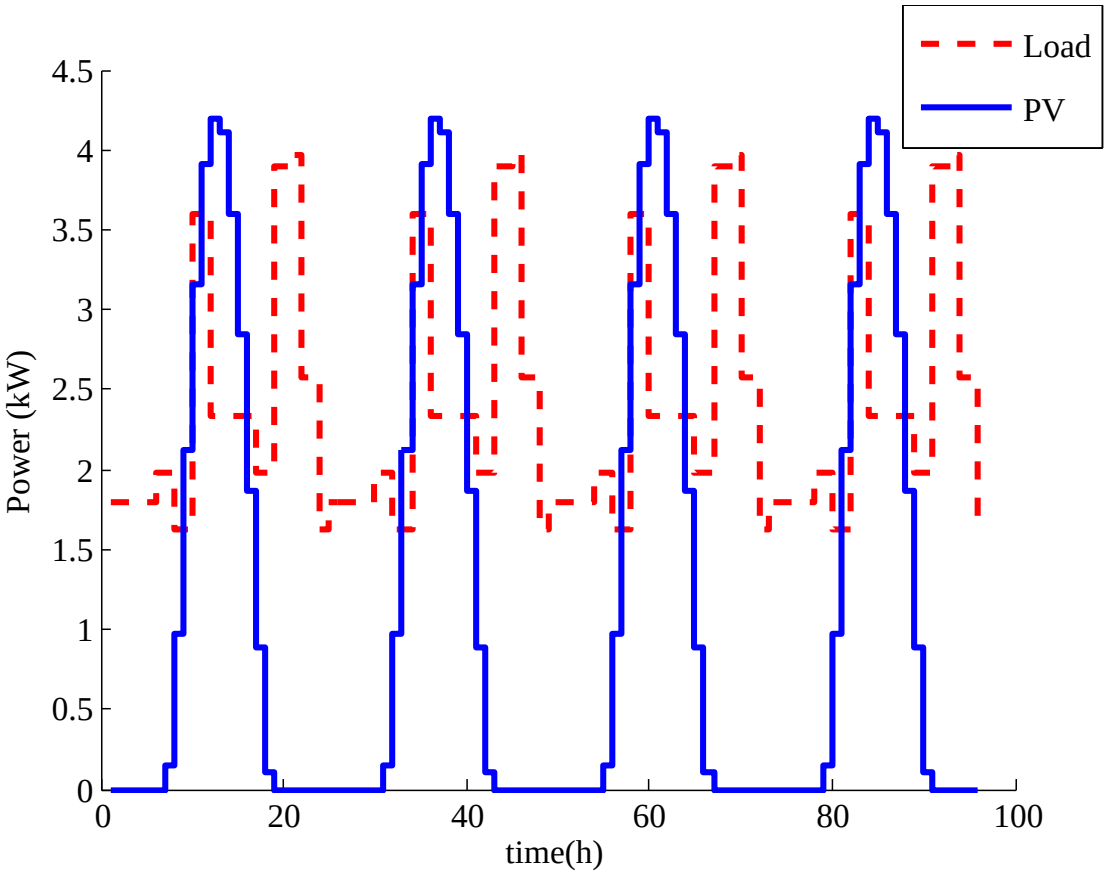

Figure 4.4: Load demand and PV power in winter

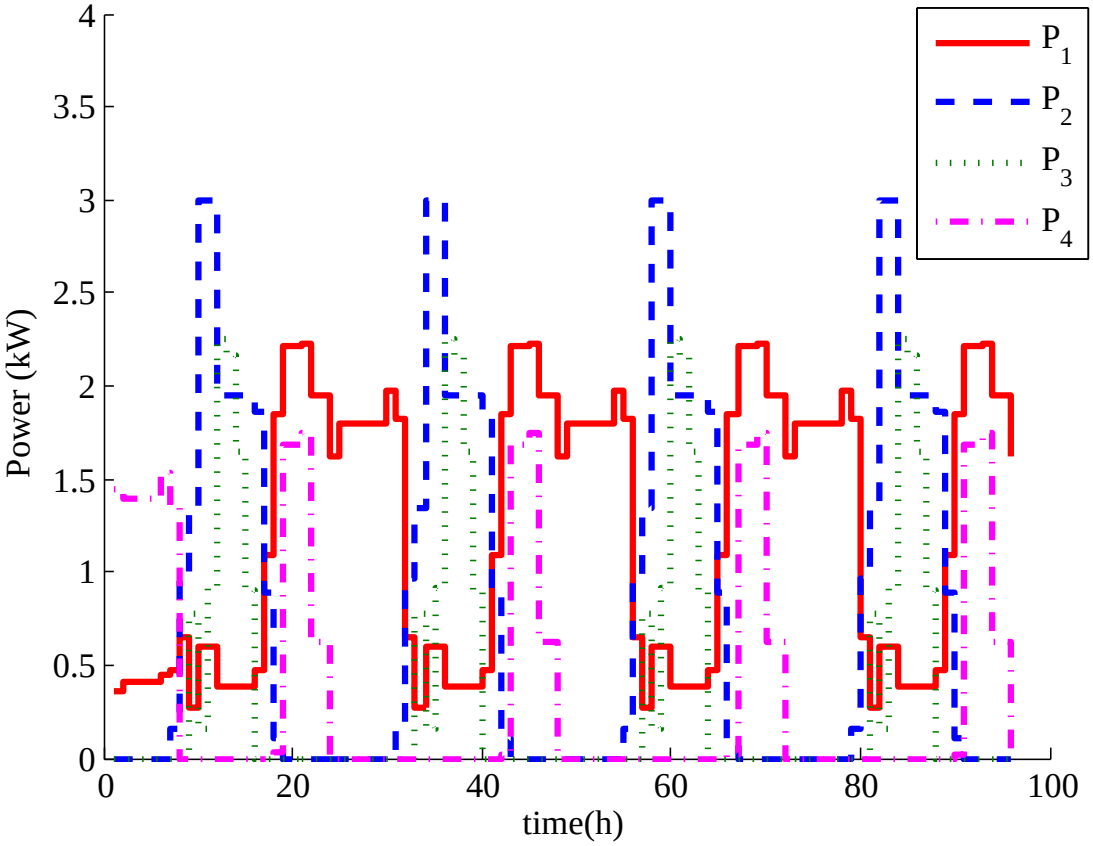

Figure 4.5: Energy flows of the closed-loop system (winter)

Table 4.5: Diesel energy consumptions (kWh) of PDB hybrid system with different strategies

	Summer	Winter
Adaptive switched MPC	63.7	118.4
Switched MPC	63.9	118.2
Intuitive strategy	68.0	125.3
Open loop optimal control	81.4	140.2

4.4.2 Comparisons and discussions

To illustrate performance of the proposed adaptive switched MPC, comparisons with other techniques are presented. The diesel consumptions of systems with different techniques are listed in Table 4.5.

The switched MPC without online estimation for uncertain parameters is designed by setting the nominal values to $\bar{\eta}_c = 1.0$ and $\bar{\eta}_d = 1.0$. As can be seen from Table 4.5, the result of the switched MPC without online estimation is fairly satisfactory. It is quite similar to that of the proposed switched MPC with online estimation, implying that the inherent robustness of MPC with respect to a certain degree of parametric uncertainties is acceptable.

The intuitive strategy can be described as follows: if sunlight is sufficient, PV array is used (P_2) to satisfy the load demand (P_L) as a priority. The PV array is also used for charging the battery bank (P_3) in case of sufficient supply for the load demand. When the sunlight is insufficient, the battery bank discharges to satisfy the load demand as the second choice, since battery power is cheaper than diesel power. Finally, if the load demand is too large for the PV array and battery bank to supply, the DG is operated to cover the imbalance. It can be indicated by the result listed in Table 4.5 that, the robustness of the proposed MPC with online estimation is superior over that of the intuitive strategy.

The open loop optimal control is designed by using the objective function and constraints of the proposed switched MPC, but without receding horizon control and online estimation. As can be seen from Table 4.5, the diesel consumption with open loop optimal control is the largest. The reason is that only one optimization is conducted at the very beginning of operation, without consideration of parametric uncertainties and external disturbances. In

Table 4.6: Diesel energy consumptions (kWh) of the closed-loop system with different battery capacities

B_C^{max}	43.6	49.1	54.5	60.0	65.4
Summer	81.3	68.1	63.9	60.2	56.7
Winter	125.3	121.8	118.4	114.9	111.5

contrast, with the proposed switched MPC, optimization is conducted in each sampling time with feedback of system states.

Another comparison can be conducted among systems with different battery capacities. As can be seen from results displayed in Table 4.6, total diesel energy consumption decreases, if the capacity of the battery bank can be increased. The reason is that, in case of larger battery capacity, the proposed MPC strategy would choose to store more PV power for future consumption rather than abandoning surplus PV power owing to the limit of the battery capacity, such that less diesel energy would be used for covering the imbalances.

4.5 CONCLUSION

A new switched MPC strategy is developed for energy dispatching of a PDB hybrid power system to ensure that simultaneous charging and discharging of the battery cannot take place. Different switched states of the battery are described by switched constraints, so that the hybrid system could be expressed by a unified linear MIMO state-space model, and the difficulty of constructing a complicated switched predictive state-space model is avoided. Uncertain battery parameters are estimated online with the adaptive updating law. Simulation results and comparisons with other strategies imply that the proposed switched MPC algorithm is satisfactory in dispatching energy usage for the PDB hybrid power system. In the next chapter battery wear cost will be incorporated into original optimal model.

CHAPTER 5

OPTIMAL POWER FLOW MANAGEMENT MODEL: CASE OF FUEL AND BATTERY WEAR COST MINIMIZATION

In this chapter an optimal energy management model of a solar PBD hybrid power supply system for off-grid applications is presented. The proposed model is a further development of the ones presented in the previous chapters which focused on minimizing only the fuel costs. The model minimizes fuel and battery wear costs and finds the optimal power flow, taking into account PV power availability, battery bank SoC and load power demand. The optimal solutions are compared for cases when the objectives are weighted equally and when a larger weight is assigned to battery wear. The work is mainly from author's published work [52]. The chapter is made up of the introduction, problem formulation, case study, results and discussion, as well as a conclusion.

5.1 INTRODUCTION

This work minimizes the operational cost of a PDB hybrid system in which lead-acid batteries are used. The main contribution is the consideration of battery wear cost, as battery wear has a great impact on battery life and this has not been considered in the optimization of RE-based distributed hybrid systems. The model considers hourly fuel and battery wear costs as components of the hybrid system operational cost. The results show the effect of the weighting factors on the system's operational cost and on the SoC of the battery. The effect of restricting the allowable DoD is also revealed, as this has a great impact on battery life.

The purpose of the PDB hybrid power system is to supply power to consumers reliably and economically, taking into account fuel and battery wear costs. This work is a follow-up of our previous work that considered only fuel costs, in [50], and also modeling of uncertainties, in [55]. Modeling of uncertainties is however not included in this paper. This paper is organized as follows: Section 2 describes the problem formulation, Section 3 is the case study and Section 4 covers the results and discussion; the last part is the conclusion.

5.2 PROBLEM FORMULATION

The PDB system is made up of the PV, DG and battery sub-systems and the configuration is as shown in Fig. 5.1. The DG supplies the load when the PV output, P_{pv}, the battery output or a combination of the two cannot meet the load. The control variables P_1 and P_2 represent the energy flows from the DG and from the PV generator and battery to the load respectively, while P_3 represents the power flow to and from the battery. Priority is given to the PV generator to supply the load. If the PV output is more than the load, charging power is supplied to the battery. When the PV output is low, the battery supplies power to the load to make up for the imbalance, provided it is within its operating limits. The DG comes on when the PV and/or battery cannot meet the load. The model is thus able to show the performance of the system in terms of battery dynamics and power flow from each sub-system at any given time interval. The sub-models in the following sub-sections are as described in our previous work [50], [111].

5.2.1 Sub-system models

The sub-system models for solar and DG are the same as used in chapter 3, but the sub-model of the battery is as follows:

The power output from the PV and the load demand at a given hour determine the charge or discharge power into and out of the battery bank. k is an integer representing the k^{th} hour interval. The SoC of the battery bank at the next time step , $SoC(k+1)$, depends on the current SoC, $SoC(k)$. At any given hour the battery SoC will be given by the expression:

$$SoC(k+1) = SoC(k) - \alpha P3(k), \tag{5.1}$$

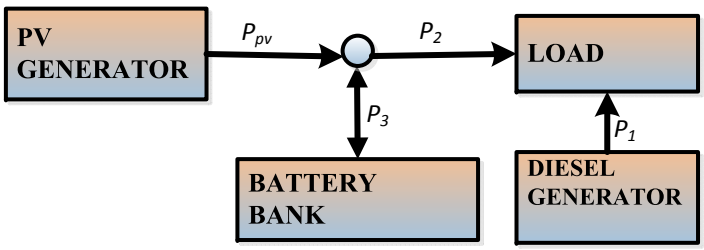

Figure 5.1: PDB configuration

in which $\alpha = \eta_B \Delta t / E^{max}$ and η_B is the battery round trip efficiency, while Δt is the time step. E is the capacity of the battery.

The following general expression applies to the battery dynamics:

$$SoC(k) = SoC(0) - \alpha \sum_{\tau=1}^{k} P_3(\tau), for 1 \leqslant \tau \leqslant k, \tag{5.2}$$

where $SoC(0)$ is the initial SoC of the battery.
$P_3(\tau)$ is the charge or discharge rate of the battery at time k.

The available battery bank capacity must not be less than the minimum allowable capacity $SoC^{\min}$ and must not be higher than the maximum allowable capacity $SoC^{\max}$ [22]:

$$SoC^{min} \leq SoC(k) \leq SoC^{max},$$

and

$$SoC^{min} = (1 - DoD) SoC^{max},$$

where DoD is expressed as a percentage.

5.2.2 Battery lifetime modeling

Modeling of the lifetime characteristics of battery energy storage systems is a vital aspect of hybrid power system simulation that has not been fully considered in many RE-based hybrid

energy management optimization studies [106]. The uncertainty associated with the expected lifetime of the batteries used in RE-based hybrid energy systems makes the estimates of cost of energy of the systems uncertain, as the life cycle cost of the batteries is one of the significant hybrid system expenses.

The two common lead acid batteries lifetime models are the post-processing models and the performance degradation models. The former are pure lifetime models in that they do not include a performance model and can be used to analyze measured data from real systems. The latter integrates a performance model with a lifetime model and the performance model is updated continuously during the simulation so that the performance of the battery can be analyzed depending on the utilization pattern of the battery [107]. There are various methods for calculating the lifetime consumption; these include the Ah-throughput and cycle counting methods. In this work the Ah-throughput counting method is employed to evaluate the lifetime consumption of the battery. This method assumes that a fixed amount of energy can be cycled through a battery before it requires replacement. The estimated throughput, λ_L (the total throughput over a battery bank lifetime), obtained mostly from the DoD vs. cycles to failure curve provided by the manufacturer, is expressed as follows [107]:

$$\lambda_L = DoD_i C_i E, \tag{5.3}$$

where E is the battery capacity, DoD_i is the DoD being considered, C_i represents the cycles to failure, and i represents each DoD and cycles to failure as given by the manufacturer. In [22], it is noted that the degradation of battery bank capacity depends most strongly on the interrelationships of the following parameters: the charging/discharging regime that the battery has experienced, the DoD of the battery over its life, its exposure to prolonged periods of low discharge and the average temperature of the battery over its lifetime. Battery wear is mainly determined by the cycles of the battery, that is, the battery completes a cycle when it is charged and discharged once. In a solar based system, the batteries are charged during the day and discharged at night and this cycle corresponds to one day.

For optimal control formulation, the total throughput of the battery bank over a daily time horizon, λ_D , is given by [120]:

$$\lambda_D = \frac{1}{2} \sum_{k=1}^{24} |P_3(k)|. \tag{5.4}$$

In order to understand any business model, the cost per cycle, measured in $\$/kWh/Cycle$, is important. This is obtained by considering the battery cost, which is the sum of the cost of batteries, transportation and installation costs (multiplied by the number of times the battery is replaced during the lifetime of the system). The sum of these costs is divided by the net consumption of the system. The battery bank operating cost over a given day as derived from literature is modeled as [121], [122]:

$$B_{op} = \frac{\lambda_D}{\lambda_L} C_b, \tag{5.5}$$

where B_{op} is the battery operational cost, and C_b is the cost of the battery bank. The battery wear cost, C_{bw}, is expressed as [122]:

$$C_{bw} = \frac{C_b}{\lambda_L}. \tag{5.6}$$

The battery bank life, B_L, is expressed as [23], [122], [123] :

$$B_L = \frac{\lambda_{yr}}{\lambda_L}, \tag{5.7}$$

where λ_{yr} denotes the annual throughput of the battery bank.

5.2.3 Diesel generator model

DGs are incorporated in hybrid power supply systems as back-ups. The DG energy dispatch strategy determines the switching on or off conditions and in this paper, a load-following strategy is employed in which the DG is switched on when the PV and/or the battery is unable to meet the load. In this strategy, the DG is dispatched only when required and this is economical in terms of usage of DG energy and fuel cost. The DG produces only enough power to meet the load demand and does not charge the battery. The DG is more likely to operate at high load factors, resulting in low specific fuel consumption and longer DG life [98]. In this work a variable speed Rush generator type is employed in which an electronic control system is used to vary the output by sensing the load and sending an electrical signal to the fuel injection system to adjust the fuel supply and engine revolutions in response to the load. The advantage of this type of generator is its ability to supply the required power output at any given time [50], [51]. The generator is also constrained by its lower and upper operating limits.

5.3 CASE STUDY

The solar radiation data used in this study are calculated from stochastically generated values of hourly global and diffuse irradiation using the simplified tilted-plane model of [71]. This is calculated for a Zimbabwean site, Harare (latitude 17.80°S) and the PV data are derived from our previous work [50]. A typical load demand profile for institutional applications based on an energy demand survey carried out in rural communities in Zimbabwe is used and the methodology for calculating the load demand profile is as described in [112] The load profile is as shown in Fig.5.2.

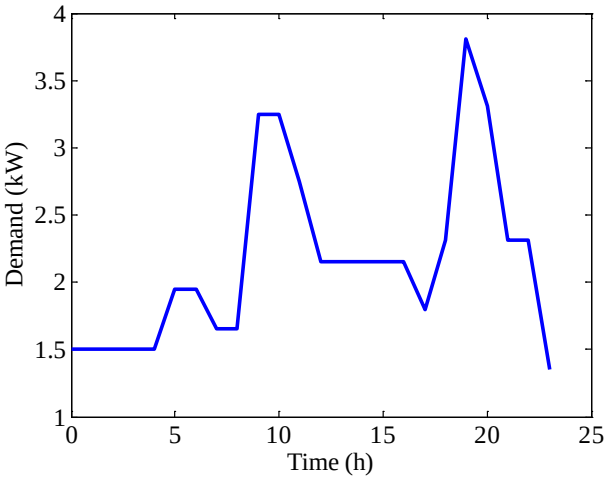

Figure 5.2: Typical demand profile

The parameters used in this model are shown in Table 5.1. The generator cost coefficients are specified by the manufacturer while the DG, PV and battery bank capacities are chosen based on a sizing model developed by [111]. The system is designed such that demand is met at any given time. A small system means demand will not always be met, while an oversized system means the demand will be met but the system will be unnecessarily costly and energy will be wasted. The sizing is within "'rule of thumb" provisions, for example the PV array area for 1 kWp varies from 7 m^2 to 20 m^2 depending on cell material used. The energy generated by the PV and the DG is consumed by the load, and the PV and WGs also charge the battery, depending on the instantaneous magnitude of the load and SoC of the storage battery. The DG on or off times depend on the DG energy dispatch strategy employed. In this work, the load-following strategy is employed whereby the DG switches on when the hourly output of PV is lower than the hourly load and the combined output of the

Table 5.1: Parameters

Battery capacity	40 kWh
Battery efficiency	85%
Battery allowable depth of discharge	50%
Battery purchase cost	\$65/kWh
Minimum state of charge	0.5
Maximum state of charge	1
Initial state of charge	0.6
PV array	47 m^2
DG capacity	5 kVA
System voltage	24 V
a	US \$0.246 /(kW)^{2}h
b	US \$0.1 /kWh
c	US \$0.01 /h
Fuel Cost	US\$1.2

battery and PV cannot meet the load.

5.3.1 Open loop optimal control model

In order to obtain an optimal operational scheme that balances the objectives in (5.8), a weighting method is employed to integrate the objectives into one. The sum of the weight coefficients w_1, w_2 and w_3 is 1 and weight factors indicate the objectives' significance. Each set of weights should generate one optimal solution. Various cases can be considered; however in this paper, two cases are elaborated, when the first two objectives are treated as equally important and when more weight is given to the battery wear cost. This problem is formulated as follows:

$$\min \sum_{k=1}^{N} (w_1 C_f (a P_1^2(k) + b P_1(k) + c) + w_2 C_{bw} |P_3(k)| - w_3 P_{pv}(k)) \tag{5.8}$$

subject to the following constraints:

$$P_1(k) + P_2(k) = P_L(k), \tag{5.9}$$

$$P_2(k) + P_3(k) \leq P_{pv}(k), \tag{5.10}$$

$$P_i^{min} \leq P_i(k) \leq P_i^{max}, \tag{5.11}$$

$$0 \leq P_1(k) \leq DG^{rated}, \tag{5.12}$$

$$P_3^{min} \leq P_3(k) \leq P_3^{max}, \tag{5.13}$$

$$SoC^{min} \leq SoC(0) - \alpha \sum_{\tau=1}^{k} P_3(\tau) \leq SoC^{max}, \tag{5.14}$$

for all $k = 1, \cdots, N$, where N is 24 and C_f is the fuel price. $w_1 - w_3$ are weight coefficients whose sum is 1. $SoC(0)$ is the initial SoC of the battery. P_i^{min} and P_i^{max} are the minimum and maximum limits for each variable. The optimization problem is solved in a MATLAB environment using the "quadprog" function. This solves problems in the form:

$$\min \frac{1}{2} x^T H x + f^T x,$$

subject to:

$$Ax \leq b,$$

$$A_{eq} x = b_{eq},$$

$$lb \leq x \leq ub.$$

The operation strategy is the same as in the previous chapter whereby the load demand is to be met by the PV generator. If the PV output is not enough to satisfy the load demand, the battery discharges to satisfy the load requirement. If the PV output is above the load requirement, the excess energy from the PV is stored in the battery until the full capacity of the batteries is reached. In some instances the solar PV power and/or battery bank power available is supplied to the load and the DG supplies the deficit in order to satisfy the load completely. The DG switches off when the PV and/or the battery bank can fully satisfy the load. The economic dispatch problem is to determine the optimum scheduling of generation at any given time that minimizes the fuel cost while completely satisfying the demand and operating limits

5.4 RESULTS AND DISCUSSION

Increasing the battery capacity reduces the DoD requirements, thus extending the life cycle of the batteries and reducing interim capital costs, but results in increased initial capital costs. Figs. 5.3 and 5.4 show the power flow in case 1: w_1 =0.45, w_2=0.45, and w_3 =0.1 while in case 2: w_1 =0, w_2 =0.9 and w_3 =0.1 respectively, revealing the effect of different optimal solutions on the operational cost. The power flows in Fig. 5.3 show that the DG operates only during the early hours of the morning when the SoC of the battery is at such a level that it cannot satisfy the load and the PV is not yet producing any output. During daytime, as soon as the PV can supply the load, the generator switches off completely. The PV system is able to satisfy the load and excess power is used to charge the battery. The total combined power from the PV system and from the battery bank is represented by Graph $P2$. Graph $P2$ shows that when the PV system ceases to generate power at the end of the daytime, the battery bank has been charged enough to satisfy the load on its own initially before the DG comes in to cover the imbalance when the battery gets depleted. In Fig. 5.4 the situation is different, as the DG supplies more power than in Fig. 5.3 in the early hours of the morning, and also continues to supply reduced power throughout the remainder of the day. The total power supplied to the load, PT, is represented by Graph PT to show the system power balance. Graph PT in both figures shows that the demand is always met completely at any given time, confirming the reliability of the hybrid system.

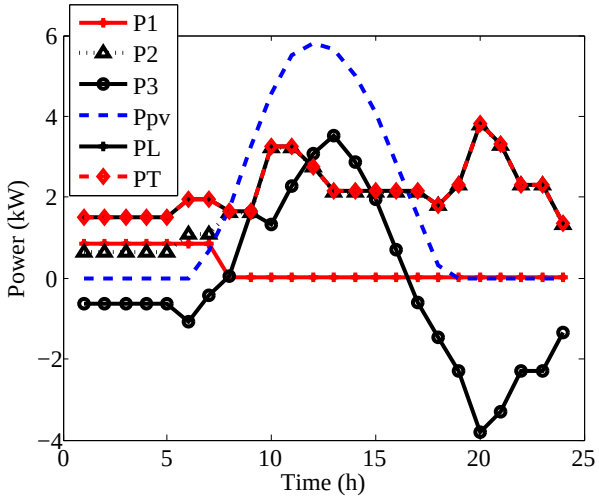

Figure 5.3: Optimal power flow for high radiation case 1

In Fig. 5.3, the objectives are treated as equally important, while in Fig. 5.4 fuel cost is given

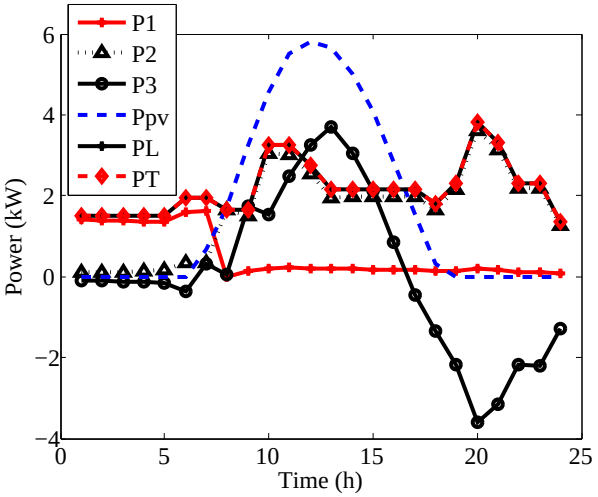

Figure 5.4: Optimal power flow for high radiation case 2

less weight. When the two cases are compared, there is a considerable increase of 43% in the annual operational cost in favor of the former case. The former case may be considered a more economic dispatch strategy that minimizes system operational costs. The latter case is an extreme case where fuel cost is given less weight, and the cost increase is due to increased usage of the DG, depicting the importance of balancing and prioritizing the objectives. In the latter case, the DG supplies the load continuously and this may be an unfavorable option for any decision maker, as it results in high DG operational cost and reduces the DG life. The system in this case limits the battery bank usage, resulting in battery life being prolonged at the cost of fuel and DG life. In such a case the DG supplies power during the early morning hours to complement what is coming from the battery. The optimization results thus provide a platform for designers, performance analyzers, control agents and decision makers who are faced with multiple objectives to make appropriate trade-offs, compromises or choices. The results demonstrate that the proposed model can be used to balance the system's operational cost effectively.

While Figs. 5.3 and 5.4 show the situation when the radiation output is high, Figs. 5.5 and 5.6 show cases where the radiation level is low in the two cases considered above. The major differences in the power flows are the increased usage of the DG to cater for the low power output from the PV system. In all cases shown in the figures the power output from the PV system is maximized. There is still a considerable increase in the operational cost for the weight factors considered. The system's operational costs are also higher than in the case of

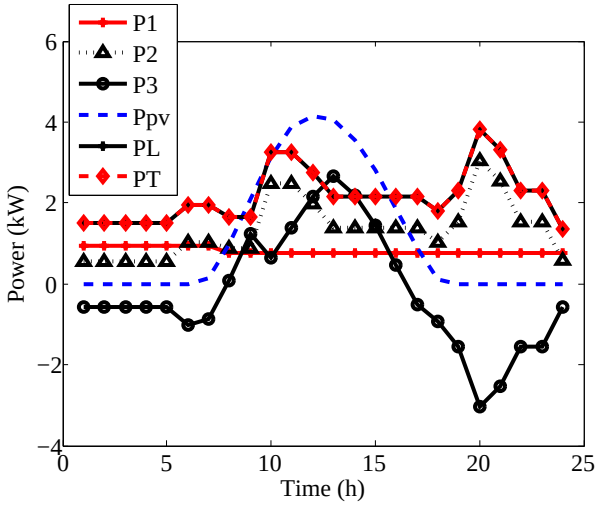

Figure 5.5: Optimal power flow for low radiation for case 1

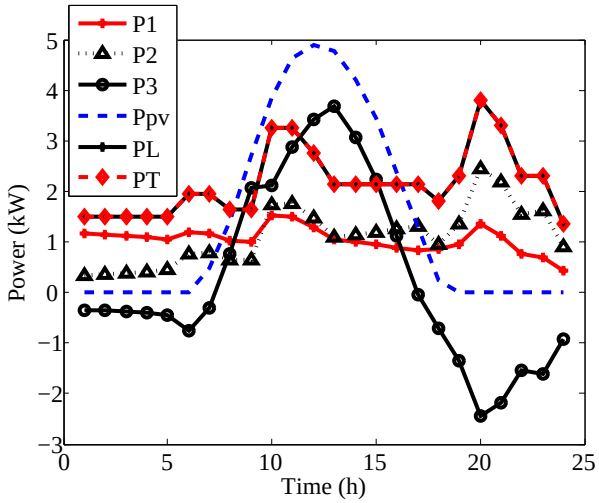

Figure 5.6: Optimal power flow for low radiation for case 2

high radiation owing to the increased fuel cost.

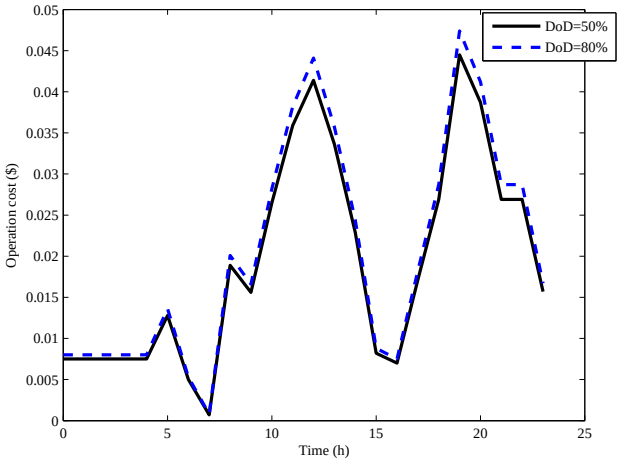

Figure 5.7: Comparison of battery wear costs at different DoDs

The daily battery operational costs are shown in Fig. 5.7 for each DoD, showing that the higher the DoD, the higher the battery operational cost. The relationship between battery operational cost and battery wear cost is as given in (5.5) and (5.6). It is therefore revealed that the operational cost increases owing to the increase in battery wear as the allowable DoD increases. Fig. 5.7 shows the fraction of the battery cost used in a 24-hour interval. The results show that during system design, it is important to restrict the allowable DoD, as this can improve the cycle life of the battery bank. It is thus shown that the more the battery works, the sooner it will fail, thus higher capacity withdrawal would result in a reduction of battery life cycle.

In Fig. 8 the SoCs of the battery bank are shown for the weighting factors considered in this work. It can be seen that although in all cases the battery bank operates within its limits, for case 1, SoC 1 and case 1, SoC 3, the battery bank is discharged more, while in case 2, SoC 2, and case 2, SoC 4, the battery operates at higher SoCs, as the system penalizes discharging. The less the battery is discharged, the less the cost per cycle, owing to the fact that the battery is operated at higher SoCs. The higher the SoC, the less the daily battery throughput, thus the battery bank is preserved more when discharging is penalized. In this work battery life increases, for instance for the high radiation case, from 4.6 years in Case 1 to nine years in Case 2. It is however important to note that Case 2 is not an ideal case, as it promotes more use of the DG. The results for the cases considered are given to illustrate the

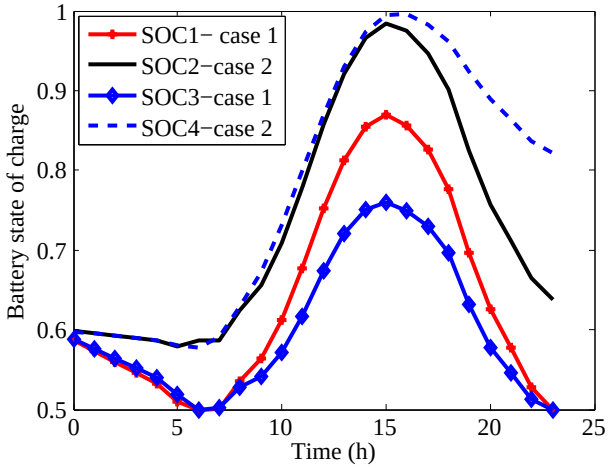

Figure 5.8: Comparison of battery states of charge

effect of limiting battery usage, for instance on fuel cost and on its life span. The results of this work provide a platform for decision makers to make informed decisions by considering various combinations of battery and fuel costs.

5.5 CONCLUSION

An optimal model of a PDB hybrid energy management system that minimizes both fuel costs and battery wear costs is presented. Insights into the significance of weight factors are provided and intuition suggests that when a larger weight is assigned to an objective, the optimization result favors that objective. The effect of DoD on battery wear cost has also been shown, confirming that limiting the allowable DoD can prolong battery life in RE based hybrid power supply systems. The optimal model results reveal how the system power flows change in response to the chosen combination of the components of the cost function. A practical platform for decision making has been presented. This chapter is based on open loop optimal control and no uncertainties are considered as it is unable to cater for them, hence the need for a closed loop system in the next chapter. The next chapter will constitute the final model, which incorporates wind energy. MPC methodologies will be applied and the optimal power flows will be evaluated by taking into account variations in RE sources and demand.

CHAPTER 6

ENERGY DISPATCH STRATEGY FOR A PHOTOVOLTAIC–WIND–DIESEL–BATTERY HYBRID POWER SYSTEM: A MODEL PREDICTIVE MODEL APPROACH

This chapter looks at a brief introduction, the hybrid system configuration, the MPC formulation for the PWDB hybrid system, the simulation results discussion and the conclusion. The work is mainly derived from author's published work [51]. An energy dispatch model that satisfies the load demand, taking into account the intermittent nature of the solar and wind energy sources and variations in demand described in which MPC techniques are applied in the management and control of such a power supply system. The emphasis is on the co-ordinated management of energy flow from the battery, wind, PV and diesel generators when the system is subject to disturbances. The results of the open loop model and the closed-loop model are compared in terms of the models' capability to attenuate against uncertainties and external disturbances in demand and renewable output. Diesel consumption is also compared for the winter and summer seasons.

6.1 INTRODUCTION

This work follows up on previous work presented in [50]. The major addition is the WG and the application of the receding horizon technique to the optimal energy management strategy of a PWDB hybrid power supply system. The work presents a more practical model when compared with the open loop model making it more favorable for real-time applications. The

optimal control model for the PWDB hybrid system is an open loop approach and there is no feedback on system states. Absence of feedback might render the system vulnerable to disturbances in both load demand and RE (solar and wind) energy. In this work, the MPC technique is applied to the open loop model for a PWDB hybrid power supply system with the aim of minimizing fuel costs, minimizing use of the battery and maximizing use of RE generators. The work considers the effect of daily energy consumption and RE variations on the system by introducing disturbances in the demand profiles and RE output for both winter and summer seasons. The multi-objective optimisation used in this work enables designers, performance analyzers, control agents and decision-makers who are faced with multiple objectives to make appropriate trade-offs, compromises or choices. Although an MPC strategy might be too sophisticated for individual domestic applications, it is certainly useful for institutional and industrial applications.

6.2 HYBRID SYSTEM CONFIGURATION

The PWDB hybrid power supply system considered in this work consists of the PV system, WG system, battery storage system and the DG, as shown in Figure 6.1. The supply priority is such that the load is initially met by the RE generators (PV and wind) and the battery comes in when the RE generators' output is not enough to meet the load, provided it is within its operating limits. The DG comes in when the RE and/or the battery cannot meet the load. The battery is charged when the total generated power is above the load requirements. The RE supplies the load and/or battery, depending on the instantaneous magnitude of the

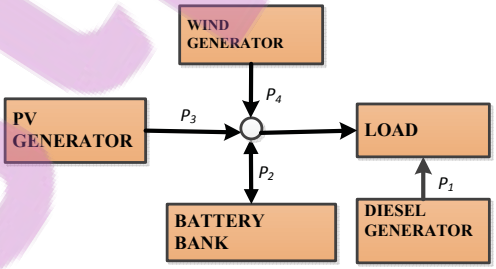

Figure 6.1: Schematic layout of the PV-wind-diesel-battery hybrid power supply system

load and the battery bank SoC. Control variables P_1, P_3 and P_4 respectively, represent the energy flows from the DG, PV and WG to the load at any hour (k), while P_2 represents the energy flow to and from the battery.

6.2.1 Sub-models

The PV, DG and battery models are described in detail in the preceding chapter where

$$P_{pv}(k) = \eta_{pv} A_c I_{pv}(k), \tag{6.1}$$

where η_{pv} is the efficiency of the PV array, $I_{pv}(k)$ (kWh/m^2) is the hourly solar irradiation incident on the PV array, A_c is the PV array area and $P_{pv}(k)$ is the hourly energy output from a PV generator [111]. The battery SoC is given by the expression:

$$SoC(k+1) = SoC(k) - \alpha(P_2(k)), \tag{6.2}$$

in which, $\alpha = \eta_B / B_C^{max}$ and η_B is the battery round trip efficiency while B_C^{max} is the maximum battery capacity. $SoC(k)$ is the current SoC of the battery. A variable speed DG is employed in this work because of its lower fuel consumption compared to the constant speed type and its ability to use optimum speed for a particular output power, resulting in higher efficiency of the generator operation. In this way, the engine is able to operate at relatively low speed for low power demand and vice versa [99].

The power output of a wind turbine depends on the wind speed pattern at the specific location, air density, rotor swept area and energy conversion efficiency from wind to electrical energy. The wind speed at the tower height can be calculated by using the power law equation as follows:

$$v_{hub}(k) = v_{ref}(k) \left(\frac{h_{hub}}{h_{ref}} \right)^{\beta}, \tag{6.3}$$

where $v_{hub}(k)$ is the hourly wind speed at the desired height h_{hub}, $v_{ref}(k)$ is the hourly wind speed at the reference height h_{ref} and β is the power law exponent that ranges from $\frac{1}{7}$ to $\frac{1}{4}$. $\frac{1}{7}$ is used in this work, which is typical for open land. Various models are used to simulate the wind turbine power output and in this work, the mathematical model used to convert hourly wind speed to electrical power is as follows [88]:

$$P_{wind} = 0.5 \eta_w \rho_{air} C_p A V^3, \tag{6.4}$$

where V is the wind velocity at hub height, ρ_{air} the air density, Cp the power coefficient of the wind turbine, which depends on the design, A the wind turbine rotor swept area, and η_w the WG efficiency as obtained from the manufacturer's data.

6.2.2 Open loop optimal control model

In this work, the WG and PV modules are modeled as variable power sources controllable in the range of zero to the maximum available power for a 24-hour interval. No operating costs are incorporated for the renewable energy sources. The DG is also modeled as a controllable variable power source with minimum and maximum output power. The battery bank is modeled as a storage entity with minimum and maximum available capacity levels. No battery operating costs are incorporated. Fuel consumption costs are modeled as a non-linear function of generator output power [14]. The optimisation problem is solved using the "quadprog" function in MATLAB.

The multi-objective function is given by the expression:

$$\min \sum_{k=1}^{N} (w_1(C_f(aP_1^2(k) + bP_1(k))) + w_2P_2(k) - w_3P_3(k) - w_4P_4(k)) \tag{6.5}$$

subject to the following constraints:

$$P_1(k) + P_2(k) + P_3(k) + P_4(k) = P_L(k), \tag{6.6}$$

$$P_i^{min} \leq P_i(k) \leq P_i^{max}, \tag{6.7}$$

$$0 \leq P_1(k) \leq DG^{rated}, \tag{6.8}$$

$$P_2^{min} \leq P_2(k) \leq P_2^{max}, \tag{6.9}$$

$$0 \leq P_3(k) \leq P_{pv}(k), \tag{6.10}$$

$$0 \leq P_4(k) \leq P_{wind}(k), \tag{6.11}$$

$$SoC^{min} \leq SoC(0) - \alpha \sum_{\tau=1}^{k} P_2(\tau) \leq SoC^{max}, \tag{6.12}$$

for all $k = 1, \cdots, N$, where N is 24 and C_f is the fuel price. $w_1 - w_4$ are weight coefficients whose sum is 1. Daily operational costs are considered, as they enable customers to make informed decisions before buying a given system, as stated earlier. The daily operational cost can then be extrapolated to get the weekly, monthly or yearly cost, but this is not within the scope of this work. $SoC(0)$ is the initial SoC of the battery.
$\alpha \sum_{\tau=1}^{k} P_2(\tau)$ is the power accepted and discharged by the battery at time k. P_i^{min} and P_i^{max} are the minimum and maximum limits for each variable.

6.2.3 Model parameters and data

The solar radiation data used in this study are calculated from stochastically generated values of hourly global and diffuse irradiation using the simplified tilted-plane model of [71]. This is calculated for a Zimbabwean site, Harare (latitude 17.80°S). Wind speed data measured at 10 m height at the site over a period of two years is used in this work. Two typical summer and winter load demand profiles for institutional applications based on an energy demand survey carried out in rural communities in Zimbabwe are used and the methodology for calculating the load demand profile is as described in [112]. These are as shown in Table 1.

Table 6.1: Summer and winter demand profiles

Time	Winter Load [kW]	Summer Load [kW]	Time	Winter Load [kW]	Summer Load [kW]
00:30	2.5	2.5	12:30	2.95	2.25
01:30	2.5	2.5	13:30	2.95	2.32
02:30	2.5	2.85	14:30	2.95	2.35
03:30	2.5	2.95	15:30	2.95	2.35
04:30	2.5	2.85	16:30	2.65	2.45
05:30	2.65	2.5	17:30	2.65	3.15
06:30	2.65	2.15	18:30	4.25	3.31
07:30	2.35	2.25	19:30	4.25	4.25
08:30	2.35	2.3	20:30	3.31	4.25
09:30	4.0	2.32	21:30	3.15	3.0
10:30	4.0	2.35	22:30	3.15	2.95
11:30	2.95	0.32	23:30	2.35	2.65

The model parameters and PV output data are as used in [111]. The generator cost coefficients are specified by the manufacturer while the DG, PV and battery bank capacities are chosen based on a sizing model developed by [111]. The system is designed such that demand is met at any given time. A small system means demand will not always be met while an oversized system means the demand will be met but the system will be unnecessarily costly and energy will be wasted. This work focuses mainly on the optimal energy management of any given system. The sizing is also within "'rule of thumb" provisions, for example PV array

area for 1 kWp varies from 7 m^2 to 20 m^2 depending on cell material used. A 5 kW Evoco endurance wind turbine is employed in this study. The energy generated by the PV, WG and DG is consumed by the load, and the PV and WGs also charge the battery, depending on the instantaneous magnitude of the load and SoC of the storage battery. The switching on or off times of the DG depend on the DG energy dispatch strategy employed, which is herein referred to as the load-following strategy. The DG switches on when the combined hourly output of PV and WG is lower than the hourly load and the combined output of the battery, WG and PV cannot meet the load.

6.3 MODEL PREDICTIVE CONTROL FOR THE PHOTOVOLTAIC-WIND-DIESEL-BATTERY HYBRID SYSTEM.

Optimal control for the PWDB hybrid system described above is an open loop approach, without feedback of system states. Absence of feedback might render the system vulnerable to disturbances (in both load demand, PV and wind energy).

In this section, a closed-loop linear MPC is proposed for the PWDB hybrid system, such that: 1) load demand at each sampling time is satisfied, 2) power provided by the DG is minimized, and 3) the closed-loop system is robust with respect to disturbances in both load demand and RE output.

6.3.1 Brief introduction of discrete linear MPC

Discrete linear MPC is a control approach for a given system expressed as follows:

$$x(k+1) = Ax(k) + Bu(k), \tag{6.13}$$

$$y(k) = Cx(k), \tag{6.14}$$

where $x \in R^n$, $u \in R^m$ and $y \in R^l$ are states, inputs and outputs, respectively. The MPC approach can minimize the cost function

$$J = \sum_{i=1}^{N_p} \left(y(k+i-1|k) - r(k+i-1)\right)^2 = (Y-R)^T(Y-R), \tag{6.15}$$

subject to constraint

$$Mu \leq \gamma, \tag{6.16}$$

where $Y(k) = [y^T(k), y^T(k+1|k), \ldots, y^T(k+N_p-1|k)]^T$, and $y(k+i|k)$ denotes the predicted value of y at step i $(i = 1, \ldots, N_p)$ from sampling time k; $R(k) = [r(k), r(k+1), \ldots, r(k+N_p-1)]$ is the predicted reference value for Y; N_p denotes the predicted horizon; and M and γ are matrices and vector with proper dimensions.

In this work, the control horizon is selected equal to the predicted horizon. Predicted states can be calculated by

$$\begin{aligned}
x(k+1|k) &= Ax(k) + Bu(k),\ y(k) = Cx(k),\\
x(k+2|k) &= Ax(k+1|k) + Bu(k+1|k)\\
&= A^2x(k) + ABu(k) + Bu(k+1|k),\\
&\vdots\\
x(k+N_p-1|k) &= \cdots = A^{N_p-1}x(k) + \sum_{i=1}^{N_p-1} A^{N_p-1-i}Bu(k+i-1|k),
\end{aligned}$$

and predicted outputs can be calculated by

$$Y(k) = [C, C, \ldots, C]X(k) = Fx(k) + \Phi U \tag{6.17}$$

where $X(k) = [x^T(k), x^T(k+1|k), \ldots, x^T(k+N_p-1|k)]^T$, $U(k) = [u^T(k), u^T(k+1|k), \ldots, u^T(k+N_p-1|k)]^T$, and

$$F = \begin{bmatrix} CA \\ CA^2 \\ \vdots \\ CA^{N_p} \end{bmatrix},\ \Phi = \begin{bmatrix} CB & 0 & \cdots & 0 \\ CAB & CB & & 0 \\ \vdots & & \ddots & \vdots \\ CA^{N_p-1}B & CA^{N_p-2}B & \cdots & CA^{N_p-N_c}B \end{bmatrix}. \tag{6.18}$$

Substitute (6.17) into (6.15). It can be deduced that minimizing (6.15) is equivalent to minimizing $\hat{J} = U^TEU + FU$, where

$$E = \Phi^T\Phi,\quad H = (Fx(k) - R(k))^T\Phi. \tag{6.19}$$

Numerical tools can be used to solve the optimization problem:

$$U = \arg\min_U U^TEU + FU,\qquad s.t.\ \ \bar{M}U \le \bar{\gamma}, \tag{6.20}$$

where the constraint is derived from (6.16).

The MPC is implemented by using receding horizontal control

$$u(k) = [I, 0, \ldots, 0]U, \tag{6.21}$$

where I is the identity matrix with proper dimension.

The key concept of MPC is that, in each time k, the control series $U(k)$ is calculated by using an optimal control technique, but only the first mth (the dimension of $u(k)$) element of $U(k)$ is implemented. Feedback is incorporated by minimizing the cost function. In the next time $k+1$, the performance of the closed-loop system can be assessed, and the control is recalculated and re-implemented based on updated information, such that unpredicted disturbances can be addressed.

6.3.2 Model transformation for MPC design

For typical MPC design, the PWDB model should be transformed into a linear state-space form, as given by (6.13) and (6.14). In this work, the charging (or discharging) rate of the battery ($P_2(k)$), the energy flow from PV ($P_3(k)$) and wind turbine ($P_4(k)$) are considered as the control inputs. Energy flow from the DG ($P_1(k) = P_L(k) - P_2(k) - P_3(k) - P_4(k)$) and the practical use of RE ($P_3(k) + P_4(k)$) are regarded as the outputs, where $P_L(k)$ denotes the load demands at the kth sampling time. The transformation process is carried out as outlined below.

Define $x_m(k) = SoC(k)$ and $u(k) = [P_2(k), P_3(k), P_4(k)]^T$. The transformation process can be started by considering the dynamic model of the battery:

$$x_m(k) = x_m(k-1) + b_m u(k-1), \tag{6.22}$$

where $b_m = [-\alpha, 0, 0]$. Define

$$y_m(k) = P_L(k) - P_1(k) = P_2(k) + P3(k) + P_4(k), \tag{6.23}$$

such that

$$y_m(k) = c_m x_m(k) + d_m u(k), \tag{6.24}$$

where $c_m = 0$ and $d_m = [1, 1, 1]$. From the definition of y_m, it can be seen that minimizing $\sum P_1$ ($P_1 > 0$) is equal to minimizing $\sum (P_L(k) - y_m(k))$.

Define an auxiliary output $y_a(k) = P_3(k) + P_4(k) = c_a x_m(k) + d_a u(k)$, where $c_a = 0$ and $d_a = [0, 1, 1]$. Usage of PV can be encouraged by minimizing $\sum (P_{pv}(k) + P_{wind} - y_a(k))$.

Define the augmented system states $x(k) = [x_m(k), y_m(k), y_a(k)]^T$ and the augmented output $y(k) = [y_m(k), y_a(k)]^T$. An augmented linear state space model can be obtained in the form of (6.13) and (6.14),

where

$$A = \begin{bmatrix} 1 & 0 & 0 \\ 0 & 0 & 0 \\ 0 & 0 & 0 \end{bmatrix}, \; B = \begin{bmatrix} -\alpha & 0 & 0 \\ 1 & 1 & 1 \\ 0 & 1 & 1 \end{bmatrix}, \; C = \begin{bmatrix} 0 & 1 & 0 \\ 0 & 0 & 1 \end{bmatrix}. \tag{6.25}$$

The augmented linear state-space equations are considered as the plant to be controlled by the MPC approach.

6.3.3 Objective function

The main objectives of the MPC control system are to minimize the use of the DG and to encourage the use of renewable energy. To this end, the objective function (or cost function) can be assigned as the sum of two parts:

1. $\min J_1 = \min \sum_k^{k+N_p} P_1^2(k) = \min \sum_k^{k+N_p} (P_L(k) - y_m(k))^2$, which indicates that usage of the DG should be minimized;

2. $\min J_2 = \min \sum_k^{k+N_p} (P_{pv}(k) + P_{wind}(k) - y_a(k))^2$, which implies that usage of renewable energy is encouraged.

Define the reference value $R(k) = [P_L(k), P_{pv}(k) + P_{wind}(k), P_L(k+1), P_{pv}(k+1) + P_{wind}(k+1), \ldots, P_L(k+N_p-1), P_{pv}(k+N_p-1) + P_{wind}(k+N_p-1)]^T$. The overall objective function is then given by

$$\min J = \min(J_1 + J_2) = \min \left(Y(k) - R(k)\right)^T \left(Y(k) - R(k)\right). \tag{6.26}$$

6.3.4 Constraints

Several types of constraints exist in this hybrid system:

1. Energy flows from generators and battery are non-negative values and are subjected to their maximum values: $0 \leq P_1(k) = P_L(k) - y_m(k) \leq P_1^{max}$, $0 \leq P_i(k) \leq P_i^{max}$ $(i = 3, 4)$, $-P_2^{max} \leq P_2(k) \leq P_2^{max}$, where P_i^{max} $(i = 1, 2, 3, 4)$ denote the maximum values of energy flows.

2. Energy flow from the PV generator ($P_{pv}(k)$) is no less than PV energy directly used on the load ($P_3(k)$): $P_{pv}(k) \geq P_3(k)$. Energy flow from the wind turbine ($P_{wind}(k)$) should be no less than the wind energy directly used on the load ($P_4(k)$): $P_{wind}(k) \geq P_4(k)$

3. Battery capacity is subjected to its minimum and maximum values: $B_C^{min} \leq x_m(k) \leq B_C^{max}$.

Constraints 1 and 2 can be rewritten into a compact form:

$$M_1 u(k) \leq \gamma_1, \tag{6.27}$$

where

$$M_1 = \begin{bmatrix} -1 & 0 & 0 \\ 0 & -1 & 0 \\ 0 & 0 & -1 \\ 1 & 1 & 1 \\ 0 & 1 & 0 \\ 0 & 0 & 1 \\ 1 & 0 & 0 \\ 0 & 1 & 0 \\ 0 & 0 & 1 \\ -1 & 0 & -1 \end{bmatrix}, \ \gamma_1 = \begin{bmatrix} P_2^{max} \\ 0 \\ 0 \\ P_L(k) \\ P_{pv}(k) \\ P_{wind}(k) \\ P_2^{max} \\ P_3^{max} \\ P_4^{max} \\ P_1^{max} - P_L(k) \end{bmatrix}. \tag{6.28}$$

They can be rewritten by using the control series

$$\bar{M}_1 U(k) \leq \bar{\gamma}_1, \tag{6.29}$$

where

$$\bar{M}_1 = \begin{bmatrix} M_1 & & \\ & \ddots & \\ & & M_1 \end{bmatrix}, \ \bar{\gamma}_1 = \begin{bmatrix} \gamma_1 \\ \vdots \\ \gamma_1 \end{bmatrix}. \tag{6.30}$$

For constraint 3, consider the battery dynamic equation (6.22), which can be written into

$$x_m(k+i|k) = x_m(k) + b_m \sum_{j=k}^{j\leq k+i} u(j), \tag{6.31}$$

or

$$X_m(k) = x_m(k)[1,1,\cdots,1]^T + B_m U(k), \tag{6.32}$$

where $X_m(k) = [x_m(k), x_m(k+1|k), \cdots, x_m(k+N_c-1|k)]^T$, and $x_m(k+i|k)$ denotes the predicted value of x_m from sampling time k; the matrix B_m has the following form:

$$B_m = \begin{bmatrix} b_m & 0 & \cdots & 0 \\ b_m & b_m & \ddots & \vdots \\ \vdots & & \ddots & 0 \\ b_m & b_m & \cdots & b_m \end{bmatrix}. \tag{6.33}$$

Consider the constraint for the battery. It then follows that

$$B_C^{min}[1,1,\cdots,1]^T \leq x_m(k)[1,1,\cdots,1]^T + B_m U(k) \leq B_C^{max}[1,1,\cdots,1]^T, \tag{6.34}$$

which can be further expressed by

$$\bar{M}_2 U(k) \leq \bar{\gamma}_2, \tag{6.35}$$

where

$$\bar{M}_2 = \begin{bmatrix} -B_m \\ B_m \end{bmatrix}, \bar{\gamma}_2 = \begin{bmatrix} (x_m(k) - B_C^{min})\,[1,1,\cdots,1]^T \\ (B_C^{max} - x_m(k))\,[1,1,\cdots,1]^T \end{bmatrix}. \tag{6.36}$$

Combining constraints (6.29) and (6.35) yields constraints in the form of (6.16), where

$$\bar{M} = [\bar{M}_1^T, \bar{M}_2^T]^T, \quad \bar{\gamma} = [\bar{\gamma}_1^T, \bar{\gamma}_2^T]^T. \tag{6.37}$$

6.3.5 MPC algorithm

With the linear state-space equations, the objective function and the constraints, a standard MPC algorithm can be applied to the PWDB hybrid system:

1. Calculate MPC gains E and H by using (6.18) and (6.19);

2. Conduct the optimization with objective function given by (6.15) subject to constraints (6.16), where $\bar{M}$ and $\bar{\gamma}$ are given by (6.37);

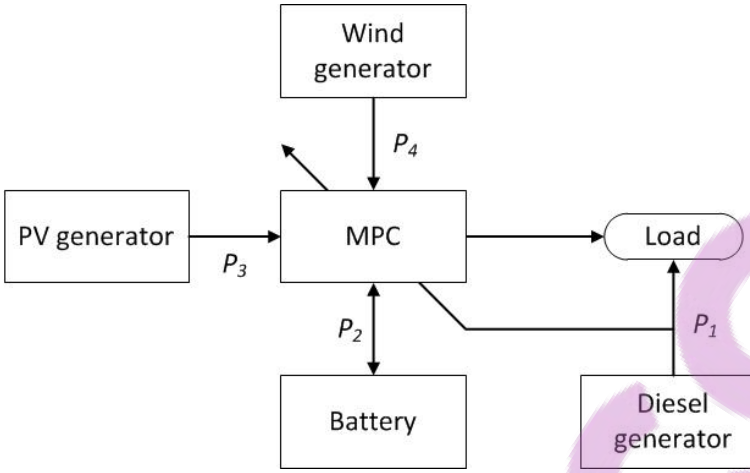

Figure 6.2: The closed-loop system for the PWDB hybrid system

3. Calculate and implement the receding horizontal control by using (6.21);

4. Set $k = k + 1$, and update system information with the control $u(k)$; repeat steps 1-5 until k reaches its predefined value.

Basic principles of MPC are given in Section 6.3.1. Detailed explanations and proofs concerning constrained MPC are outline in [118].

Based on the proposed MPC algorithm, the closed-loop system could be illustrated by Fig.6.2. Energy flows from the PV panel, the WG and the battery are dispatched by the proposed MPC, based on the information of diesel consumption. The inclined line implies that the real-time information of diesel consumption is fed back to MPC for decision making, but P_1 is not dispatched directly by MPC.

6.4 SIMULATION RESULTS AND DISCUSSION

In this section, simulation results of the PWDB hybrid system in different situations are presented. Data concerning the daily load demand and system parameters of the PWDB system for a Zimbabwean site are presented in Section 6.2.3. The initial values of $P_i(k)(i = 1, 2, 3, 4)$ are set to zeros. The initial values of the SoC are set to $x_m(1) = 0.5B_c^{max}$. The time spans of simulation cases are assigned to four days (96 hours).

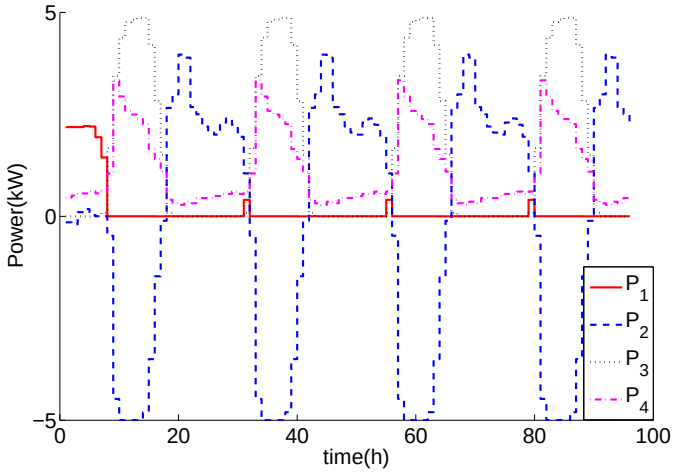

Figure 6.3: Simulation result of the closed-loop system without disturbances (in summer)

6.4.1 Simulation results of the PWDB hybrid system without disturbances

In this simulation case, MPC is simply applied to the ideal PWDB hybrid system without any disturbances. The results of the closed-loop system are displayed in Fig. 6.3 and Fig. 6.4.

From the figures, it can be seen that the closed-loop system can automatically schedule the use of the different generators to satisfy the demand load. With the effect of MPC, the hybrid system uses P_3 and P_4 as a priority when there is enough energy from PV and WG. At the same time, the surplus energy from PV and WG is utilized to charge the battery (negative P_2). In case of insufficient PV energy, the discharge of the battery (positive P_2) is used as a priority to meet the demand load. The DG (P_1) is operated as the final choice.

For comparison purposes, results of the open loop system without MPC are presented in Fig. 6.5 and Fig. 6.6. In open loop control, the optimization scheme is identical to that of the closed-loop MPC control, but without receding horizon control. It can be seen from the figures that, without disturbances, the performances of both controllers are fairly similar.

The consumption of diesel energy is indicated in Table 6.2. From the table, it seems that performances of the open loop system and the closed-loop system are almost the same in terms of diesel consumption.

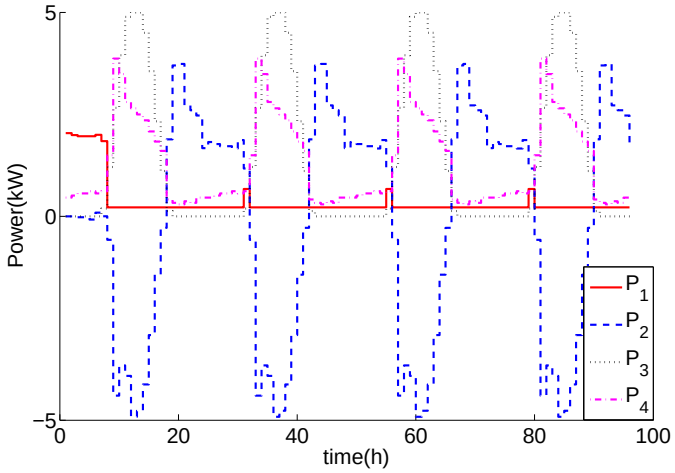

Figure 6.4: Simulation result of the closed-loop system without disturbances (in winter)

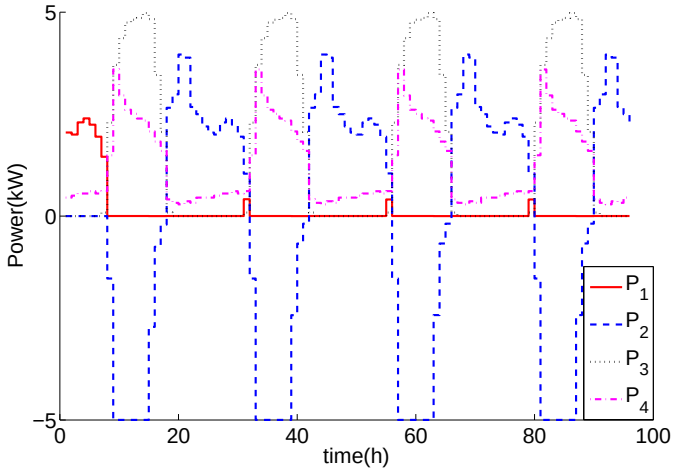

Figure 6.5: Simulation result of the open loop system without disturbances (in summer)

Table 6.2: Diesel energy consumption (kWh) of PWDB hybrid system without disturbances

	Closed-loop system	open loop system
Summer	15.61	15.66
Winter	30.63	30.92

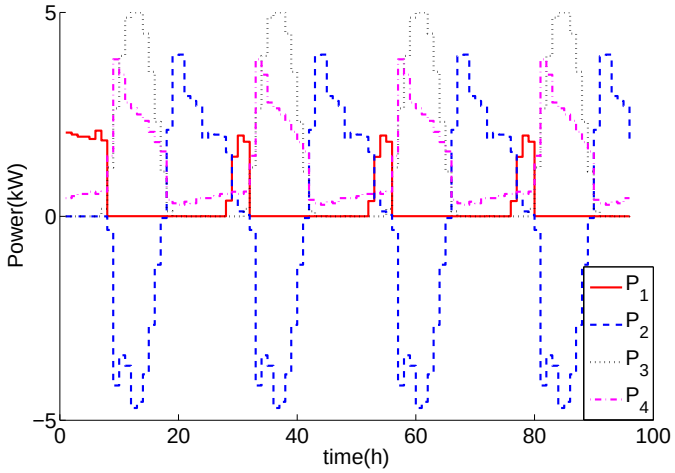

Figure 6.6: Simulation result of the open loop system without disturbances (in winter)

6.4.2 Results of the PWDB hybrid system with disturbances

The load demand and RE energy presented in Section 6.2.3 are only expectations based on previous experiences, and there are always disturbances resulting from weather conditions, disasters and migration. In this subsection, it is supposed that the hybrid system encounters a particularly bad condition: actual load demand is 20% greater than expected, and the energy provided by the PV and wind turbine is 20% less than expected.

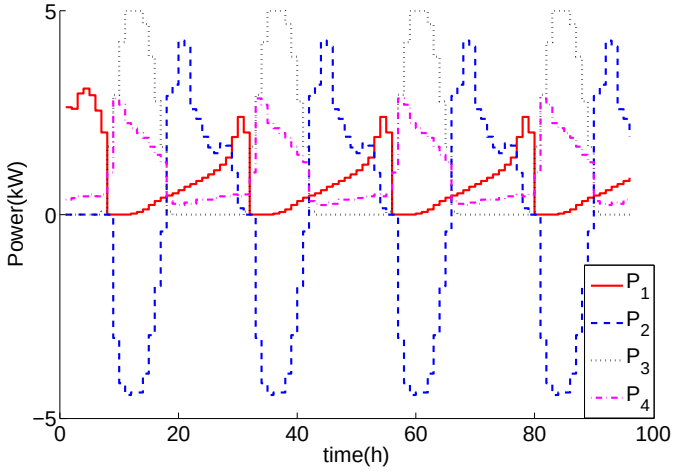

Figure 6.7: Simulation result of the closed-loop system with disturbances (in summer)

The performances of the closed-loop system with disturbances are displayed in Fig. 6.7 and

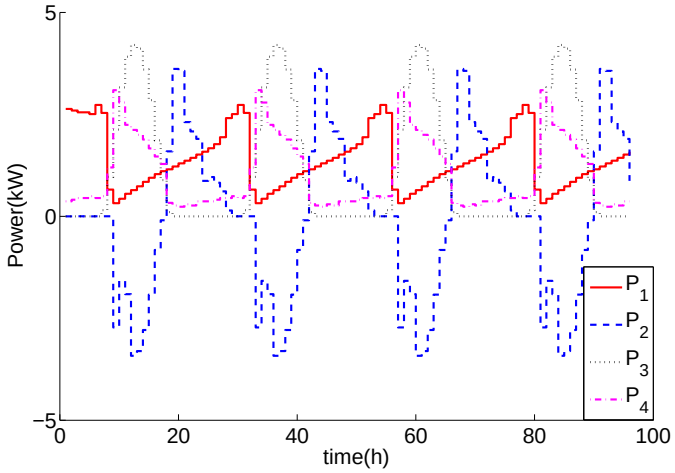

Figure 6.8: Simulation result of the closed-loop system with disturbances (in winter)

Fig. 6.8, and the performances of the open loop system with disturbances are illustrated by Fig. 6.9 and Fig. 6.10. It can be seen from the figures that the performances of the closed-loop system are generally better, indicating that its robustness with respect to disturbances is superior to that of the open loop system. The reason is that MPC is capable of predicting future states based on feedback of current states (which are influenced by disturbances). In contrast, open loop control is unable to respond to unpredictable disturbances, and it simply starts the DG when the load demand is greater than expected.

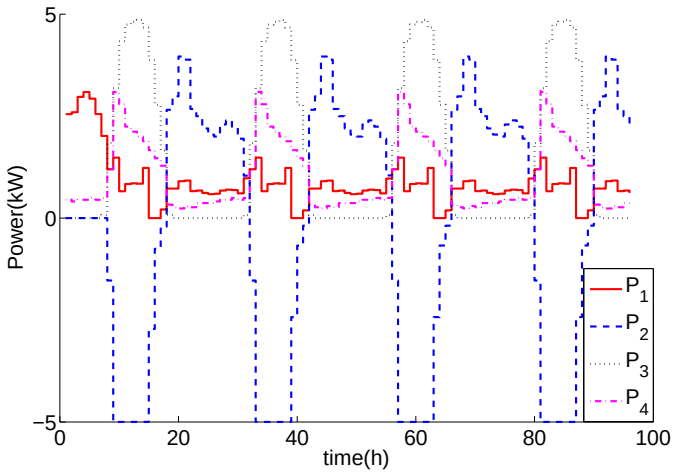

Figure 6.9: Simulation result of the open loop system with disturbances (in summer)

Diesel energy consumption is listed in Table 6.3 and also indicates that the performance and robustness of the closed-loop system are superior.

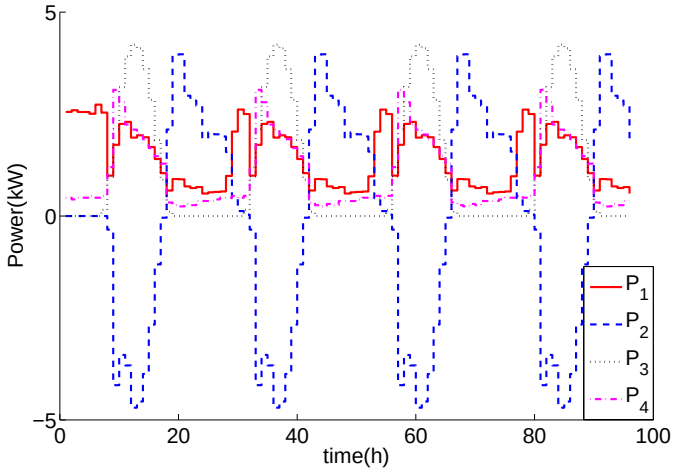

Figure 6.10: Simulation result of the open loop system with disturbances (in winter)

Table 6.3: Diesel energy consumption (kWh)of PWDB hybrid system with disturbances

	Closed-loop system	open loop system
Summer	75.62	83.17
Winter	132.11	137.32

6.5 CONCLUSION

The MPC technique has been applied to the energy management of a PWDB power supply system. Comparisons have been made of the performances of the open loop model and the MPC model without disturbances and with disturbances for both winter and summer times. The performances of the closed-loop system have been found to be generally better, indicating that its robustness with respect to disturbances is superior to that of the open loop system. The simulation results show promising applications of MPC approach in the energy dispatch problem. Although an MPC technique might be too sophisticated for individual domestic applications, it can be beneficial for institutional and industrial applications. The following chapter will deal with the final conclusion of all the work done in this thesis.

CHAPTER 7

CONCLUSIONS

This thesis presents an optimal planning and operational platform for hybrid energy systems for off-grid applications through the development of an optimal power flow management system for the hybrid system. The work enables optimization and coordination of the power flow among the hybrid power system components in order to satisfy the load requirements completely. Specific optimization cases considered in this thesis for minimizing system operational costs are ways of illustrating the benefits of energy management and system reliability provided RE-based hybrid systems. A brief summary of each chapter and the important conclusions are included in this chapter.

7.1 SUMMARY

In this thesis, each chapter has provided vital information that supports the the implementation of optimal energy management of RE hybrid energy systems in isolated areas or in an area where it is difficult to connect to the grid, with the objective of minimizing system operational cost and ensuring supply reliability.

Chapter 2 reviews literature with regards to modeling, optimization, and control studies of the PDB and PWDB hybrid systems in terms of what has been done by various authors and their applications. It goes further to review the system components, such as the DGs, battery storage, solar and wind energy generation including methodologies for incorporating the data for power output calculations. The need for the usage of DGs as back-up systems in hybrid energy systems is explored. The problems associated with the use of conventional constant speed DGs such as low part-load efficiency and minimum loading are explained

and act as motivating factors for the proposed usage of variable speed DGs. It explains how variable speed types of DGs can overcome these problems and the possibilities this offers in terms of fuel savings. It goes further to highlight the need for storage systems to cater for times when there is excess production by providing storage and for times of low production by supply power to the load to make up for the imbalance. In this respect usage of the lead acid battery in off-grid applications is motivated, as well as the need to improve battery life since these batteries are subjected to various operating conditions. The drivers for the usage of solar and wind energy resources are explored in light of their modularity and complementary characteristics though variable in nature, and in terms of the global need for use of clean, environmentally friendly technologies. The methodologies for incorporating the meteorological data in the RE sub-models are also explored.

In order to develop the energy management strategies and to investigate the performances of the RE hybrid systems, models were developed by way of upgrading the first one in Chapters 3-6. The optimization models, which include the objective function, constraints, parameters and the system configurations, are implemented in MATLAB. In chapter 3, the proposed hybrid system consists of the PV system, battery bank and DG, and considers the daily energy consumption variations for winter and summer weekdays and weekends in order to compare the corresponding fuel costs and evaluates the operational efficiency of the hybrid system for a 24-hour period. The model presents an open loop platform that gives a new dimension to the time correlation of intermittent renewable energy sources while minimizing fuel costs. A load following diesel dispatch strategy is employed and the fuel costs and power flows are analyzed. A comparison is made in terms of fuel savings achieved by the PDB hybrid model case and by the DG-only case, for winter and summer days.

Chapter 4 introduces a new adaptive switched MPC strategy for energy dispatching of a PDB hybrid power system, to ensure that the battery bank charge and discharge processes do not occur simultaneously. The distinguishing feature of the proposed switched MPC is that, new switched constraints are constructed to describe the different modes (charging and discharging) of the battery, such that the burden of using a switched MIMO state-space model could be circumvented. The parameters of the battery are unknown constants, and are estimated online with an adaptive updating law. In the switched MPC algorithm, the predictive horizon and the control horizon vary according to the predefined switching schedule. Based on optimization with the switched constraints, the receding horizon control is utilized to obtain

the dispatching strategy for the hybrid power system. The performance of the closed-loop system with the proposed switched MPC is verified by simulation results.

Chapter 5 deals with the need to improve battery life, as the battery constitutes a considerable cost during the life span of the project, since it needs to be replaced from time to time. The optimal energy management model of a solar PDB hybrid power supply system developed in the previous chapters is upgraded to cater for battery wear costs. The proposed model minimizes fuel and battery wear costs and finds the optimal power flow, taking into account PV power availability, battery bank state of charge and load power demand. The optimal solutions are compared for cases when the objectives are weighted equally and when a larger weight is assigned to battery wear. The model provides a platform for decision makers, as it considers trade-offs between the two conflicting objectives.

In chapter 6, the model is further developed into a PWDB hybrid system by incorporating wind energy. The energy dispatch model developed satisfies the load demand, taking into account the intermittent nature of the solar and wind energy sources and variations in demand. MPC techniques are applied in the management and control of such a hybrid power supply system with the aim of minimizing fuel costs, minimizing use of the battery and maximizing the use of RE generators. The emphasis is on the co-ordinated management of energy flow from the battery, wind, PV and diesel generators when the system is subject to disturbances. The results of the open loop model and the closed-loop model are compared in terms of the model capability to attenuate against uncertainties and external disturbances in demand and renewable output. Diesel consumption is also compared for the winter and summer seasons. This model presents a more practical solution to the energy dispatch problem and is evaluated using actual community load obtained from a survey carried out by the author in previous research works, as well as actual RE meteorological data for a Zimbabwean site. The simulation cases are run for a four-day period.

7.2 CONCLUSIONS AND CONTRIBUTIONS

An optimal energy dispatch model of a PDB hybrid system is presented and the optimal energy flows are analyzed. The optimization model developed is shown to achieve more savings than the diesel-only scenario. The results show how daily and seasonal variations in demand affect the operational cost of the PDB power supply system. For the both summer

and winter seasons, the weekend fuel costs are higher than weekday costs. Winter fuel costs are found to be higher than summer fuel cost owing to higher demand in winter and the lower winter radiation levels also mean more use of supplementary sources. This shows that daily and seasonal demand changes are important aspects to be considered, as they affect the operation cost and the energy flows considerably. It has been shown that the developed optimization model achieves optimal fuel costs and can be used in the analysis of the energy flows in any given system. A more practical estimate of the fuel costs reflecting variations of power consumption behavior patterns is thus presented in this thesis, which can be extrapolated to give an accurate estimate of the daily diesel fuel cost. In contrast to most previous works on hybrid systems, this work focuses on the minimization of the operational cost during a 24-hour period for a chosen diesel dispatch strategy. It looks at the optimization of the operation cost of the PDB power supply system from an energy efficiency perspective, as one of the key characteristics of energy efficiency is the search for optimality. As already mentioned, energy efficiency can be summarized as composed of performance efficiency, operational efficiency, equipment efficiency and technology efficiency. Operational efficiency is a system-wide measure, which is evaluated in this thesis by considering matching of different system components, time control and human coordination. Operational efficiency is improved through mathematical optimization and optimal control approaches implemented. In this work the operational efficiency is also measured in monetary terms so as to minimize the fuel cost. Another import aspect emphasized in this work is that unlike most works in literature, this work does not assume a constant load or a uniform daily operational cost, which does not reflect the variation of radiation output throughout the year and varying consumption patterns. The model can thus assist solar energy practitioners or companies to give consumers accurate estimates of fuel costs they will expect to incur daily, seasonally and yearly.

The optimal model that minimizes both fuel costs and battery wear costs is also a unique approach that has been proposed. The main contribution in this case is the consideration of battery wear cost, as battery wear has a great impact on battery life and this has not been considered in the optimization of RE-based distributed hybrid systems. It gives insights into the significance of the use of weight factors, and intuition suggests that when a larger weight is assigned to an objective, the optimization result favors that objective. The effect of DoD on battery wear cost is also been shown, and the effect of restricting the allowable DoD is

revealed, as this has a great impact in terms of prolonging battery life in renewable based hybrid power supply systems. The optimal model results reveal how the system power flows change in response to the chosen combination of the components of the cost function. This work thus presents a practical platform for decision makers, as it considers hourly fuel and battery wear costs as part of the hybrid system operational cost. The results of this work thus enable consumers and practitioners to obtain ideas of the system operations and also to appreciate the need for optimal control of the system.

The application of the receding horizon technique to the optimal energy management strategy of a PWDB hybrid power supply system is an important aspect that has not been explored for this particular configuration. This thesis thus presents a more practical model when compared with the open loop model, making it more favorable for real-time applications. The paper considers the effect of daily energy consumption and RE variations on the system by introducing disturbances in the demand profiles and RE output for winter and summer seasons. The multi-objective optimization used in this work enables designers, performance analyzers, control agents and decision-makers who are faced with multiple objectives to make appropriate trade-offs, compromises or choices. Although an MPC strategy might be too sophisticated for individual domestic applications, it is certainly useful for institutional and industrial applications. The performance of the closed-loop system has been found to be generally better, indicating that its robustness with respect to disturbances is superior to that of the open loop system. The simulation results show promising applications of the MPC approach in the energy dispatch problem. The main contributions of the switched MPC are the modeling of the optimal dispatching problem into a control problem that can be solved by the approach of MPC, so that the closed-loop system could benefit from advantages such as feedback and prediction; description of switched modes (charge and discharge) of the battery by switched constraints (instead of the switched state-space model), such that a unified linear MIMO state-space model could be used to design a simple predictive model; and adaptive parameters with updating law are employed to estimate uncertain constant parameters of the battery. Simulation results demonstrate that, with the proposed switched MPC strategy, the energy efficiency of the closed-loop system is satisfactory.

Future work may constitute an extension of the work to include a techno-economic analysis of the system, taking into account various cost combinations. Reduced time steps may also be the subject of future work for locations that have suitable data, as the current one-hour

time step is somewhat coarse. The thesis considers solar PV, wind, DG and lead acid battery storage systems; further development of this work may incorporate more RE and storage technologies. The model may be upgraded to cater for thermal loads by including solar thermal and other clean thermal technologies; and the model and actual experimental results may be compared. The hybrid system may also be grid-tied to sell any excess power to the grid and/or use grid power during off-peak periods in the absence of the DG system.

REFERENCES

[1] H. Post and M. Thomas, "Photovoltaic systems for current and future applications," *Solar Energy*, vol. 41, no. 5, pp. 465–473, 1988.

[2] S. Shaahid and M. Elhadidy, "Economic analysis of hybrid photovoltaic–diesel–battery power systems for residential loads in hot regions: A step to clean future," *Renewable and Sustainable Energy Reviews*, vol. 12, no. 2, pp. 488–503, 2008.

[3] R. Battisti and A. Corrado, "Evaluation of technical improvements of photovoltaic systems through life cycle assessment methodology," *Energy*, vol. 30, no. 7, pp. 952–967, 2005.

[4] G. N. Tiwari and S. Dubey, *Fundamentals of Photovoltaic Modules and Their Applications*. RSC Publishing„ 2010, no. 2, Cambridge.

[5] A. Roy, S. B. Kedare, and S. Bandyopadhyay, "Application of design space methodology for optimum sizing of wind–battery systems," *Applied Energy*, vol. 86, no. 12, pp. 2690–2703, 2009.

[6] M. Datta, T. Senjyu, A. Yona, T. Funabashi, and C.-H. Kim, "A coordinated control method for leveling pv output power fluctuations of pv–diesel hybrid systems connected to isolated power utility," *IEEE Transactions on Energy Conversion*, vol. 24, no. 1, pp. 153–162, 2009.

[7] Y.-Y. Hong and R.-C. Lian, "Optimal sizing of hybrid wind/pv/diesel generation in a stand-alone power system using markov-based genetic algorithm," *IEEE Transactions on Power Delivery*, vol. 27, no. 2, pp. 640–647, 2012.

[8] S. Agrawal and A. Tiwari, "Experimental validation of glazed hybrid micro-channel solar cell thermal tile," *Solar Energy*, vol. 85, no. 11, pp. 3046–3056, 2011.

[9] M. Deshmukh and S. Deshmukh, "Modeling of hybrid renewable energy systems," *Renewable and Sustainable Energy Reviews*, vol. 12, no. 1, pp. 235–249, 2008.

[10] H. Yang, Z. Wei, and L. Chengzhi, "Optimal design and techno-economic analysis of a hybrid solar–wind power generation system," *Applied Energy*, vol. 86, no. 2, pp. 163–169, 2009.

[11] M. Elhadidy and S. Shaahid, "Optimal sizing of battery storage for hybrid (wind+ diesel) power systems," *Renewable Energy*, vol. 18, no. 1, pp. 77–86, 1999.

[12] R. Dufo-Lopez and J. L. Bernal-Agustín, "Design and control strategies of pv-diesel systems using genetic algorithms," *Solar Energy*, vol. 79, no. 1, pp. 33–46, 2005.

[13] R. Belfkira, L. Zhang, and G. Barakat, "Optimal sizing study of hybrid wind/pv/diesel power generation unit," *Solar Energy*, vol. 85, no. 1, pp. 100–110, 2011.

[14] M. Muselli, G. Notton, and A. Louche, "Design of hybrid-photovoltaic power generator, with optimization of energy management," *Solar Energy*, vol. 65, no. 3, pp. 143–157, 1999.

[15] J. Talaq, F. El-Hawary, and M. El-Hawary, "A summary of environmental/economic dispatch algorithms," *IEEE Transactions on Power Systems*, vol. 9, no. 3, pp. 1508–1516, 1994.

[16] H. Dagdougui, R. Minciardi, A. Ouammi, M. Robba, and R. Sacile, "Modeling and optimization of a hybrid system for the energy supply of a green building," *Energy Conversion and Management*, vol. 64, pp. 351–363, 2012.

[17] M. Bouzerdoum, A. Mellit, and A. Massi Pavan, "A hybrid model (sarima–svm) for short-term power forecasting of a small-scale grid-connected photovoltaic plant," *Solar Energy*, vol. 98, pp. 226–235, 2013.

[18] D. Jenkins, J. Fletcher, and D. Kane, "Lifetime prediction and sizing of lead–acid

batteries for microgeneration storage applications," *IET Renewable Power Generation*, vol. 2, no. 3, pp. 191–200, 2008.

[19] V. Svoboda, H. Wenzl, R. Kaiser, A. Jossen, I. Baring-Gould, J. Manwell, P. Lundsager, H. Bindner, T. Cronin, P. Nørgård *et al.*, "Operating conditions of batteries in off-grid renewable energy systems," *Solar Energy*, vol. 81, no. 11, pp. 1409–1425, 2007.

[20] R. W. Wies, R. A. Johnson, A. N. Agrawal, and T. J. Chubb, "Simulink model for economic analysis and environmental impacts of a pv with diesel-battery system for remote villages," *IEEE Transactions on Power Systems*, vol. 20, no. 2, pp. 692–700, 2005.

[21] M. S. Adaramola, M. Agelin-Chaab, and S. S. Paul, "Analysis of hybrid energy systems for application in southern ghana," *Energy Conversion and Management*, vol. 88, pp. 284–295, 2014.

[22] R. Kaiser, "Optimized battery-management system to improve storage lifetime in renewable energy systems," *Journal of Power Sources*, vol. 168, no. 1, pp. 58–65, 2007.

[23] D. Jenkins, J. Fletcher, and D. Kane, "Model for evaluating impact of battery storage on microgeneration systems in dwellings," *Energy Conversion and Management*, vol. 49, no. 8, pp. 2413–2424, 2008.

[24] Y. Riffonneau, S. Bacha, F. Barruel, and S. Ploix, "Optimal power flow management for grid connected pv systems with batteries," *IEEE Transactions on Sustainable Energy*, vol. 2, no. 3, pp. 309–320, 2011.

[25] C. A. Hernandez-Aramburo, T. C. Green, and N. Mugniot, "Fuel consumption minimization of a microgrid," *IEEE Transactions on Industry Applications*, vol. 41, no. 3, pp. 673–681, 2005.

[26] R. Dufo-Lopez, J. L. Bernal-Agustin, J. M. Yusta-Loyo, J. Dominguez-Navarro, I. J. Ramirez-Rosado, J. Lujano, and I. Aso, "Multi-objective optimization minimizing cost and life cycle emissions of stand-alone pv–wind–diesel systems with batteries storage," *Applied Energy*, vol. 88, no. 11, pp. 4033–4041, 2011.

[27] C. Dennis Barley and C. Byron Winn, "Optimal dispatch strategy in remote hybrid power systems," *Solar Energy*, vol. 58, no. 4, pp. 165–179, 1996.

[28] K. Sopian, A. Zaharim, Y. Ali, Z. M. Nopiah, R. J. Ab, and M. N. Salim, "Optimal operational strategy for hybrid renewable energy system using genetic algorithms," *WSEAS Transactions on Mathematics*, no. 4, 2008.

[29] A. Elaiw, X. Xia, and A. Shehata, "Application of model predictive control to optimal dynamic dispatch of generation with emission limitations," *Electric Power Systems Research*, vol. 84, no. 1, pp. 31–44, 2012.

[30] J. Lee and Z. Yu, "Tuning of model predictive controllers for robust performance," *Computers & Chemical Engineering*, vol. 18, no. 1, pp. 15–37, 1994.

[31] A. Kaabeche and R. Ibtiouen, "Techno-economic optimization of hybrid photovoltaic/wind/diesel/battery generation in a stand-alone power system," *Solar Energy*, vol. 103, pp. 171–182, 2014.

[32] A. Vahidi, A. Stefanopoulou, and H. Peng, "Current management in a hybrid fuel cell power system: A model-predictive control approach," *IEEE Transactions on Control Systems Technology*, vol. 14, no. 6, pp. 1047–1057, 2006.

[33] X. Xia, J. Zhang, and A. Elaiw, "An application of model predictive control to the dynamic economic dispatch of power generation," *Control Engineering Practice*, vol. 19, no. 6, pp. 638–648, 2011.

[34] J. Zhang and X. Xia, "A model predictive control approach to the periodic implementation of the solutions of the optimal dynamic resource allocation problem," *Automatica*, vol. 47, no. 2, pp. 358–362, 2011.

[35] J. Siroky, F. Oldewurtel, J. Cigler, and S. Prívara, "Experimental analysis of model predictive control for an energy efficient building heating system," *Applied Energy*, vol. 88, no. 9, pp. 3079–3087, 2011.

[36] E. Gallestey, A. Stothert, M. Antoine, and S. Morton, "Model predictive control and the optimization of power plant load while considering lifetime consumption," *IEEE*

Transactions on Power Systems, vol. 17, no. 1, pp. 186–191, 2002.

[37] X. Zhuan and X. Xia, "Development of efficient model predictive control strategy for cost-optimal operation of a water pumping station," *IEEE Transactions on Control Systems Technology*, vol. 21, no. 4, pp. 1449–1454, 2013.

[38] L. Xie and M. D. Ilic, "Model predictive dispatch in electric energy systems with intermittent resources," in *Proceedings of IEEE International Conference on Systems, Man and Cybernetics*. IEEE, 2008, pp. 42–47, Singapore .

[39] H. Zhang, X. Xia, and J. Zhang, "Optimal sizing and operation of pumping systems to achieve energy efficiency and load shifting," *Electric Power Systems Research*, vol. 86, pp. 41–50, 2012.

[40] S. Zhang and X. Xia, "Modeling and energy efficiency optimization of belt conveyors," *Applied Energy*, vol. 88, no. 9, pp. 3061–3071, 2011.

[41] P. Mhaskar, N. H. El-Farra, and P. D. Christofides, "Predictive control of switched nonlinear systems with scheduled mode transitions," *IEEE Transactions on Automatic Control*, vol. 50, no. 11, pp. 1670–1680, 2005.

[42] A. Bemporad and M. Morari, "Control of systems integrating logic, dynamics, and constraints," *Automatica*, vol. 35, no. 3, pp. 407–427, 1999.

[43] V. Dua, N. A. Bozinis, and E. N. Pistikopoulos, "A multiparametric programming approach for mixed-integer quadratic engineering problems," *Computers & Chemical Engineering*, vol. 26, no. 4, pp. 715–733, 2002.

[44] M. R. Irving and Y.-H. Song, "Optimisation techniques for electrical power systems. part 1: Mathematical optimisation methods," *Power Engineering Journal*, vol. 14, no. 5, pp. 245–254, 2000.

[45] P. H. Shaikh, N. B. M. Nor, P. Nallagownden, I. Elamvazuthi, and T. Ibrahim, "A review on optimized control systems for building energy and comfort management of smart sustainable buildings," *Renewable and Sustainable Energy Reviews*, vol. 34, pp. 409–429, 2014.

[46] H. Yang, L. Lu, and W. Zhou, "A novel optimization sizing model for hybrid solar-wind power generation system," *Solar Energy*, vol. 81, no. 1, pp. 76–84, 2007.

[47] J. A. Momoh, M. El-Hawary, and R. Adapa, "A review of selected optimal power flow literature to 1993. part i: Nonlinear and quadratic programming approaches," *IEEE Transactions on Power Systems*, vol. 14, no. 1, pp. 96–104, 1999.

[48] Z. Hu and W. T. Jewell, "Optimal power flow analysis of energy storage for congestion relief, emissions reduction, and cost savings," in *Power Systems Conference and Exposition,*. IEEE/PES, 2011, pp. 1–8, Phoenix.

[49] R. J. Vanderbei, "Loqo: An interior point code for quadratic programming," *Optimization Methods and Software*, vol. 11, no. 1-4, pp. 451–484, 1999.

[50] H. Tazvinga, X. Xia, and J. Zhang, "Minimum cost solution of photovoltaic–diesel–battery hybrid power systems for remote consumers," *Solar Energy*, vol. 96, pp. 292–299, 2013.

[51] H. Tazvinga, B. Zhu, and X. Xia, "Energy dispatch strategy for a photovoltaic–wind–diesel–battery hybrid power system," *Solar Energy*, vol. 108, pp. 412–420, 2014.

[52] H. Tazvinga, Z. Bing, and X. Xia, "Optimal power flow management for distributed energy resources with batteries," *Energy Conversion and Management*, vol. 102, pp. 104 – 110, 2015, clean, Efficient, Affordable and Reliable Energy for a Sustainable Future.

[53] H. Tazvinga, B. Zhu and X. Xia, "Optimal power flow management for distributed energy resources with batteries," *Energy Conversion and Management*, DOI: 10.1016/j.enconman.2015.01.015, 2015.

[54] H. Tazvinga, X. Xia, and B. Zhu, "Optimal energy management strategy for distributed energy resources," *Energy Procedia*, vol. 61, pp. 1331–1334, 2014.

[55] B. Zhu, H. Tazvinga, and X. Xia, "Switched model predictive control for energy dispatching of a photovoltaic-diesel-battery hybrid power system," *IEEE Transactions on Control Systems Technology*, vol. 23, no. 3, pp. 1229–1236, 2015.

[56] H. Tazvinga, X. Xia, and Z. Jiangfeng, "Fuel cost minimisation for an off-grid photovoltaic hybrid power supply system," in *Applied Energy*, 2013, Pretoria SA.

[57] B. Zhu, H. Tazvinga, and X. Xia, "Model predictive control for energy dispatch of a photovoltaic-diesel-battery hybrid power system," in *Proceedings of the IFAC World Congress*, vol. 19, no. 1, 2014, pp. 11 135–11 140, Cape Town SA.

[58] A. M. Noorian, I. Moradi, and G. A. Kamali, "Evaluation of 12 models to estimate hourly diffuse irradiation on inclined surfaces," *Renewable Energy*, vol. 33, no. 6, pp. 1406–1412, 2008.

[59] G. A. Kamali, I. Moradi, and A. Khalili, "Estimating solar radiation on tilted surfaces with various orientations: a study case in karaj (iran)," *Theoretical and Applied Climatology*, vol. 84, no. 4, pp. 235–241, 2006.

[60] D. Reindl, W. Beckman, and J. Duffie, "Evaluation of hourly tilted surface radiation models," *Solar Energy*, vol. 45, no. 1, pp. 9–17, 1990.

[61] P. Loutzenhiser, H. Manz, C. Felsmann, P. Strachan, T. Frank, and G. Maxwell, "Empirical validation of models to compute solar irradiance on inclined surfaces for building energy simulation," *Solar Energy*, vol. 81, no. 2, pp. 254–267, 2007.

[62] J. A. Duffie and W. A. Beckman, *Solar Engineering of Thermal Processes*. John Wiley & Sons, 2013, New York .

[63] S. Klein, "Calculation of monthly average insolation on tilted surfaces," *Solar energy*, vol. 19, no. 4, pp. 325–329, 1977.

[64] M. Iqbal, *An introduction to solar radiation*. Academic Press, INC, 1983, Canada.

[65] B. Liu and R. Jordan, "Daily insolation on surfaces tilted towards equator," *ASHRAE J.*, vol. 3, pp. 53–59, 1961.

[66] V. Badescu, "3d isotropic approximation for solar diffuse irradiance on tilted surfaces," *Renewable Energy*, vol. 26, no. 2, pp. 221–233, 2002.

[67] T. M. Klucher, "Evaluation of models to predict insolation on tilted surfaces," *Solar*

energy, vol. 23, no. 2, pp. 111–114, 1979.

[68] R. C. Temps and K. Coulson, "Solar radiation incident upon slopes of different orientations," *Solar Energy*, vol. 19, no. 2, pp. 179–184, 1977.

[69] J. E. Hay, "Calculation of monthly mean solar radiation for horizontal and inclined surfaces," *Solar Energy*, vol. 23, no. 4, pp. 301–307, 1979.

[70] J. A. Duffie and W. A. Beckman, *Solar Engineering of Thermal Processes*. John Wiley & Sons, 2006, New York .

[71] M. Collares-Pereira and A. Rabl, "The average distribution of solar radiation-correlations between diffuse and hemispherical and between daily and hourly insolation values," *Solar Energy*, vol. 22, no. 2, pp. 155–164, 1979.

[72] S. Agrawal, *Comparative Analysis of Hybrid Photovoltaic Thermal Air Collectors: Design, modeling and Experiment to improve the overall efficiency of PV system*. Lambert Academic Publishing, 2012, Germany.

[73] T. Hove, "A method for predicting long-term average performance of photovoltaic systems," *Renewable Energy*, vol. 21, no. 2, pp. 207–229, 2000.

[74] D. Erbs, S. Klein, and J. Duffie, "Estimation of the diffuse radiation fraction for hourly, daily and monthly-average global radiation," *Solar Energy*, vol. 28, no. 4, pp. 293–302, 1982.

[75] D. T. Reindl, W. A. Beckman, and J. A. Duffie, "Diffuse fraction correlations," *Solar Energy*, vol. 45, no. 1, pp. 1–7, 1990.

[76] C. Ma and M. Iqbal, "Statistical comparison of solar radiation correlations monthly average global and diffuse radiation on horizontal surfaces," *Solar Energy*, vol. 33, no. 2, pp. 143–148, 1984.

[77] T. Hove and J. Göttsche, "Mapping global, diffuse and beam solar radiation over zimbabwe," *Renewable Energy*, vol. 18, no. 4, pp. 535–556, 1999.

[78] E. Skoplaki and J. Palyvos, "On the temperature dependence of photovoltaic module

electrical performance: A review of efficiency/power correlations," *Solar Energy*, vol. 83, no. 5, pp. 614–624, 2009.

[79] M. Siegel, S. Klein, and W. Beckman, "A simplified method for estimating the monthly-average performance of photovoltaic systems," *Solar Energy*, vol. 26, no. 5, pp. 413–418, 1981.

[80] D. Evans, "Simplified method for predicting photovoltaic array output," *Solar Energy*, vol. 27, no. 6, pp. 555–560, 1981.

[81] A. Shariah, M.-A. Al-Akhras, and I. Al-Omari, "Optimizing the tilt angle of solar collectors," *Renewable Energy*, vol. 26, no. 4, pp. 587–598, 2002.

[82] V. Morcos, "Optimum tilt angle and orientation for solar collectors in Assiut, Egypt," *Renewable Energy*, vol. 4, no. 3, pp. 291–298, 1994.

[83] W. Zhou, C. Lou, Z. Li, L. Lu, and H. Yang, "Current status of research on optimum sizing of stand-alone hybrid solar–wind power generation systems," *Applied Energy*, vol. 87, no. 2, pp. 380–389, 2010.

[84] H. Yang, W. Zhou, L. Lu, and Z. Fang, "Optimal sizing method for stand-alone hybrid solar–wind system with lpsp technology by using genetic algorithm," *Solar energy*, vol. 82, no. 4, pp. 354–367, 2008.

[85] T. Burton, N. Jenkins, D. Sharpe, and E. Bossanyi, *Wind Energy Handbook*. John Wiley & Sons, 2011, New York.

[86] E. W. E. Association *et al.*, *Wind Energy-The Facts: A Guide to The Technology, Economics and Future of Wind Power*. Earthscan, 2012, London, UK.

[87] M. R. Patel, *Wind and Solar Power Systems: Design, Analysis, and Operation*. CRC Press, 2006, Boca Raton, FL.

[88] S. Ashok, "Optimised model for community-based hybrid energy system," *Renewable Energy*, vol. 32, no. 7, pp. 1155–1164, 2007.

[89] L. Lu, H. Yang, and J. Burnett, "Investigation on wind power potential on Hong

Kong islands : An analysis of wind power and wind turbine characteristics," *Renewable Energy*, vol. 27, no. 1, pp. 1–12, 2002.

[90] C. Bueno and J. Carta, "Technical–economic analysis of wind-powered pumped hydro-storage systems. part i: model development," *Solar Energy*, vol. 78, no. 3, pp. 382–395, 2005.

[91] M. Alhusein, O. Abu-Leiyah, and G. Inayatullah, "A combined system of renewable energy for grid-connected advanced communities," *Renewable Energy*, vol. 3, no. 6, pp. 563–566, 1993.

[92] S. Diaf, D. Diaf, M. Belhamel, M. Haddadi, and A. Louche, "A methodology for optimal sizing of autonomous hybrid pv/wind system," *Energy Policy*, vol. 35, no. 11, pp. 5708–5718, 2007.

[93] F. O. Hocaoğlu, Ö. N. Gerek, and M. Kurban, "A novel hybrid (wind–photovoltaic) system sizing procedure," *Solar Energy*, vol. 83, no. 11, pp. 2019–2028, 2009.

[94] C. Nayar, "Remote area micro-grid system using diesel driven doubly fed induction generators, photovoltaics and wind generators," in *IEEE International Conference on Sustainable Energy Technologies*, 2008, pp. 1081–1086, Singapore .

[95] P. Lim and C. Nayar, "Photovoltaic-variable speed diesel generator hybrid energy system for remote area applications," in *IEEE Universities Power Engineering Conference, 2010 20th Australasian*, 2010, pp. 1–5, Christchurch, New Zealand.

[96] E. Koutroulis, D. Kolokotsa, A. Potirakis, and K. Kalaitzakis, "Methodology for optimal sizing of stand-alone photovoltaic/wind-generator systems using genetic algorithms," *Solar Energy*, vol. 80, no. 9, pp. 1072–1088, 2006.

[97] J. Fulzele and S. Dutt, "Optimium planning of hybrid renewable energy system using homer," *International Journal of Electrical and Computer Engineering*, vol. 2, no. 1, pp. 68–74, 2011.

[98] J. Manwell, W. Stein, A. Rogers, and J. McGowan, "An investigation of variable speed operation of diesel generators in hybrid energy systems," *Renewable Energy*, vol. 2,

no. 6, pp. 563–571, 1992.

[99] G. Seeling-Hochmuth, "A combined optimisation concept for the design and operation strategy of hybrid-pv energy systems," *Solar Energy*, vol. 61, no. 2, pp. 77–87, 1997.

[100] K. Divya and J. Østergaard, "Battery energy storage technology for power systemsŮan overview," *Electric Power Systems Research*, vol. 79, no. 4, pp. 511–520, 2009.

[101] H. Ibrahim, A. Ilinca, and J. Perron, "Energy storage systems: Characteristics and comparisons," *Renewable and Sustainable Energy Reviews*, vol. 12, no. 5, pp. 1221–1250, 2008.

[102] D. Nelson, M. Nehrir, and C. Wang, "Unit sizing and cost analysis of stand-alone hybrid wind/pv/fuel cell power generation systems," *Renewable Energy*, vol. 31, no. 10, pp. 1641–1656, 2006.

[103] S. Vosen and J. Keller, "Hybrid energy storage systems for stand-alone electric power systems: optimization of system performance and cost through control strategies," *International Journal of Hydrogen Energy*, vol. 24, no. 12, pp. 1139–1156, 1999.

[104] D. Guasch and S. Silvestre, "Dynamic battery model for photovoltaic applications," *Progress in Photovoltaics: Research and Applications*, vol. 11, no. 3, pp. 193–206, 2003.

[105] L. Zhang, G. Barakat, and A. Yassine, "Deterministic optimization and cost analysis of hybrid pv/wind/battery/diesel power system," *International Journal of Renewable Energy Research*, vol. 2, no. 4, pp. 686–696, 2012.

[106] N. Achaibou, M. Haddadi, and A. Malek, "Lead acid batteries simulation including experimental validation," *Journal of Power Sources*, vol. 185, no. 2, pp. 1484–1491, 2008.

[107] H. Bindner, T. Cronin, P. Lundsager, J. F. Manwell, U. Abdulwahid, and I. Baring-Gould, "Lifetime modelling of lead acid batteries," Riso National Laboratory, Tech. Rep., 2005.

[108] R. Luna-Rubio, M. Trejo-Perea, D. Vargas-Vázquez, and G. Ríos-Moreno, "Optimal

sizing of renewable hybrids energy systems: A review of methodologies," *Solar Energy*, vol. 86, no. 4, pp. 1077–1088, 2012.

[109] D. Connolly, H. Lund, B. V. Mathiesen, and M. Leahy, "A review of computer tools for analysing the integration of renewable energy into various energy systems," *Applied Energy*, vol. 87, no. 4, pp. 1059–1082, 2010.

[110] O. Erdinc and M. Uzunoglu, "Optimum design of hybrid renewable energy systems: Overview of different approaches," *Renewable and Sustainable Energy Reviews*, vol. 16, no. 3, pp. 1412–1425, 2012.

[111] T. Hove and H. Tazvinga, "A techno-economic model for optimising component sizing and energy dispatch strategy for pv-diesel-battery hybrid power systems," *Journal of Energy in Southern Africa*, vol. 23, no. 4, pp. 18–28, 2012.

[112] H. Tazvinga and T. Hove, *Photovoltaic/Diesel/Battery Hybrid Power Supply System*. VDM Publishers, 2010, Germany.

[113] H. Tazvinga and S. Fore, "An energy performance analysis for a photovoltaic/diesel/battery hybrid power supply system," *International Conference on Domestic Use of Energy*, pp. 68–73, 2010, Cape Town, SA.

[114] G. Tina, S. Gagliano, and S. Raiti, "Hybrid solar/wind power system probabilistic modelling for long-term performance assessment," *Solar Energy*, vol. 80, no. 5, pp. 578–588, 2006.

[115] Y. SÖNMEZ, "Estimation of fuel cost curve parameters for thermal power plants using the abc algorithm," *Turkish Journal of Electrical Engineering and Computer Science*, vol. 21, no. Sup. 1, pp. 1827–1841, 2013.

[116] H. Suryoatmojo, A. Elbaset, A. Syafaruddin, and T. Hiyama, "Genetic algorithm based optimal sizing of pv-diesel-battery system considering co2 emission and reliability," *International Journal of Innovative Computing Information and Control*, vol. 6, no. 10, pp. 4631–4649, 2010.

[117] P. A. Ioannou and J. Sun, *Robust Adaptive Control*. Dover, 2012, New York, USA.

[118] L. Wang, *Model Predictive Control System Design and Implementation Using MATLAB®*. Springer Science & Business Media, 2009, Australia.

[119] A. A. Sousa, G. L. Torres, and C. A. Canizares, "Robust optimal power flow solution using trust region and interior-point methods," *IEEE Transactions on Power Systems*, vol. 26, no. 2, pp. 487–499, 2011.

[120] S. F. Woon, V. Rehbock, and A. A. Setiawan, "Modeling a pv-diesel-battery power system: An optimal control approach," in *Proceedings of the World Congress on Engineering and Computer Science,*, 2008, San Francisco, USA.

[121] B. Zhao, X. Zhang, J. Chen, C. Wang, and L. Guo, "Operation optimization of standalone microgrids considering lifetime characteristics of battery energy storage system," *IEEE Transactions on Sustainable Energy*, vol. 4, no. 4, pp. 934–943, 2013.

[122] C. Zhou, K. Qian, M. Allan, and W. Zhou, "Modeling of the cost of ev battery wear due to v2g application in power systems," *IEEE Transactions on Energy Conversion*, vol. 26, no. 4, pp. 1041–1050, 2011.

[123] D. J. Spiers and A. A. Rasinkoski, "Limits to battery lifetime in photovoltaic applications," *Solar Energy*, vol. 58, no. 4, pp. 147–154, 1996.